

ABSTRACT

Analysis of the *Staphylococcus aureus* collagen adhesin B domain

James L. Snodgrass

Department of Microbiology and Immunology, University of Arkansas for Medical Sciences,
Little Rock, AR 72205

Staphylococcus aureus has the capacity to colonize essentially any tissue including bone. The ability to colonize diverse tissues appears to involve bacterial surface proteins (adhesins) that bind specific host proteins. For instance, the ability to bind collagen appears to contribute to the ability to colonize bone and cartilage. Our previous studies suggest the ability to bind collagen is due to the production of a single adhesin encoded by a gene designated *cna*. Indeed, the only exception to the correlation between the presence of *cna* and the ability to bind collagen are heavily-encapsulated strains that encode and express *cna* but do not bind collagen. The fact that non-encapsulated mutants bind collagen suggests that the capsule can mask the adhesin on the surface of *S. aureus* cells. Based on the recognized role of the capsule in the pathogenesis of staphylococcal infections, and the apparent role of the collagen adhesin in musculoskeletal infections, these results present the bacterium with a paradox. Specifically, previous results imply that *S. aureus* utilizes two virulence factors, one of which (the capsule) is not compatible with the other (the collagen adhesin). That is consistent with our studies demonstrating that heavily-encapsulated strains are particularly virulent in a murine peritonitis model of staphylococcal disease but did not cause disease in a rabbit model of osteomyelitis. However, the *cna*-encoded collagen adhesin occurs in at least four forms that differ in the number (1-4) of a 187 amino acid domain called the B domain. Although the function of the B domain is unknown, the fact that it is located between the ligand binding A domain and the C-terminal wall and membrane-spanning domains suggest that it may act as a stalk to extend the ligand-binding A domain away from the cell surface. Presumably, that would be a particularly important attribute in strains that are heavily encapsulated. To determine whether the B domain is required, a *cna* gene lacking a B domain was constructed and evaluated on its ability to adhere to collagen. Additionally, to address whether multiple B domains can overcome the inhibition associated with the production of an extensive capsule, four naturally-occurring B domain variants and three isogenic B domain variants were introduced into both microencapsulated and heavily encapsulated strains and evaluated on their ability to bind collagen. We conclude that (i) the B domain of Cna is not required for expression of the A domain which enables functional collagen binding, and (ii) multiple B domain repeats do not serve as a recognizable stalk in microencapsulated or heavily-encapsulated strains.

Analysis of the *Staphylococcus aureus* collagen adhesin B domain

A thesis submitted in partial fulfillment of
the requirements for the degree of
Masters of Science

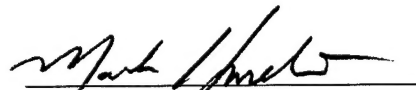
By

JAMES LEE SNODGRASS
B.S., Utah State University, 1994

1999
University of Arkansas for Medical Sciences


This thesis is approved
for recommendation to the
Graduate Council

Major Professor



Mark S. Smeltzer, Ph. D.

Thesis Committee



Shouguang Jin, Ph. D.



William G. Stroop, Ph. D.

ACKNOWLEDGEMENTS

I would like to sincerely thank Dr. Mark S. Smeltzer for providing me the essential resources and guidance which made this research possible. I am also grateful to Dr. Shouguang Jin and Dr. William Stroop for their extensive time and effort in support of this work.

A special thanks goes to Dr. Allison Gillaspy, Dr. Marie Chow and Dr. David Wennerstrom for their endless assistance and “behind the scenes” input.

I would like to especially thank my wife, Shonna, who consistently provided unparalleled loving support and encouragement. A million special “thanks” go to my three daughters, Brittany, Katy and Samantha, and my son, Keaton, who always went out of their way to bring a smile to my face when I came home.

Finally, I am grateful to the United States Air Force for affording me this valuable educational opportunity.

TABLE OF CONTENTS

Acknowledgements.....	4
List of Figures and Table	6
Introduction.....	8
Materials and Methods.....	22
Creation and confirmation of 0B <i>cna</i> variant.....	22
DNA amplification and confirmation of natural <i>cna</i> variants.....	27
Creation and confirmation of isogenic <i>cna</i> variants.....	28
Transformation and transduction of <i>S. aureus</i> strains.....	31
Purification of RNA from bacterial cells.....	34
Northern slot blot analysis.....	36
Preparation of bacterial cell lysates.....	37
Western blot analysis.....	38
Detection of surface associated Cna by fluorescent activated cell-sorting.....	40
Adherence of bacterial cells to immobilized collagen.....	41
Adherence of bacterial cells to soluble collagen.....	42
Adherence of bacterial cells to soluble fibrinogen.....	43
Results.....	44
Discussion.....	77
Bibliography.....	90

LIST OF FIGURES AND TABLE

FIGURE	PAGE
1. Schematic diagram of natural <i>cna</i> variants	54
2. Construction of the 0B <i>cna</i> variant from the Phillips' 2B <i>cna</i> gene	55
3. Construction of the isogenic <i>cna</i> variants from the UAMS-639 <i>cna</i> gene	56
4. Toxicity of the pLI50:: <i>cna</i> constructs in <i>E. coli</i>	57
5. Northern slot blot and Western blot of UAMS-128 comparing the pLI50::0B <i>cna</i> variant with the pLI50::2B <i>cna</i> variant	58
6. Determination of surfaced expressed Cna in UAMS-128 by flow cytometry comparing the pLI50::0B <i>cna</i> variant with the pLI50::2B <i>cna</i> variant	59
7. Qualitative collagen binding assay of UAMS-128 possessing the pLI50::0B <i>cna</i> variant with the pLI50::2B <i>cna</i> variant	60
8. ¹²⁵ I-labeled collagen binding assays comparing the pLI50::0B <i>cna</i> variant and the pLI50::2B <i>cna</i> variant	61
9. Northern slot blot and Western blot analysis of UAMS-128 possessing the pLI50::natural <i>cna</i> variants	62
10. Determination of surface expressed Cna in UAMS-128 by flow cytometry comparing the pLI50:: natural <i>cna</i> variants	63
11. ¹²⁵ I-labeled collagen binding assays comparing the pLI50::natural <i>cna</i> variants in UAMS-128	64
12. Northern slot blot and Western blot analysis of UAMS-128 possessing the pLI50::isogenic <i>cna</i> variants	65

13.	Determination of surface expressed Cna in UAMS-128 by flow cytometry comparing the pLI50::isogenic <i>cna</i> variants	66
14.	Qualitative collagen binding assay of UAMS-128 possessing the pLI50::isogenic <i>cna</i> variants	67
15.	¹²⁵ I-labeled collagen binding assays comparing the pLI50::isogenic <i>cna</i> variants in UAMS-128	68
16.	Combined ¹²⁵ I-labeled collagen binding assays comparing the pLI50::isogenic <i>cna</i> variants as an average from seven different strains	69
17.	¹²⁵ I-labeled collagen binding assays comparing the pLI50::natural <i>cna</i> variants in Newman and Newman (<i>cap</i> ⁻)	70
18.	¹²⁵ I-labeled collagen binding assays comparing the pLI50::natural <i>cna</i> variants in Smith Diffuse and Smith Compact	71
19.	¹²⁵ I-labeled collagen binding assays comparing the pLI50::isogenic <i>cna</i> variants in strains Newman and Wright	72
20.	¹²⁵ I-labeled collagen binding assays comparing the pLI50::isogenic <i>cna</i> variants in strain Wright during a 12-hour time course study	73
21.	¹²⁵ I-labeled collagen binding assays comparing the pLI50::isogenic <i>cna</i> variants in strain Wright grown on a solid surface	74
22.	¹²⁵ I-labeled collagen binding assays comparing the pLI50::isogenic <i>cna</i> variants in strains Smith Diffuse and M	75
23.	¹²⁵ I-labeled fibronectin binding assays comparing the pLI50::natural <i>cna</i> variants in strain UAMS-182	76
TABLE 1 Bacterial strains, plasmids, and PCR primers utilized		53

INTRODUCTION

Purpose of this study

Staphylococcal infections are at the forefront of many debilitating and life-threatening diseases. Among the staphylococci, *S. aureus* stands out as the primary extracellular pathogen. It alone induces upward of one million serious infections each year giving rise to some of the most insidious of diseases including endocarditis, septic shock, and osteomyelitis. Patients, often elderly, afflicted with osteomyelitis undergo agonizing recovery procedures associated with surgical implants. The ability of *S. aureus* to cause this wide array of diseases stems from its many virulence factors.

One factor, the capsular polysaccharide, serves as an antiphagocytic barrier. Other factors include a vast assortment of adhesins, which facilitate attachment to host proteins. One adhesin, Cna, affords the organism the ability to colonize bone. Our preliminary results demonstrate that the use of an extensive capsule impairs the function of Cna (19). However, Cna has been shown to exist in multiple forms, varying in the number (1 to 4) of a 187 amino acid domain called the B domain (17). Therefore, to investigate potential functions associated with the B domain, we addressed two specific aims: (1) Is a single B domain essential for collagen binding? (2) Can multiple B domains act collectively to enhance collagen binding?

Overview of Staphylococci

Within the family Micrococcaceae, members of the *Staphylococcus* genus possess qualities that enable them to be easily distinguished from other bacteria. Closely related to the *Bacillus* genus, staphylococci are gram positive, facultative anaerobes

approximately 1µm in diameter. Additionally, staphylococci are catalase positive, usually oxidase negative, and can grow in environmental conditions with a 10% salt concentration (27). At the genetic level, they possess a low G+C DNA content which ranges from 30 to 40% (27). Unlike most bacteria, staphylococci are inherently unique in their maintenance of a highly evolved cell wall architecture.

Heavily cross-linked peptidoglycan, intermixed with teichoic acid, comprise over 60% of the overall dry weight of the cell wall (27). This intricate cross-linking affords the organism a rigid protective barrier capable of withstanding osmotic pressures as high as 30 atmospheres (40). It also offers innate resistance to lysozyme, an enzyme found in many bodily secretions that degrades most bacterial wall components. As a result, staphylococci are able to proliferate in niches intolerable to other bacteria. Finally, staphylococci can be easily differentiated from other micrococci based on their cell division (27).

Microscopic analysis reveals staphylococci typically divide in more than one plane (27). By doing so, several bacteria will remain grouped, forming the characteristic grape-like clusters. This is in contrast to the related streptococci, which divide on a single plane. As a result, they too remain linked but form branched chains of variable length. As these pathogens share similarities both in morphology and disease, distinguishing between them can be important. Of the many staphylococci, three species are considered opportunistic pathogens capable of inducing human disease.

Coagulase-negative staphylococci and disease

Staphylococci are often differentiated on their ability to produce coagulase, an enzyme that activates thrombin for the clotting of plasma. Among the coagulase-negative species are *Staphylococcus saprophyticus* and *Staphylococcus epidermidis*.

Only recently identified as a human pathogen, *S. saprophyticus* is generally associated with urinary tract infections in females. The majority of infections occur in sexually active young women or elderly women. Though these infections can be painful and moderately dangerous if untreated, most are easily diagnosed and resolved with proper antibiotic therapy. Fortunately, its frequency in human disease is relatively rare. This is in contrast to *S. epidermidis*, the more common coagulase-negative staphylococcal pathogen.

This general commensal organism is the primary bacterium associated with the human epidermal layer. Once considered to be strictly nonpathogenic, we now know *S. epidermidis* causes opportunistic infections in debilitated and immunocompromised patients. Most notably, it utilizes a polysaccharide capsule to efficiently colonize medical devices, particularly catheters, orthopedic implants, and prosthetic heart valves. Additionally, this extracellular slime provides a protective layer, a biofilm glycocalyx, which serves as an effective barrier against antibiotic treatment. After the biofilm formation, septicemia can result as bacteria disassociate and proliferate within the patient's bloodstream (57). With the increased use of plastic devices in modern medicine, the incidents of *S. epidermidis*-induced disease is expected to rise. Despite this foreseen rise, the coagulase-positive *S. aureus* is expected to remain at the forefront of bacterial pathogenesis.

Coagulase-positive staphylococci and disease

Prior to antibiotics, *Staphylococcus aureus* was among the most devastating of human pathogens. Patients afflicted with *S. aureus* bacteremia had an 80% mortality rate (62). Following the development of antibiotics, the fatalities associated with *S. aureus* diseases dropped substantially. However, it was not long before the selective pressure of antibiotics, coupled with the organism's unprecedented ability to evolve, resulted in unforeseen antibiotic resistance. Today, with the emergence of complete antibiotic resistance, the likelihood of preantibiotic-era mortality rates resulting from *S. aureus* infections is increasingly possible (39).

Presently, *S. aureus*-associated diseases range from superficial skin infections to life-threatening deep tissue and systemic conditions. Among the most common of clinical diseases are the superficial infections of impetigo, folliculitis, and carbuncles. These are best characterized as local tissue necrosis often coupled with the formation of pus-filled abscesses. Additionally, *S. aureus* is a well-described etiologic agent of numerous toxin-mediated diseases. Examples include exfoliatins (scalded skin syndrome) (37, 42), heat- and protease-stable enterotoxins (food poisoning) (26), and pyrogenic exotoxin (toxic shock syndrome) (10, 11). It is also a major causative agent of numerous life-threatening musculoskeletal diseases such as endocarditis (6, 24), septic arthritis (5, 20, 51), and osteomyelitis (9, 69). It is this diversity of diseases which has impelled scientists to investigate the transmission of *S. aureus* (38).

Interestingly, epidemiological studies have concluded that the primary reservoir for *S. aureus* is the human being (38). Ironically, as much as 50% of the general population are intermittently colonized with little or no manifestation of disease (38).

Colonization of hospital workers can be even higher, giving rise to nosocomial infections. Clearly, many mechanisms control the fine balance of disease induction versus mere colonization. The determination of disease induction lies not only in the complex blend of host conditions, but also with the invading strain's possession of marked virulence factors.

The crucial role of virulence factors

A virulence factor is a product which contributes to an organism's ability to cause disease. However, virulence factors are generally not essential elements for the bacterium's survival in all conditions. As such, no single strain has been shown to possess all of the *S. aureus*-associated virulence factors. This does not imply that the ability to colonize or survive within a particular environment does not require a specific factor or factors. Therefore, the ability of a strain to promote a specific disease is often linked to its possession of specific virulence factors. Interestingly, *S. aureus* has been shown to effectively control the expression of its virulence factors. This promotes the bacterium's efficient colonization of target tissues without the consistent metabolic burden.

Most virulence factors are not constitutively expressed. Rather, they are regulated and produced during specific growth conditions or in response to certain environmental stimuli. This affords the organism an effective means of metabolic control. Without this control, the bacterium would be unable to adapt to rapid changes in pH, osmotic pressure, nutrient availability, temperature or cell density, among others. The two well-characterized regulatory elements within *S. aureus* are *agr* (accessory gene regulator) and *sar* (staphylococcal accessory regulator). These, along with potentially unidentified

regulatory elements, allow *S. aureus* to efficiently utilize its virulence factors. Of the many virulence factors, those which promote evasion of host immune responses are particularly important.

Occurrence of capsules in *S. aureus*

Many bacterial cell surface components are considered virulence factors, critical in pathogenesis. One such component is the bacterial capsular polysaccharide, or capsule. A capsule is generally characterized as being loosely associated with the cell wall. Within the *S. aureus* population, nearly 90% of all isolates produce some kind of capsular polysaccharide (25, 29, 54, 63). Of these, at least 11 distinct capsule types have been differentiated serologically (63).

Among all the identified capsule types, only 2 are considered heavily encapsulated, presenting an extensive mucoid appearance when grown on solid medium. These have been classified serotypes 1 and 2 (33, 45). Interestingly, despite these strains being highly virulent in animal models, they are rarely isolated as commensals or pathogenic organisms in humans (33, 45). In contrast, most strains appear to produce capsular polysaccharide of a lower density. These strains are referred to as microencapsulated. Of all the clinically-isolated *S. aureus* strains, 75-80% possess microcapsules with serotypes 5 or 8 (2, 3, 25, 29, 54, 63). With such an overwhelming presence in human disease, it is understandable why more research is focused on microcapsules, over extensive capsules, in *S. aureus* pathogenesis.

The capsule and pathogenesis

As many bacterial capsules are thought to have antiphagocytic properties, it is believed to be a key virulence factor (38). However, the distinct relevance of

microcapsules in staphylococcal pathogenesis is somewhat controversial. Many scientists have attempted to interpret conflicting virulence studies, presence and regulation of capsule genes, and overall immunogenicity of capsular products to determine its role in pathogenesis (1, 12, 14, 45, 65).

Microcapsules, particularly types 5 and 8, have been shown to provide little or no protection when compared to unencapsulated mutants *in vivo* (1). This suggests the microcapsule fails to provide the antiphagocytic properties associated with extensive capsules. Recently, others claim that *in vitro* growth conditions are the limiting factor (65), outlining the microcapsule as antiphagocytic in an animal model. The mere fact that 90% of all *S. aureus* strains produce capsules, most of which are microcapsules, implies it provides the organism some benefit. Otherwise one could expect such a genetic and metabolic burden would be naturally selected out of the population. Searching for increased evidence supporting the capsule as a virulence factor, others have addressed this issue based on the antigenicity of capsular polysaccharides (12, 45).

Many virulence factors have been shown to be immunogenic (capable of generating a host immune response). Similar to the above-cited studies, conflicting reports regarding the immunogenicity of capsule antigens are also prevalent. In one study, antibodies raised to capsular polysaccharides failed to provide protection against *S. aureus* induced experimental endocarditis (45). Yet a more recent study demonstrated that human antibodies raised from capsule-derived conjugative vaccines are highly efficient in opsonophagocytosis (12). The disparity between these studies probably comes from the differences in experimental designs. Clearly, more research regarding the *S. aureus* capsule is needed as we search to neutralize this pathogen. Specifically,

exploration focused on understanding how capsules interact with other surface bound virulence factors, particularly adhesins, is needed.

The capsule: does it play well with others?

It has been previously shown that certain types of capsules inhibit the function of other known virulence factors, particularly adhesins (19). However, to best serve the organism, the surface proteins beneath the capsule layer should be functional. This may offer the pathogen the dual benefit of protection from an immune response while maintaining the ability to colonize target sites.

The presence of a capsule, even a microcapsule, has been suggested to obscure adherence resulting in decreased virulence (4). This is unlike related studies involving the closely related *Bacillus anthracis*, where the relationship between the capsule and the surface components (including adhesins) are completely compatible (43). Likewise, Gillaspay et al. (19) demonstrated that surface-bound adhesins are virtually unaffected in the presence of a microcapsule. However, significant inhibition occurred in strains which produced extensive capsules. Clearly, this inhibition does not restrict the passage or attachment of all substances. Others have demonstrated, using heavily encapsulated strains, that the capsule is porous, allowing the passage of certain substrates while restricting others (30, 31, 70, 71). With nearly all strains producing some kind of capsule, it is necessary to address the relationship between it and the underlying surface components, particularly adhesins.

Adhesins

Adherence to host proteins by all microorganisms is a fundamental process of pathogenesis. Typically, most organisms have specific target tissues to which they adhere

and colonize, resulting in disease. Failure to adhere directly correlates to the inability to cause disease at that site. Corresponding with its wide range of diseases, *S. aureus* has been shown to adhere to multiple extracellular matrices (ECMs).

The *S. aureus* adhesins responsible for binding ECMs have been termed microbial surface components recognizing adhesive matrix molecules (MSCRAMMs) (49). Some MSCRAMM gene products, which exhibit high-specificity binding of surface components, have been identified. These include Fib, ClfA, and FbpA (fibrinogen binding), FnbA and FnbB (fibronectin binding), EbpS (elastin binding), and Cna (collagen binding) (49). In contrast, the *map* gene appears to encode a broad-specificity MSCRAMM. It has been shown to mediate low-level binding of fibronectin, fibrinogen, vitronectin, osteopontin, thrombospondin, collagen and bone sialoprotein (28, 41). This large assortment of surface adhesins, most with high specificity for a single host protein, contributes to the many *S. aureus*-associated diseases.

The presence of a specific adhesin has been linked to the increased ability of the organism to cause specific diseases. For example, strains which express the FnbA or FnbB adhesins have a greater ability to colonize intravascular devices (68). Such colonization, especially in hospital patients with weakened immune systems, can lead to bacterial sepsis, then death (39, 40). Other strains possessing Cna have an increased likelihood of causing septic arthritis (64). Notably, many *S. aureus* MSCRAMMs, such as Cna, may have arisen from frequent exposure to host proteins, such as collagen. Therefore, to fully comprehend the disease process, an understanding of the host protein that serves as a site for bacterial attachment is required.

Collagen as a target for bacterial adherence

Collagen is one of the most abundant proteins found within the human body, making it an attractive matrix for colonization. Essential for strength, collagen is found in many connective tissues including cartilage, tendons, bone tissue, and the cornea of the eye. At the amino acid level, it is composed primarily of glycine, proline, and hydroxyproline. Found in repeating tripeptides of Gly-X-Pro or Gly-X-Hyp, a single molecule assumes an α -helical secondary structure. However, collagen's final structure has many unique features which may directly impact the binding capability *S. aureus*.

Being one of the few left-handed triple helices found in proteins, this secondary structure provides rigid strength, able to support up to 10,000 times its own weight (35). Such tensile strength is stronger than steel wire of equal size (35). The collagen superhelix, referred to as tropocollagen, is an extended rod-shaped molecule approximately 1.5nm thick by 300nm long. However, since tropocollagen molecules frequently cross link one another, the overall length and thickness can be quite variable. Interestingly, such a structure may impair collagen binding by heavily encapsulated strains (Brian Wilkinson, personal communication).

Presumably, such a long rod-shaped molecule could frequently lie across the capsule pores. This, in turn, may prevent binding by the underlying adhesins. Such a limitation, observed only in heavily encapsulated strains, could be deleterious to the organism and may affect a broad range of adhesins. This may explain why heavily-encapsulated *S. aureus* strains are rarely found in human disease. This is not surprising as many adhesins, including Cna, share several common features.

Commonalties associated with Cna and other adhesins

The gene encoding Cna possesses fundamental characteristics which define many staphylococcal surface proteins (49). For example, all MSCRAMMs begin with an N-terminal signal sequence. The presence of such a sequence ensures the protein is targeted to the cell wall. Upon translation and trafficking to the cell wall, this region is cleaved as the protein is transported out of the cell.

The individual domains of many *S. aureus* cell surface associated proteins, including adhesins, share common features. For example, the outermost region of the adhesin is a unique, nonrepetitive sequence (50). Most of these have been identified as essential for ECM binding. Like other adhesins, truncation of this domain within the *cna* gene results in the loss of function (50). Immediately following the ECM binding domain lies one or more repeated elements. Between adhesins, these regions exhibit great variation in both size and apparent function. The C-terminus of all MSCRAMMs concludes with the characteristic wall-spanning domain, LPXTG motif, and hydrophobic membrane spanning domain (58). Despite the genetic similarities between *cna* and other adhesin genes, *cna* has been shown to possess some unique properties.

The unique properties of *cna*

Unlike the majority of identified adhesin genes, which are highly conserved in most strains, the prevalence of *cna* is relatively rare (found in only 40% of examined strains) (61). Additionally, most adhesins are linked to the cell wall in a similar manner (66). The LPXTG sorting signal, recognized by a hypothetical sortase, facilitates direct incorporation of the MSCRAMM into the peptidoglycan layer. This sorting signal is found within *cna*. Yet for unknown reasons, it remains one of the few adhesins not

incorporated into the cell wall. Instead, it remains bound to the cytoplasmic membrane (59). The most striking difference between *cna* and other *S. aureus* MSCRAMMs lies in its repetitive domains, each termed the B domain.

Cna, from several clinical isolates, has been found to express multiple B domains (1-4) each comprised of 187 amino acid repeat regions. Most MSCRAMM repetitive sequences are significantly smaller when compared to *cna*. For comparison, the *clfA* gene has a total repeat region of 308 residues comprised of 31 repetitive sequences (20). The sheer size of each B domain is unprecedented, carrying 561 residues. With 4 direct repeat regions, probably arising from gene duplication events, the resulting *cna* has a total of 2,244 residues. This marks over a 7-fold increase in repetitive sequence when compared to other MSCRAMMs. More strikingly, following transcription and translation, as much as 49% of the overall protein can be comprised of B domain. This, taken together with the inability to identify any Cna lacking such a domain, suggests the B domain serves a function.

Function of repetitive elements

DNA sequences, containing tandem repeat regions, are found in many bacterial-wall associated proteins. Some have been shown to be essential in functional expression of the ligand binding domain (20). Others remain uncharacterized. Until now, similar experiments with Cna have not been conducted. Presumably, if the role of the B domain is to properly orient the ECM binding domain, similar to that seen in ClfA, one could truncate the B domain and observe some functional loss. In addition to presenting the binding domain, repeated protein sequences have also been shown to function in ECM binding.

Studies involving the *S. aureus* fibronectin binding proteins have shown that the repeat sequences are themselves directly involved in ligand binding (60, 67). This does not appear to be the case in Cna. If the B domain served to bind collagen, one would expect the multimers to have a distinct advantage in collagen binding. However, it has been previously demonstrated that variations in collagen binding among *cna*-positive strains are associated with the level of transcription (19). As such, the repetitive B domain has yet to be associated with any function.

Therefore, the aim of this present study was twofold. First, we investigate the requirement for a single B domain in collagen binding. Second, we assessed whether multiple B domains might enhance the ability of the organism to bind collagen, particularly in encapsulated strains.

The design of this study

To determine whether a single B domain is required for functional expression of the collagen binding domain, we first constructed a B domain knockout mutant. After cloning into several *S. aureus* cell lines, we assessed transcription, translation, expression, and overall collagen binding capability.

It has been previously shown that Cna-positive strains possessing capsule types 1 and 2 fail to bind collagen at significant levels (19). However, both of these heavily encapsulated strains expressed Cna with a single B domain. Experiments involving their respective capsule knockout mutants restored collagen binding. This provided direct evidence that overproduction of capsular polysaccharide directly masks Cna's function. Therefore, the possibility exists that a Cna variant with multiple B domains could restore binding capability. Such restoration could be attributed to the repeat regions acting

collectively, as a stalk, projecting the collagen domain past the capsule boundary.

Therefore, we cloned naturally-occurring (1-4) B domain variants and created a 1B, 2B, and 3B isogenic variant from our 4B *cna*-positive parent. After expression in several nonencapsulated, microencapsulated, and heavily encapsulated cell lines, we assayed them for expression and overall collagen binding capacity.

MATERIALS AND METHODS

Bacterial strains, plasmids, and oligonucleotide primers

All bacterial strains, plasmids, and primers used in this study are summarized in Table 1. As *cna* has been found to express multiple B domains (1-4) each comprised of 187 amino acid repeat regions, we selected four natural variants for this study (Fig 1).

DNA amplification via Polymerase Chain Reaction (PCR)

For amplification of 0B domain mutant and natural *cna* variants, oligonucleotide primers were purchased from Integrated DNA Technologies, Inc (Coralville, IA.).

Amplification of the 0B domain gene fragments was performed utilizing the chromosomal DNA from strain Phillips. As shown in Figure 2a, primers B1 and B3 were utilized to produce the 2,070 bp gene fragment (promoter region and A domain). Primers B2 and B4 were used to amplify the 380 bp gene fragment (wall, membrane, and cytoplasmic domains). Each PCR mix contained 1 μ l genomic DNA, 1 μ l of each primer (5' and 3'), 10 μ l 10 \times buffer, 8 μ l deoxynucleotides (dNTPs), 0.5 μ l Taq polymerase and 78.5 μ l sterile water. The 10 \times buffer, dNTPs, and Taq polymerase were purchased from Qiagen (Valencia, CA.). PCR was accomplished utilizing the M.J. Research (Watertown, MA.) PTC-100 Programmable Thermal Controller. Each cycle consisted of a 1 minute denaturation step (94° C), 1.5 minute annealing step (50° C), and 1.5 minute extension step (72° C) for 30 cycles.

Purification of DNA

Following amplification, the PCR mix was transferred to a 0.8% agarose gel and DNA fragments separated utilizing the Bio-Rad (Hercules, CA.) Mini-sub Cell GT Gene

electrophoretic instrument. Fragments were excised from the gel and purified utilizing the Qiagen Gel Extraction kit following manufacture's guidelines. Specifically, 300 μ l of Buffer QG were added to each 100 mg of gel and incubated at 50° C for 10 minutes. After the gel was dissolved, 100 μ l of isopropanol was added, mixed, and poured into a QIAquick spin column. All centrifugation steps were accomplished at room temperature (RT) at 15,000 \times g. Samples were spun in an IEC Micromax (Needham Heights, MA.) centrifuge for 1 minute and the flow-through material discarded. The column was then washed with 750 μ l of Buffer PE by centrifugation and the flow-through material discarded. Finally, after placing the QIAquick column in a clean 1.5 ml microcentrifuge tube, 50 μ l of sterile water was delivered to column and centrifuged for 1 minute.

Creation of TOPO 2.1::0B *cna*

To facilitate the direct insertion of *Taq*-amplified PCR products into a plasmid vector, the TOPO2.1 cloning vector from Invitrogen (Carlsbad, CA.) was utilized. Specifically, fragment DNA products were resuspended in a PCR mix at a ratio of 20:1 small fragment to large fragment ratio. The sense strand of the larger A domain will anneal to the antisense strand of the W domain, as primers B3 and B4 were designed with complementary ends (Fig 2b). Without the addition of oligonucleotide primers, 5 cycles of amplification using *Taq* polymerase were performed as described above. Immediately following, the B1 and B2 oligonucleotides were added and the full 30-cycle PCR completed. The 2,450 bp gene products were harvested, gel purified, and cloned into the TOPO 2.1 vector as described by the manufacturer. Specifically, TOPO-cloning mix was created with 2 μ l of PCR product, 2 μ l of sterile water, and 1 μ l of pCR-TOPO vector.

The sample was mixed and incubated at RT for 5 minutes. Top10F' competent cells (Invitrogen) were thawed on ice for 15 minutes followed by the addition of 2 μ l of 0.5 M β -mercaptoethanol. Immediately, 2 μ l of the TOPO-cloning mix was added to the cells and incubated on ice for 15 minutes. The cells were heat shocked for 30 secs at 42° C without shaking. Finally, 250 μ l of SOC medium (2% Tryptone, 0.5% Yeast Extract, 10 mM NaCl, 2.5 mM KCl, 10 mM MgCl₂, 10 mM MgSO₄, and 20 mM glucose) was added, mixed, and incubated for 1 hr at 37° C with heavy shaking. Cells were plated on Difco Trypticase Soy Agar (TSA) each containing 100 μ g/ml ampicillin, 4 μ l \times -gal and 40 μ l 100 mM IPTG. All Difco broth and agar products, X-gal, and IPTG were utilized from Fisher Scientific (Pittsburgh, PA.). Following overnight incubation at 37° C, white colonies were screened by restriction digest (Fig 2c) and confirmed with sequencing analysis.

Small scale purification of plasmid DNA (Miniprep)

Plasmid DNA for cloning and sequence analysis was purified utilizing the QIAprep Spin Miniprep kit following the manufacture's protocol (Qiagen). Briefly, individually picked colonies were grown overnight at 37° C in 5 ml of Difco trypticase soy broth (TSB) with appropriate selection (100 μ g/ml of ampicillin for *E. coli* and 20 μ g/ml of chloramphenicol for *S. aureus*). Bacterial cells were pelleted at RT at 9,300 \times g, resuspended in 250 μ l of Buffer P1 (50 mM glucose, 25 mM Tris Cl at pH 8.0, and 10 mM EDTA at pH 8.0), and transferred to a 1.5 ml microcentrifuge tube. If bacteria were staphylococci, 3 μ l of lysostaphin was added and incubated at 37° C for 1 to 2 hours. Cells were then lysed for 5 minutes with the addition and gentle mixing of 250 μ l of

Buffer P2 (0.2 N NaOH and 1% SDS). Immediately, 350 μ l of buffer N3 (5 M potassium and 11.5% glacial acetic acid) was added to precipitate proteins followed by centrifugation for 10 minutes at $15,000 \times g$. The supernatant was decanted onto a QIAprep spin column and recentrifuged for 1 minute at $15,000 \times g$. Following discard of flow-through, the column was washed with 750 μ l of Buffer PE (70% ethanol) and centrifuged with two separate 1-minute individual spins. DNA was eluted with 50 μ l of sterile water.

Large scale purification of plasmid DNA (Midiprep)

Plasmid DNA for cloning, sequence analysis, and generation of isogenic *cna* variants was purified utilizing Qiagen's Midiprep Kit following the manufacture's protocol. Briefly, individually picked colonies were grown overnight at 37° C in 25 ml of TSB with appropriate selection (100 μ g/ml of ampicillin for *E. coli* and 20 μ g/ml of chloramphenicol for *S. aureus*). Bacteria were centrifuged at $8,000 \times g$ for 10 minutes and resuspended in 4 ml of Buffer P1 (50 mM glucose, 25 mM Tris Cl, and 10 mM EDTA at pH 8.0). If bacteria were staphylococci, 30 μ l of lysostaphin was added and incubated at 37° C for 1 to 2 hours. Cells were then lysed with the addition and 5 minute incubation of 4 ml of Buffer P2 (0.2 N NaOH and 1% SDS). After which, 4 ml of chilled buffer P3 (5 M potassium and 11.5% glacial acetic acid) was added, mixed, and incubated on ice for 20 minutes. The lysate was then centrifuged at $20,000 \times g$ for 30 minutes, the supernate collected and poured over an equilibrated Qiagen-tip 100 column. Following complete flow through, the column was washed twice with 10 ml of Buffer QC (1.0 M NaCl, 50 mM MOPS, and 15% isopropanol, pH 7.0). The DNA was then eluted with 5 ml of

Buffer QF (1.25 M NaCl, 50 mM Tris - Tris Cl, 15% isopropanol, pH 8.5), precipitated with the addition of 3.5 ml of 99% isopropanol, and centrifuged for 30 minutes at 20,000 × g. Finally, the DNA pellet was washed in cold 70% ethanol, air dried for 10 minutes at RT, and resuspended in 100 µl of sterile water.

Restriction digest of pCR-TOPO::0B *cna* mutant

All DNA restriction enzymes and buffers were purchased from New England Biolabs (Beverly, MA.). *SacI* and *XbaI* (1µl each) and 2 µl of 10 × NEBuffer 4 (50 mM potassium acetate, 20 mM Tris-acetate, 10 mM magnesium acetate, and 1 mM dithiothreitol) was added to 10 µl of miniprep DNA and incubated at 37° C for 1 hr. The expected 3.9kbp plasmid with 2.5 kbp vector was confirmed by electrophoresis (described above).

Sequencing of pCR-TOPO::0B *cna* mutant

Sequencing of the pCR-TOPO::0B *cna* mutant was performed by the UAMS Molecular Resource Laboratory (Little Rock, AR.) using an automated version of the Sanger dideoxy method. Briefly, this method utilizes DNA synthesis by PCR (described above) containing a mix of regular dNTPs with ddNTPs (each base linked to a specific and unique fluorescent molecule). Following PCR, the DNA mix is loaded into a gel and fragments of a given length migrate via electrophoresis. Passing through a laser beam, each fluorescently-labeled ddNTP base yields a specific peak. The DNA sequence is read by determining the sequence of colors in the peaks as they pass a detector. This information is directly fed into a computer and the sequence compiled. As M13 forward

and M13 reverse sites flank the multicloning site of the TOPO2.1 vector, we utilized primers specific for these sites.

Amplification, cloning, and confirmation of natural *cna* variants

Chromosomal DNA from strains UAMS-1 and Phillips (with their respective upstream promoters) were utilized to amplify the 1B and 2B *cna* variants, respectively. PCR was performed using the B1 and B2 primers (Table 1 and Fig 2a) as described above. In order to amplify the larger 4.5 kbp 4B domain *cna* variant (Fig 1), the Boehringer Mannheim (Indianapolis, IN.) Extended Long PCR kit was utilized with the B1 and B2 primers and UAMS-639 chromosomal DNA. Specifically, mix one contained 7 μ l dNTPs, 2 μ l B1 primer, 2 μ l B2 primer, 3 μ l U-639 DNA, and 11 μ l sterile water. Mix two contained 5 μ l buffer one, 0.75 μ l polymerase, and 19.25 μ l sterile water. The mixes were combined, vortexed for 20 sec, and PCR amplified using the same protocol as described above. Following amplification, electrophoresis confirmed the presence of an expected size DNA fragment. The PCR mix was then transformed into the TOPO 2.1 cloning vector (as described above for the 0B variant). Restriction digest and confirmation by sequencing of the variants were also accomplished as described above for the 0B variant. The pLI50::3B *cna* variant from FDA-574 (UAMS-102) used in this study was previously created by Patti, et al. (18).

Ligation of the natural *cna* variants into the pLI50 staphylococcal shuttle vector followed by transformation into *E. coli* and subsequently *S. aureus*

Following a *SacI* and *XbaI* restriction digest of vector and insert, pLI50 and *cna* fragments were excised and gel purified as described above. Ligations were performed

using 0.5 µl of New England Biolab's T4 ligase and 1 µl 10 × ligase buffer, 0.5 µl pLI50 shuttle vector, and 8 µl of purified *cna* insert. The ligation reaction was allowed to proceed overnight at 16° C. All ligation reactions were first transformed into the *E. coli* DH5α strain. These constructs appeared phenotypically toxic in several *E. coli* strains. To overcome the apparent toxicity, the final pLI50::*cna* constructs were transformed into the *E. coli* Top10F' cells (as described above) and grown at 30° C on 50% Luria-Bertani (LB) agar selecting with Ampicillin (100 µg/ml). At 24 hours, the smaller colonies were subcultured to 50% LB agar making wide streaks with each. Following a second 24 hour incubation at 30° C, the streaked *E. coli* growth was collected with a sterile toothpick and purified with the QIAprep miniprep kit (described above). Ten microliters of each recombinant pLI50::*cna* product was screened by restriction digest (described above). Upon confirmation of in tact plasmid containing the appropriate size of insert, the remaining 40 µl of miniprep DNA was used to transform *S. aureus* strain RN4220. Once in *S. aureus*, the toxicity was not observed and the pLI50::*cna* constructs could be subsequently transformed into the various experimental *S. aureus* strains (Table 1).

Generation of isogenic *cna* variants from pCR-TOPO::UAMS 639 *cna* construct

Isogenic *cna* variants were created utilizing the pCR-TOPO::4B *cna* variant (described above) in the TOP10F' cell line. Specifically, bacterial cells harboring the TOPO2.1::4B *cna* construct were grown overnight in 25 ml of TSB with Ampicillin (100 µg/ml). Plasmid DNA was then extracted and purified utilizing the Qiagen Midiprep Kit. Constructs were confirmed with a *SacI/XbaI* digest followed by electrophoresis and verification of expected sizes of DNA fragments. Once confirmed, supercoiled plasmid

DNA was partially digested at 37° C for 45 minutes with 140 µl of plasmid DNA (approximately 95 µg), 15.6 µl of 10 × buffer 4 (described above) and 0.5 µl of *AccI* enzyme (New England Biolabs). After heat inactivating the enzyme at 80° C for 20 minutes, a ligation reaction was set up using 9 µl sample, 1 µl of 10 × ligase buffer and 0.5 µl T4 ligase (2,000,000 units/ml). Subsequently, the ligation reaction was incubated at 16° C overnight. As the 4B *cna* variant has 6 *AccI* sites (Fig 3a), while the TOPO vector can not be digested with this enzyme, individual B domains can be excised while keeping the majority of the *cna* gene attached to the TOPO vector. The ligation reaction was then cloned back into the *E. coli* TOP10F' cell line. Specifically, Top10F' competent cells (Invitrogen) were thawed on ice for 15 minutes followed by the addition of 2 µl of 0.5 M β-mercaptoethanol. Immediately, 2 µl of the TOPO-cloning mix was added to the cells and incubated on ice for 15 minutes. Cells were heat shocked for 30 secs at 42° C without shaking. Finally, 250 µl of SOC medium (2% Tryptone, 0.5% Yeast Extract, 10 mM NaCl, 2.5 mM KCl, 10 mM MgCl₂, 10 mM MgSO₄, and 20 mM glucose) was added, mixed, and incubated for 1 hr at 37° C with heavy shaking. Cells were plated on Difco Trypticase Soy Agar (TSA) each containing 100 µg/ml ampicillin, 4 µl X-gal and 40 µl 100 mM IPTG. All Difco broth and agar products, X-gal, and IPTG were utilized from Fisher Scientific (Pittsburgh, PA.). Following overnight incubation at 37° C, white colonies were screened by restriction digest and confirmed with sequencing analysis.

Confirmation of isogenic *cna* variants in pCR2.1-TOPO vector

After subculturing individual colonies to 5 ml of TSB with Ampicillin (100 µg/ml), cells were minipreped and plasmid DNA purified as described above. *AccI* has

two cut sites in the A domain (Fig 3a) in addition to a single cut site in each B domain. As such, stringent screening of each clone was critical and occurred in a three-part process. First, a *SacI/XbaI* digest followed by electrophoresis revealed *cna* fragments of expected sizes (Fig 3b). Clones which exhibited *cna* fragments which were smaller than 3 kbp or larger than 4 kbp were discarded. PCR, utilizing primers Cna 1555 with Cna B3 and also Cna 2237 with Cna B3, was then used to confirm the presence of an A domain. Only those clones that gave a positive amplification using both sets of primers were retained. Finally, sequencing utilizing the Cna 1555 primer confirmed the presence of the A domain and that its junction between the B domain was unaffected.

Creation of electrocompetent (EC) *S. aureus* cells

All the *S. aureus* strains outlined in table 1 were made electrocompetent by the following method. *S. aureus* cells were cultured in TSB at 37° C for 24 hours. Subsequently, 10 ml of the overnight culture was transferred to 500 ml of TSB and incubated at 37° C with vigorous shaking. At approximately 3.5 hours, the optical density (OD A₅₆₀) was measured. When the OD A₅₆₀ was between 0.3-0.5, the bacterial cells were pelleted at 8,000 × g for 10 minutes and the supernatant discarded. The pellet was then resuspended in 500 ml of 500 mM sucrose, repelleted at 8,000 × g for 10 minutes, and the supernatant again discarded. Two washes, each in 500 ml of 500 mM sucrose, were performed with 15 minute ice-incubation steps. After the final centrifugation of 8,000 × g for 10 minutes, EC cells were resuspended in 5 ml of 500 mM sucrose and immediately frozen at -70° C in 100 µl aliquots.

Transformation of pLI50::*cna* variants (natural) into *S. aureus* strains

EC *S. aureus* cells (created as described above) were transformed via electroporation. Briefly, cells were thawed on ice for approximately 15 minutes. Two microliters of supercoiled DNA was added to 50 μ l of cells and incubated at RT for 30 minutes. BTX 2 mm cuvettes (San Diego, CA.) and 2.5 ml SMMP50 mix were placed on ice. SMMP50 mix is composed of 523 μ l 2XSMM (34.2 g sucrose, 0.46 g maleic acid, 0.812 g MgCl_2 in 100 ml sterile H_2O , pH 6.5), 380 μ l of 4X Panassay broth, 47.5 μ l of filter sterilized 10% bovine serum albumin (BSA), and 1 μ g chloramphenicol. Following a 30 minute incubation step, cells were transferred to the ice-cold 2 mm cuvette and electroporated at 10 kV/cm for 2.5 seconds. After the pulse, the cells were quickly resuspended in SMMP50 mix and subsequently shaken at 37° C for 90 minutes. The cells were then subcultured to TSA with chloramphenicol (10 μ g/ml) and incubated at 37° C overnight. Following subculture, individual colonies were screened by cracking buffer analysis (described below).

Plasmid screening of pLI50::*cna* transformants in *S. aureus* by cracking buffer analysis

Cracking buffer was prepared by mixing 35 ml deionized water with 10 g of sucrose. Once mixed, 2 ml of 5 M NaOH and 2.5 ml of 10% SDS were added. Once in solution, the total volume was brought up to 50 ml by adding deionized water. For plasmid isolation, 25 μ l of sterile water was placed into a 1.5 ml microcentrifuge tube. Using a sterile toothpick, single colonies were picked, suspended in water and subcultured to TSA with chloramphenicol (10 μ g/ml). A total of 25 μ l of cracking buffer was

added to the culture and allowed to incubate at RT for 3 minutes. Two microliters of DNA loading dye was added to each tube and thoroughly mixed. Suspensions were then electrophoresed using 0.8% agarose gels. Colonies with plasmids of approximate expected sizes were purified, digested and electrophoresed (as described above) to confirm the presence of the 5.2 kbp pLI50 with each *cna* variant (Fig 3b).

Generation of transducing lysates containing pLI50::isogenic *cna* constructs

Isogenic *cna* variants were delivered into recipient strains by transduction. Each chloramphenicol (10 µg/ml) TSA plate was coated with a moderately heavy inoculum of particular donor strain (RN4220) and grown overnight at 37° C. The next day, the growth from the plate was harvested with a flame-sterilized loop and resuspended into a sterile 1.5 ml tube containing 500 µl of TSB. Several bacteriophage ϕ 11 concentrations (10^{-1} to 10^{-7}) were prepared by gently mixing 100 µl of ϕ 11 phage stock in 900 µl TSB followed by serial dilutions. Once prepared, 4 ml of liquefied soft agar (0.6% Bacto-agar in TSB) equilibrated to 50° C, 40 µl of 500 mM CaCl₂, and 100 µl of donor suspension were gently mixed with 100 µl of each bacteriophage dilution. The soft agar suspension was then poured over a 37° C pre-warmed TSA plate and gently rotated for even distribution. Subsequently, the plate was incubated overnight at RT. The next day, the plate with the concentration of phage forming a completely cleared appearance and the two adjacent plates with lower phage concentrations were selected. Frequently, selected plates would often have concentrations of 10^{-2} (completely cleared), 10^{-3} (lacy appearance), and 10^{-4} (many individual plaques). Once selected, 4 ml of TSB were poured onto the completely cleared plate, spread evenly breaking up the soft agar, and then poured directly onto the

next plate. When phage from the last plate was harvested, the mix was poured into a 25 ml Corex tube (Fisher Scientific) and centrifuged at $8,000 \times g$ for 15 minutes. Once complete, the supernatant was removed and sterilized by passage through a $0.45 \mu\text{m}$ syringe filter. To ensure the phage lysate was completely void of donor bacteria, $100 \mu\text{l}$ of filtered lysate was plated on TSA and grown at 37°C overnight. Once verified, the phage lysate was stored at 4°C until use.

Titration of bacteriophage lysates

Phage lysates were titrated on donor and recipient strains in order to assess the overall quality of the lysate. Particularly, moderately heavy overnight plate cultures of donor and recipient strains were grown and each resuspended in $500 \mu\text{l}$ of TSB. Four milliliters of soft agar was mixed with $40 \mu\text{l}$ of 500 mM CaCl_2 and $100 \mu\text{l}$ of the bacterial suspension. Once gently mixed, the suspension was poured directly onto a 37°C prewarmed TSA plate and allowed to set up 15-30 minutes. While setting up, several 10-fold dilutions of transducing lysate were prepared in TSB by gently mixing. Ten microliters of each dilution was pipetted onto the soft agar lawn and allowed to incubate at RT overnight. The titer of phage were determined the following day.

Transduction of pLI50::*cna* variants (isogenics) into *S. aureus* strains

A very heavy suspension of recipient bacterial strains was grown on chloramphenicol ($10 \mu\text{g/ml}$) TSA plates overnight and resuspended in 2 ml of TSB. Next, $500 \mu\text{l}$ of the bacterial suspension were pipetted into a 25 ml Corex tube containing $20 \mu\text{l}$ of 500 mM CaCl_2 in TSB. An amount of phage suspension was added to attain a multiplicity of infection of 1.0. Once the phage were added, the mixture was incubated

for 20 minutes at 37° C with vigorous shaking. Immediately following, 1.0 ml of ice-cold 0.02 M sodium citrate was added and the mixture centrifuged for 10 minutes at 8,000 × g. Finally, the cells were resuspended in 1.0 ml of ice-cold 0.02 M sodium citrate, plated on chloramphenicol (10 µg/ml) TSA plates containing 500 µg/ml sodium citrate, and grown at 37° C overnight. Individual colonies were screened as described below.

Growth conditions used to enhance capsule production

Enhanced capsule production for CP8 strain Wright was obtained by growing overnight cultures at 37° C on Columbia agar at different oxygen conditions. Specifically, we conducted experiments involving bacteria grown overnight at room air and overnight under microaerophilic conditions (in a candle jar).

Purification of RNA from bacterial cells

Total cellular RNA was isolated as previously described (19). All strains were taken from an overnight culture, standardized by OD A_{560} to 0.05, and subcultured to TSB with chloramphenicol (10 µg/ml). Once in exponential phase, approximately 4 hours, 10 ml of cells were harvested and resuspended in an equal amount of 1:1 acetone:ethanol solution. Cells were pelleted at 10,000 × g for 15 minutes, washed in 10 ml of TES (150 mM NaCl, 78 mM disodium salt EDTA, 100 mM Tris, pH 7.5), and repelleted. After removal of the supernatant, cells were resuspended in 1 ml high-salt TES (2.5 M NaCl, 78 mM disodium EDTA, 100 mM Tris at pH 7.5). Recombinant lysostaphin was then added to a final concentration of 100 µg/ml and incubated at 37° C for 30 minutes. Once the cells had become protoplasts, 5 ml of RNazol B (Tel-Test, Inc., Friendswood, TX.) was added and the samples were rocked at RT. After complete lysis, 0.6 ml of chloroform

were added to the cells followed by vigorous shaking. The cell suspension was then placed on ice for 15 minutes followed by centrifugation at $15,000 \times g$ for 15 minutes. Three 0.6 ml portions were removed from the aqueous phase (top) of each sample and transferred to sterile microcentrifuge tubes. RNA precipitation was carried out as 0.6 ml of 99% isopropanol was added, mixed, placed in a -70°C freezer for 24 hours. The RNA was then pelleted at 4°C for 30 minutes at $15,000 \times g$ and resuspended in 100 μl of DEPC water. Following, an OD A^{260} was read and the RNA concentration calculated for each sample prior to storage at -70°C .

Creation of *cna* probe for Northern slot blot analysis

UAMS-501, containing full length UAMS-1 *cna* in the pT7 vector, was harvested from an overnight culture by small scale purification of plasmid DNA (described above) and digested with *Hae*III (New England Biolabs) to liberate *cna*. Following gel purification, approximately 500 ng of DNA in a volume of 15 μl was heated at 95°C for 10 minutes. Immediately following a quick 10-second spin, 2 μl of hexanucleotide primers and 2 μl of digoxigenin-DNA nucleotide mixture (Boehringer Mannheim), and 1 μl of Klenow (Promega, Madison, WI.) were added and incubated at 37°C overnight. The probe was precipitated with 2 μl 0.2 M EDTA (pH 8.0), 2.5 μl 4 M LiCl, 1.0 μl glycogen and 75 μl ice-cold 95% ethanol followed by an overnight incubation at -70°C . The sample was then centrifuged at $15,000 \times g$ and the supernatant was removed. Finally, the pellet was dried for 15 minutes and then resuspended in 100 μl of sterile water.

Northern slot blot analysis

Positively-charged nylon membranes (Boehringer Mannheim) were washed with 6XSSC diluted from 20XSSC stock (350 g NaCl and 176 g sodium citrate in DEPC water to final volume of 2,000 ml at pH 7.0). An RNA sample mix was prepared using 22.5 μ l DMSO, 4.5 μ l 0.1 M NaPO₄ buffer (pH 7.0), 6.6 μ l glyoxal, and 10 μ g RNA in DEPC water to a final volume of 50 μ l. Subsequently, each 50 μ l sample was transferred to the nylon membrane utilizing the Bio-Dot SF Microfiltration Apparatus (Bio-Rad). Following transfer, each slot was washed twice with 50 μ l TE (pH 8.0) and then once with 50 μ l DEPC water. The membrane was then removed from the microfiltration apparatus, crosslinked on an optimal setting using the Fisher Scientific FB-UVXL-1000 UV crosslinker, and incubated in 50 mM NaOH for 15 seconds. Immediately following NaOH incubation, the membrane was washed in 1XSSC buffer with 0.2 M Tris (pH 7.5) for 15 minutes. The membrane was then placed in a prewarmed 65° C bottle with the RNA side was up (interior of the bottle wall). Ten microliters of prewarmed 65° C pre-hybridization solution (4 ml of 10% dextran sulfate, 1 ml of 1% SDS, 2 ml of 1 M NaCl and 3 ml sterile water) was then added followed by a 15 minute incubation at 65° C in a Scientific Consultants Inc. Hybaid rotator (Baton Rouge, La.). Approximately 150 ng (25 μ l) of full length UAMS-1 digoxigenin-labeled *cna* probe (described above) was added to 75 μ l of herring sperm and denatured at 95° C for 15 minutes in the M.J. Research Thermocycler. Upon completion, DNA-herring sperm samples were centrifuged for 20 seconds, added directly to the nylon membrane, and hybridized at 65° C overnight. Following hybridization, the pre-hybridization solution was discarded. The membrane

was then put through several stringency washes: twice for 5 minutes in 2X SSC at RT, twice for 30 minutes in 2X SSC with 1%SDS at 65° C, and twice for 30 minutes in 0.1X SSC at RT. The membrane was then rocked for 5 minutes at RT in washing buffer (0.1 M maleic acid, 0.15 M NaCl, 0.3% Tween 20 and pH to 7.5 with solid NaOH). Following an initial 5 minute wash, the membrane was incubated for 30 minutes at RT in 100 ml of blocking buffer (1/10 dilution of 0.1 M maleic acid with 0.15 M NaCl in water, pH7.5). Final incubation was done for 30 minutes at RT with anti-digoxigenin-alkaline phosphatase fab fragments (Boehringer Mannheim) diluted 1:10,000 in blocking buffer (1/10 dilution of 0.1 M maleic acid with 0.15 M NaCl in water, pH 7.5). The membrane was then washed twice for 5 minutes each in 0.1 M Tris, 0.1 M NaCl, 50 mM magnesium chloride, pH 9.5 and sealed in a plastic bag. After cutting a corner of the bag, CSPD purchased from Boehringer Mannheim (disodium 3-(4-methoxyspiro(1,2-dioxetane-3,2'-tricyclo[3.3.1.1^{3,7}] decan)-4-yl)phenyl phosphate with a substituted chlorine moiety on adamantine ring) was diluted 1:100 in 0.1 M Tris, 0.1 M NaCl, 50 mM magnesium chloride, pH 9.5. The bag was resealed and the membrane was incubated with spreading of the CSPD solution for 3 minutes. Finally, the bag was reopened, the CSPD removed, and the bag resealed. Blots were exposed for 30 seconds on Fuji medical X-ray film (Tokyo, Japan).

Preparation of bacterial cell lysates for Western analysis

Bacterial cells from an overnight TSB culture were standardized to an OD A_{560} of 0.05 and subcultured to 20 ml TSB with chloramphenicol (10 µg/ml), where applicable. After approximately 4 hours, the cells were immediately harvested, pelleted and washed

in 20 ml TEG buffer (25 mM Tris-HCl, pH8.0 with 25 mM EGTA). Following centrifugation at $10,000 \times g$ for 10 minutes, the cells were resuspended in 1 ml TEG buffer and incubated with 200 μ g recombinant lysostaphin at 37° C for 20 minutes. Protoplast cells were then transferred to a BioPulverizer Blue Tubes (Bio 101, Vista, CA.) containing 0.1 mm silica spheres as a lysing matrix. Cells were subsequently lysed in the FP120 FastPrep instrument (Savant Instruments, Inc., Holbrook, NY) at a speed of 6.5 meters/second for 40 seconds. Approximately 100 μ l of supernatant were removed and the amount of protein quantitated by a Bradford assay (Bio-Rad, Richmond, CA.) and stored at -70° C until use.

Western blot analysis

A 60 μ l suspension containing 50 μ g of total protein in a 3X SDS sample buffer was prepared. Specifically, 3X SDS sample buffer is comprised of 187.5 mM Tris-HCl at pH 6.8, 6% SDS, 30% glycerol, 125 mM DTT and 0.03% bromophenol blue. Protein samples were then thoroughly mixed, denatured at 100° C for 20 minutes and centrifuged at $15,000 \times g$ for 5 minutes. Twenty-five microliters of each protein suspension and a biotinylated protein marker were loaded into two separate 10-20% Tris-HCl polyacrylamide precast gels (Bio-Rad). One gel would be used for the total stain control while the other for Western blotting. Utilizing the Bio-Rad Mini-PROTEAN II Cell system, gels were run at 100 volts constant for 90 minutes. Immediately following, the voltage was increased to 150V for an additional 15 minutes. Upon completion, the total control gel was stained with Coomassie Blue for 15 minutes and destained overnight with gentle rocking in 7% methanol with 10% acetic acid. The proteins were transferred from

the second gel to a 0.2 μ m PVDF (polyvinylidene fluoride) membrane (Bio-Rad) for Western analysis. Cold transfer buffer (25 mM glycine, 25 mM ethanolamine in a 20% methanol solution) was used to equilibrate the membrane 5 minutes prior to actual transfer. The transfer of proteins was completed in the Bio-Rad transfer system using the above transfer buffer (25 mM glycine, 25 mM ethanolamine in a 20% methanol solution) running at 100 volts for 90 minutes. Upon completion, the membrane was then prepared for development. All incubation steps in the development were carried out at RT with gentle rocking. First, the membrane was incubated for 2 hours in 20 ml of blocking buffer (1X TBS, 0.1% Tween 20, in a 5% powdered dry milk solution). The membrane was then incubated with 20 ml of fresh blocking buffer containing 100 μ g of human Fc (Jackson ImmunoResearch Laboratories, Inc., West Grove, PA.) for 1 hour. Next, the membrane was then washed three times for 5 minutes each in 50 ml of wash buffer (1XTBS and 0.1% Tween 20). The membrane was subsequently incubated for 1 hour in 20 ml blocking buffer containing 10 μ l anti-Cna antibody and 100 μ g of human Fc. Subsequently, the membrane was washed three separate times, each for 5 minutes in 50 ml wash buffer (1XTBS and 0.1% Tween 20). A final 1 hour incubation contained 10 μ l of horse radish peroxidase (HRP)-conjugated anti-rabbit IgG antibody and 10 μ l of HRP-conjugated anti-biotin antibody (both from New England Biolabs) in 20 ml of blocking buffer. The membrane was again washed three separate times, each for 5 minutes in 50 ml wash buffer (1XTBS and 0.1% Tween 20). Finally, the membrane was incubated for 1 min in 10 ml of LumiGlo® substrate (0.5 ml of 20X LumiGlo® with 0.5 ml 20X peroxide and 9 ml dH₂O) purchased from New England Biolabs. LumiGlo®, in the

presence of H^2O^2 and HRPO, is an oxidized substrate and gives off blue light. Excess LumiGlo® was removed from the membrane, the membrane sealed in a plastic bag, and exposed for 30 seconds on Fuji medical X-ray film.

Detection of Cna antigen by fluorescent activated cell-sorting analysis (FACS)

Surface expression of the collagen-binding domain of *S. aureus* strains expressing pLI50::*cna* variants was monitored by flow cytometry as previously described (22). Cells from an overnight TSB culture were standardized to an OD A_{560} of 0.05 and subcultured to 20 ml TSB with chloramphenicol (10 μ g/ml), where applicable. At approximately 4 hours, cells were harvested and standardized to approximately 10^8 colony forming units (c.f.u.). Once standardized, the cells were resuspended in FACS buffer (100 mM $NaPO_4$ buffer containing 0.1% BSA and 0.1% Tween 20, pH 7.5). To minimize nonspecific binding of protein A, 27 μ g of purified human Fc was added to the cells and incubated with end-over-end rocking for 30 minutes. The cells were then pelleted at $9,300 \times g$ at 4° C, the supernatant discarded, and the cells resuspended in FACS buffer. Eight microliters ($\approx 45 \mu$ g) of purified rabbit anti-*cna* antibody was added and incubated for 30 minutes with end-over-end rocking. Following centrifugation and resuspension in FACS buffer, 25 μ l of commercially available FITC-conjugated goat anti-rabbit IgG Fab² fragments (Jackson ImmunoResearch Laboratories, Inc.) were added. Cells were then rocked for 30 minutes, pelleted, and resuspended in fixing buffer (2% paraformaldehyde in water) for 15 minutes. Following centrifugation and resuspension in 100 mM $NaPO_4$ buffer, pH 7.5, the average mean fluorescent intensity of 10,000 cells was assessed using the Becton Dickinson FACScan (Franklin Lakes, NJ.).

Adherence of bacterial cells to immobilized collagen

All pLI50::*cna* variants expressed in RN4220 and 8325-4 were qualitatively screened for their ability to adhere to immobilized collagen as previously described (618). Sigma 0.1% type I collagen (St. Louis, MO.) was diluted 1/10 in 10% bicarbonate. Wells of a 96-well "U" bottomed microtiter plate were then precoated with a 200 μ l solution containing 20 μ g of type I collagen in 10% bicarbonate. For negative controls, the designated wells were precoated with a blocking buffer solution (2% BSA in phosphate-buffered saline) instead of collagen. The plate was subsequently incubated at 4° C for 24 hours. Bacterial cultures were grown to exponential phase (4 hours), standardized to an OD A_{560} of 0.5, pelleted at $9,300 \times g$ for 10 minutes, and resuspended in 200 μ l of 100 mM NaPO_4 buffer, pH 7.5. After removing the blocking buffer solution from the 96-well plate, bacterial cell suspensions were added followed by a 1 hour incubation at 37° C. The plate was then centrifuged at $650 \times g$ for 10 minutes. Cells capable of binding collagen bound the side of the wells and failed to pellet.

Radiolabeling of soluble collagen with ^{125}I Iodine

Radiolabeling of Sigma type I collagen was performed as previously described (17) utilizing calf skin type I collagen from Sigma and ^{125}I sodium salt purchased from ICN Radiochemicals (Costa Mesa, CA.). First, a Sephadex G25-M column (Pharmacia Biotech, Piscataway, NJ.) was equilibrated with 25 ml of 100 mM NaPO_4 buffer, pH 7.5. Once the column was equilibrated, 490 μ l of 100 mM NaPO_4 buffer (pH 7.5) was added to the 100 μCi ^{125}I sodium salt vial. Three Iodo Beads (Pierce, Rockford, IL.) were added to the vial and the reaction was able to proceed at RT for 5 minutes. Immediately

following, 50 μg of collagen (in a 500 μl volume) was added and the reaction was incubated for 2 minutes at RT. Labeled solution was then removed and transferred to the equilibrated column. To facilitate entry of the collagen into the column, 1.5 ml of 100 mM NaPO_4 (pH 7.5) was added. Next, 3.5 ml of 100 mM NaPO_4 (pH 7.5) were added to elute the labeled collagen in sterile 1.5 ml microcentrifuge tubes (approximately 7 fractions). Utilizing a BIOSCAN QC2000 gamma counter (Washington, D.C.), decays per minute (dpm) of each 500 μl aliquot were measured. Approximately 40 μg of labeled protein were recovered with the highest radioactivity measured in fractions 2-4, which were combined and the dpm remeasured. Next, the dpm per microliter was calculated. Finally, the total volume of labeled protein needed to yield 1×10^5 to 3×10^5 dpm per binding reaction was assessed.

Adherence of bacterial cells to soluble collagen

All collagen binding assays were done with ^{125}I -labeled type I collagen as previously described (17). Cells from an overnight TSB culture were standardized to an OD A_{560} of 0.05 and subcultured to 20 ml of TSB with chloramphenicol (10 $\mu\text{g}/\text{ml}$), where applicable. After approximately 4 hours, cells were harvested, standardized to an OD A_{560} of 1.0, and pelleted. Once standardized, the cells were resuspended in binding buffer (100 mM NaPO_4 buffer containing 0.1% BSA and 0.1% Tween 20, pH 7.5). Analysis of cells grown on solid support was performed with overnight cultures grown on TSA or Columbia agar, with 20 $\mu\text{g}/\text{ml}$ of chloramphenicol. At 16 to 24 hours post plating, colonies were scraped from the agar, resuspended in 100 mM NaPO_4 buffer (pH 7.5), and also standardized to an OD A_{560} of 1.0 in 1 ml. Supernatant from

microcentrifuge tubes, precoated with 100 mM NaPO₄ buffer containing 2% BSA (pH 7.5), was removed and the standardized cell suspension transferred. The 1.0 ml aliquot of standardized cell suspension was transferred to the microcentrifuge tube followed by the addition of 10⁵ dpm of ¹²⁵I-labeled collagen. Cells were incubated at RT with end-over-end mixing for 1 hour, pelleted at 15,000 × g for 10 minutes and the supernatant removed. Samples were then recentrifuged and the remaining supernatant pipetted off. The radioactivity retained in the pellet was measured in a BIOSCAN QC2000 gamma counter (BIOSCAN, Inc., Washington, D.C.). Binding assays were performed in duplicate and reported as an average.

Adherence of bacterial cells to soluble fibronectin

Strain UAMS-182, a *fnbA* and *fnbB* knockout derivative of UAMS-128, was transformed with the natural pLI50::*cna* variants. All fibronectin binding assays were performed following the same protocol as described with soluble collagen (described above). However, prelabeled ¹²⁵Iodine fibronectin purchased from ICN Radiochemicals was utilized.

RESULTS

Toxicity of pLI50::*cna* in *E. coli* cell lines

Following excision of the *cna* inserts from the pCR 2.1-TOPO vector, and subsequent ligation into the pLI50 shuttle vector, we transformed the pLI50::*cna* constructs into the *E. coli* DH5 α cell line. However, transformed cells grown at 37°C consistently demonstrated extremely poor efficiencies, generally 6-10 transformants per 10^8 to 10^{10} total cells. In attempt to increase transformation efficacy, several *E. coli* cell lines were used. However, similar results were observed with each. Purification and restriction digest of transformants consistently revealed plasmids which had not only lost *cna*, but were missing much of the original vector as well.

As shown by electrophoresis (Fig 4a), supercoiled plasmids from isolated clones continually ran below 2 kbp. Likewise, almost all the obtained plasmid DNA failed to digest with enzymes known to cut the multicloning site. According to the pLI50 map, this truncated plasmid would possess little more than the *E. coli* origin of replication and the ampicillin resistant gene. Additionally, we observed that young transformants, shown to initially possess *cna* by PCR, experienced cell death when subcultured to TSB and grown at 37°C. This suggested our pLI50::*cna* constructs were toxic in many *E. coli* cell lines when grown under the above mentioned conditions. With this understanding, we developed a protocol to overcome this barrier.

To overcome the pLI50::*cna* toxicity problem, we attempted to slow down cell's replication rate in order to reduce the toxicity by diverting the cell's transcriptional and translational machinery to more essential pathways. Specifically, we grew the cells on

reduced media (50% LB or M9) at 30°C. Shown in figure 4b, we obtained a greater than 17-fold increase in harvesting stable plasmids containing intact *cna*. By maintaining these conditions, the pLI50::*cna* constructs were successfully collected, screened, and subsequently transformed into *S. aureus*. Throughout the remainder of the study, the constructs remained stable.

Transcriptional, translational, and expressional analysis of the 0B *cna* variant

We conducted Northern slot blot analysis to effectively compare mRNA production between the 0B and 2B variants. UAMS-128, the well characterized *cna*-negative 8325-4 strain, was transformed with the pLI50::0B clone and its pLI50::2B parent. Northern analysis revealed no detectable differences in the amount of *cna* mRNA between the two strains (Fig 5a). To assess if similar amounts of mRNA resulted in equal amounts of Cna protein, Western blot analysis was performed. Total cellular proteins, detected with polyclonal anti-Cna IgG antibodies, revealed a slight increase in the amount of the 2B Cna protein (Fig 5b). As shown by the gel stained with Coomassie Blue, this difference did not appear to result from a processing error, such as unequal loads of total protein. To further investigate this issue, flow cytometry was utilized.

Flow cytometry provided an effective means to quantitate the amount of expressed cell-surface associated protein. As shown in figure 6, no significant differences could be measured in the amount of surface expressed Cna. The error bars represent the average standard deviation calculated from a series of two separate trials, each ran in duplicate. To ensure such an observation was not strain dependent, we assessed expression in three strains (Fig 6). However, the mean fluorescent intensity remained

consistent. Collectively, these results suggest that the processing and expression of the 0B *cna* variant was unaffected by the removal of the B domain. However, because expression does not guarantee function, we performed a series of collagen binding assays.

Collagen binding capability of the 0B Cna protein

Once equivalent expression levels between the 0B and 2B Cna variants were confirmed, we investigated whether the removal of B domains affected collagen binding using an immobilized collagen binding assay. As shown in figure 7, the 0B variant effectively bound collagen. This provided early evidence that the proper presentation of the known collagen binding A domain was not effected by the absence of the B domain. However, as this assay is purely qualitative, subtle binding differences between the two proteins could go undetected. As such, we utilized an ¹²⁵I-labeled collagen binding assay to quantitatively compare the soluble collagen binding capability of each variant.

The 0B Cna mutant consistently bound collagen at levels equal, or slightly greater, than that of the 2B Cna parent (Fig 8). Again, the designated error bars represent the average deviation calculated from two separate trials. Overall, the ability of the 0B Cna variant consistently bound collagen at a level equal, or slightly greater than, its 2B domain parent.

Transcriptional, translational, and expressional analysis of the natural *cna* variants

We utilized four distinct natural *cna* variants, each obtained from clinical isolates and varying in their number of B domains (Table 1). We initially utilized Northern slot blot analysis to compare mRNA production between the variants. As shown in figure 9a, we observed differential mRNA production between the four variants. Speculating that

the increase in mRNA could be promoter driven, as each variant was under the control of its own promoter, we sequenced each of the construct's promoter regions.

Sequence analysis of the promoter regions revealed only subtle differences between the variants. Interestingly, these sequences matched previously identified chromosomal sequences taken from their respective parent strains (18). Still, these differences may prove to be significant. For example, sequence data obtained from the UAMS-1 (1B) and UAMS-639 (4B) strains possessed base changes that were common to each other. Furthermore, these changes were not identified in the Phillips (2B) and FDA 574 (3B) clones. This, taken in concert with the increased amounts of *cna* mRNA produced from the UAMS-1 and UAMS-639 genes, suggests potential *cis*-acting transcriptional preferences among these two *cna* genes. Not surprisingly, the differences observed in *cna* mRNA corresponded with the varying amounts of translated Cna protein (Fig 9b).

As shown in figure 9b, we also observed a similar trend in the amount of translated Cna protein. In addition, we observed nonspecific binding of the anti-Cna antibody to an approximate 140kD protein. The mass of this protein appeared greater than protein A. This protein has also been observed by other researchers in our laboratory in strains other than UAMS-128, suggesting it is not a strain dependent phenomenon. To date, its identity remains unknown.

In addition to Western analysis, we analyzed each variant by flow cytometry. Figure 10 summarizes the amount of surface expressed Cna protein using the UAMS-128 cell line. Remaining consistent with the established trend, analysis of 10,000 cells revealed the 1B and 4B variants exhibited higher quantities of surface expressed Cna

when compared to the 2B and 3B variants. Despite the B domain-independent expressional differences, we assessed the ability of each of the variants to bind soluble collagen.

Comparison of the ^{125}I collagen binding capacity between natural *cna* products in several unencapsulated/microencapsulated strains

To investigate the soluble collagen binding capacity between the natural *cna* variants, we used the UAMS-128, Newman *cap*⁻, Newman, Smith Compact, and Wright. However, as compared with our translation data presented above, a slightly different trend was observed when assessing the collagen binding capacity between variants (Fig 11). In particular, repeated analysis revealed the 4B Cna variant overall bound less collagen than that of the 1B version. The remaining Cna variants showed collagen binding patterns correlating to their respective amounts of surfaced expressed protein. Though a slight trendline increase was observed between 2, 3, and 4B domain variants, the 1B domain variant demonstrated significantly higher binding capability in almost every strain assayed ($p \leq 0.016$). However, to remove the apparent promoter-driven transcriptional variables, we created isogenic *cna* variants and evaluated them using the same criteria.

Transcriptional, translational, and expressional analysis of the isogenic *cna* variants

Isogenic variants, created from the UAMS-639 gene, allowed us to evaluate collagen binding without the varying expression levels. Initially, we again utilized the Northern slot blot protocol to confirm expression. As expected, we observed similar levels of transcribed mRNA (Fig 12a) and translated protein (Fig 12b) between these four

variants. These data were also confirmed by flow cytometry. Analysis of 10,000 cells demonstrated similar amounts of surface bound protein (Fig 13). With the elimination of differential expression, we assessed the ability of the isogenic Cna variants to bind collagen.

Comparison of the collagen binding capacity between strains with the pLI50::isogenic *cna* variants

We first addressed whether a specific number of B domains possessed the innate ability to increase collagen binding, possibly by enhancing the presentation of the collagen binding domain. To do so, we first assessed the ability of each to bind immobilized collagen. As shown in figure 14, all the isogenic Cna variants in UAMS-128 failed to form a pellet after centrifugation, maintaining their ability to bind collagen affixed to the sides of the wells. Between variants, no differences in binding were observed.

In addition to immobilized collagen binding assays, binding assays using ^{125}I -labeled soluble collagen showed similar levels of activity (Fig 15). Though not statistically significant in the UAMS-128 studies alone, a slight decrease in binding was observed with the increase in B domains. However, upon increasing the sample size, by combining binding averages from all 7 strains assayed, we observed a regression line with a statistically real difference (Fig 16). As calculated by the students paired T-test, the 1B version bound significantly more collagen than both that of the 3B or 4B counterparts ($p < 0.001$). This provided evidence that multiple B domains may actually, to some degree,

impair collagen binding. However, this did not preclude the ability of multiple B domains to enhance collagen binding in encapsulated strains.

It remained possible that multiple B domains, though sacrificing some affinity for collagen, may compensate by surpassing the capsule barrier. By doing so, Cna molecules with multiple B domains would have a distinct advantage in collagen binding. To address this hypothesis, we used our natural and isogenic variants in a wide variety of strains and capsule types.

Collagen binding of encapsulated strains with natural pLI50::*cna* variants

Initially, we assessed the ability of the natural pLI50::*cna* variants to enhance collagen binding in encapsulated strains. However, as the natural *cna* variants demonstrated differential expression, we were unable to directly compare the obtained binding data between individual variants (i.e. 1B Cna to 2B Cna). Therefore, we had to factor out the promoter-driven variables. To do so, we first cloned each variant into an encapsulated strain known to have a capsule knockout complement. After the collagen binding capacity of each variant was assessed in both strains, we looked for a change in binding patterns. Specifically, if multiple B domains enhanced binding, by overcoming capsule inhibition, a decrease in the interval between the unencapsulated collagen binding capacity and the encapsulated collagen binding capacity could be observed. As a result, we performed ¹²⁵I-labeled collagen binding assays using strains Newman with Newman *cap⁻* and Smith Diffuse with Smith Compact.

Strain Newman, grown in TSB and harvested in exponential phase, failed to produce enough capsule to inhibit collagen binding (Fig 17a). This suggested that Newman produced insignificant amounts of capsule at the time when Cna is maximally

expressed. As shown by the ratio of Newman over Newman *cap⁻* in figure 17b, multiple B domains served no advantage in collagen binding. Yet, when utilizing a heavily encapsulated strain, a completely different phenotype was observed.

When compared with the capsule-deficient Smith Compact, grown in TSB and harvested during exponential phase, Smith Diffuse was shown to produce a substantial capsule able to mask Cna's function (Fig 18a). Figure 18b represents the same data, only presented in ratio form (encapsulated/unencapsulated). If multiple B domains enhanced collagen binding, one could expect the larger proteins to have values approaching 1.0. Such a trend was not observed in any of the heavily-encapsulated strain assays. Though the initial data suggested that multiple B domains do not efficiently function as a stalk, we wanted to further investigate the question by utilizing our isogenic variants.

Soluble collagen binding of encapsulated strains with isogenic pLI50::*cna* variants

Utilizing encapsulated strains carrying the isogenic pLI50::*cna* constructs, we assessed the ability of multiple B domains to act as a stalk. Binding assays using strains Newman and Wright (Fig19a and 19b) grown to exponential phase displayed binding patterns similar to those previously observed in UAMS-128. However, analyzing the collagen binding capacity data obtained from our natural *cna* studies, the possibility existed where heavily encapsulated strains produced an over abundance of capsule with microencapsulated strains failing to produce enough. As such, we searched for a condition known to enhance the capsule production of microencapsulated strains. Previous work by Lee et. al has demonstrated growth conditions which effectively enhance capsule production in CP8 cell lines. We therefore focused the remainder of our

experiments on the microencapsulated strain Wright (CP8) and the heavily encapsulated strains Smith Diffuse (CP-2) and M (CP-1).

Initially, a 12-hour timecourse study of strain Wright, grown in Columbia broth, was performed. During this extensive experiment, we measured the collagen binding capacity of each variant in 2 hour intervals. As shown in figure 20, a distinct increase in inhibition occurred between 6 and 8 hours. Additionally, this inhibition was maintained throughout the remainder of the experiment. However, an elevation in collagen binding activity, associated with increased B domains, was not observed. Similarly, Wright variants grown on Columbia agar, exhibiting maximal capsule production, revealed a similar trend in collagen binding capacity (Fig 21). Regardless of environmental changes, we could not identify a condition where multiple B domains correlated with an increase in collagen binding. Finally, we conducted a series of collagen binding assays with the heavily encapsulated strains Smith Diffuse and M. However, similar binding patterns were observed (Fig 22).

Fibronectin binding assays

In searching for an alternative function of the B domain, we performed a BLAST database search utilizing the known B domain DNA and protein sequences as templates. Surprisingly, the B domain exhibited 30%-40% homology, at the protein level, with fibronectin binding proteins of three individual streptococcal species. Utilizing UAMS-182, which is a UAMS-128 *fnbA* and *fnbB* knockout strain, we performed soluble fibronectin binding assays. As shown in figure 23, the pLI50::*cna* variants failed to enhance fibronectin binding, regardless of the number of B domains.

Table 1.
S. aureus strains, plasmids, and primers used in this study.

<u><i>S. aureus</i> strain</u>	<u><i>cna</i> (B domains)</u>	<u>Reference</u>	<u>Description/Comments</u>
UAMS-1	Yes (1)	(16)	Clinical isolate (osteomyelitis)
Phillips	Yes (2)	(51)	Clinical isolate (osteomyelitis)
FDA 574	Yes (3)	(52)	Source of <i>cna</i> for cloning experiments
UAMS-639	Yes (4)	(7)	Clinical isolate (tracheal culture)
UAMS-128	No	(47)	Wild type 8325-4 strain
Newman	No	(44)	Microencapsulated strain (CP5)
Newman <i>cap</i> ⁻	No	This study	<i>cap</i> ⁻ mutant from <i>cat</i> gene insertional inactivation
Wright	No	(15)	Microencapsulated strain (CP8)
Smith Diffuse	Yes (1)	(8)	Heavily-encapsulated strain (CP2)
Smith Compact	Yes (1)	(8)	Spontaneous capsule mutant of Smith Diffuse
M	Yes (1)	(8)	Heavily-encapsulated strain (CP1)
M <i>cap</i> ⁻	Yes (1)	(32)	Spontaneous capsule mutant of M

<u>Plasmids</u>	<u><i>cna</i> (B domains)</u>	<u>Reference</u>	<u>Description/Comments</u>
pCna0	No	This study	pLI50:: <i>cna</i> 0B domain variant created from Phillips
pCna1	Yes (1)	This study	pLI50:: <i>cna</i> variant derived from UAMS-1
pCna2	Yes (2)	This study	pLI50:: <i>cna</i> variant derived from Phillips
pCna3	Yes (3)	(51)	pLI50:: <i>cna</i> variant derived from FDA-574
pCna4	Yes (4)	This study	pLI50:: <i>cna</i> variant derived from UAMS-639
pCna1-iso	Yes (1)	This study	pLI50:: <i>cna</i> variant created from UAMS-639
pCna2-iso	Yes (2)	This study	pLI50:: <i>cna</i> variant created from UAMS-639
pCna3-iso	Yes (3)	This study	pLI50:: <i>cna</i> variant created from UAMS-639

<u>Primer</u>	<u>Sequence (5' to 3')</u>
B1	ggatccacagctccgggttaataaggta
B2	ggatccagggccactcttagctgcttacat
B3	tcgggtttttgattggttttcagtattag
B4	aaacccaatcaaaaaaacccgaataaaccaatc
Cna 1555	gatcagattcaaggtggacagc
Cna 2237	ctgctcaaaagggttgggaagg

Figure 1.

Schematic diagram of each of the four chosen natural *cna* genes with their respective sizes. The 1B *cna* gene was amplified from UAMS-1, the 2B *cna* gene was amplified from Phillips, the 3B *cna* variant was amplified from FDA-574, and the 4B *cna* gene was amplified from UAMS-639. The individual domains are as follows: p=promoter, A=A domain or collagen binding domain, B=B domain or repetitive sequence, W=wall spanning domain, M=membrane spanning domain, and C=cytoplasmic tail.

p	A	B1	W	M	C
---	---	----	---	---	---

UAMS-1

≈ 3,000 base pairs

p	A	B1	B2	W	M	C
---	---	----	----	---	---	---

Phillips

≈ 3,500 base pairs

p	A	B1	B2	B3	W	M	C
---	---	----	----	----	---	---	---

FDA-574

≈ 4,000 base pairs

p	A	B1	B2	B3	B4	W	M	C
---	---	----	----	----	----	---	---	---

UAMS-639

≈ 4,500 base pairs

Figure 2.

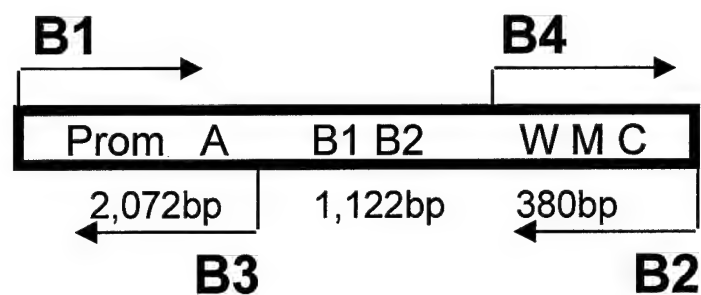
The creation of the 0B *cna* variant from the 2B Phillips' gene.

Figure 2a is a schematic outlining the location of the primers used in relationship to the chromosomal gene.

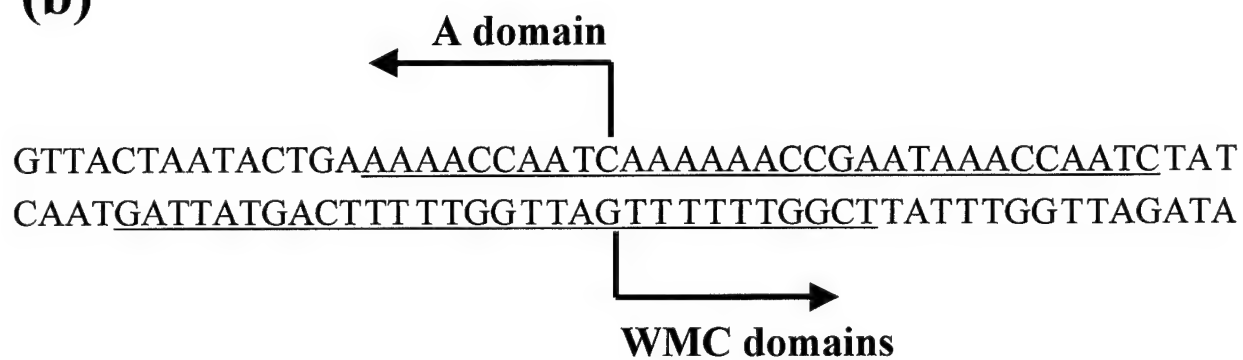
Figure 2b diagrams the engineered cohesive ends found in the B3 and B4 primers (underlined) and their location with respect to the newly created 0B *cna* gene.

Figure 2c represents the amplified DNA fragments used to create the 0B variant as well as the p2.1TOPO::*cna* construct. Lane 1 shows the B2-B4 (WMC domains) fragment and lane 2 shows the B1-B3 (promoter and A domain) fragment prior to final construction. Lane 3 contains the 1Kb marker. Lane 4 shows the p2.1TOPO::0B *cna* construct digested with *Sac*I and *Xba*I, liberating the approximate 2.5Kb 0B *cna* variant from the 3.9Kb vector.

(a)



(b)



(c)

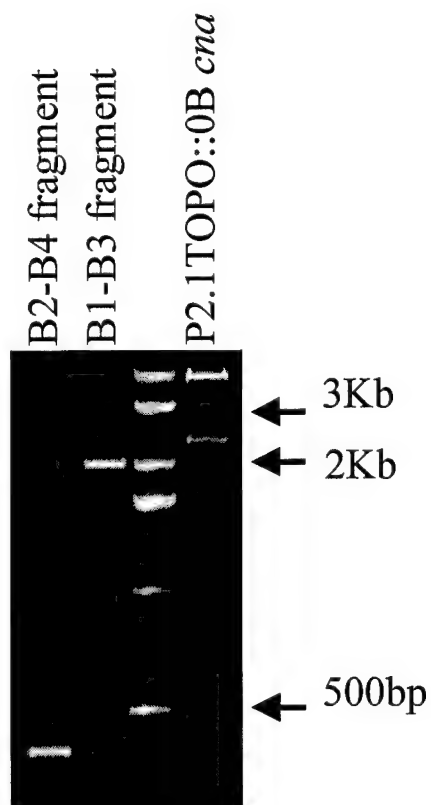


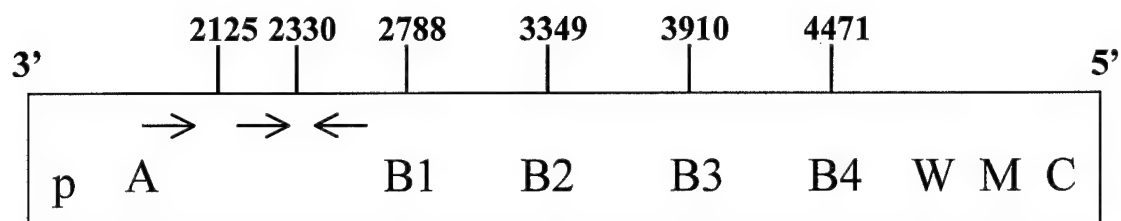
Figure 3.

The construction of the isogenic *cna* variants from the UAMS-639 parent strain.

Figure 3a is a diagram outlining the locations of the *AccI* sites with respect to the UAMS-639 gene. Figure 3a also shows the approximate location of the 3' primers (*cna* 1555 and *cna* 2237) and the location of the 5' B3 primer used to verify that the two *AccI* sites located within the A domain were not altered in the creation of the isogenic *cna* variants. The individual domains are as follows: p=promoter, A=A domain or collagen binding domain, B=B domain or repetitive sequence, W=wall spanning domain, M=membrane spanning domain, and C=cytoplasmic tail.

Figure 3b shows the *SacI* and *XbaI* digest of the isogenic *cna* variants in the pLI50 *S. aureus* shuttle vector.

(a)



(b)

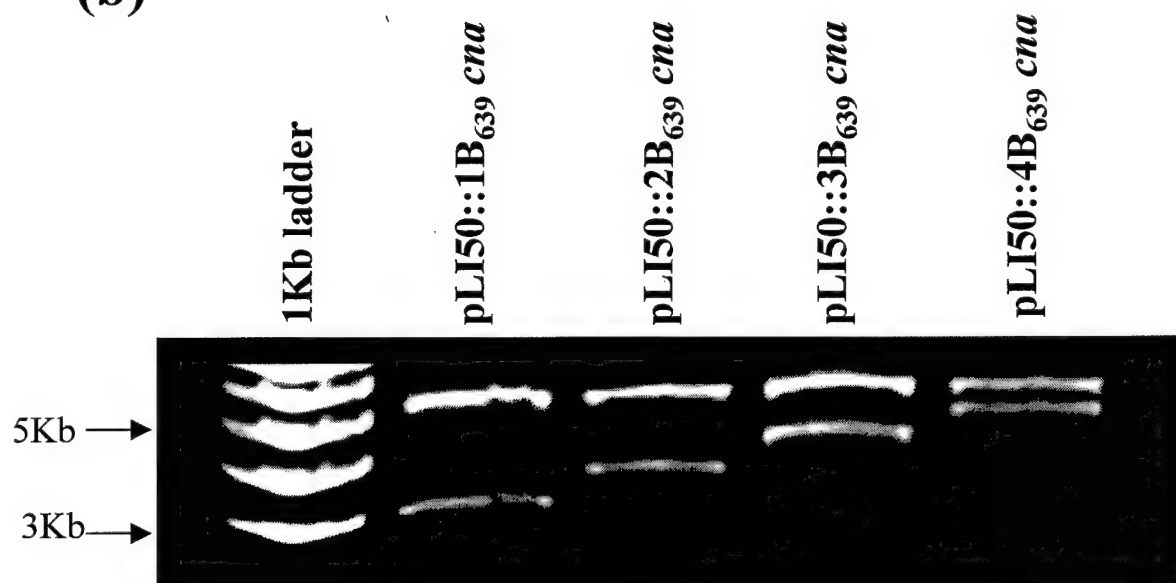


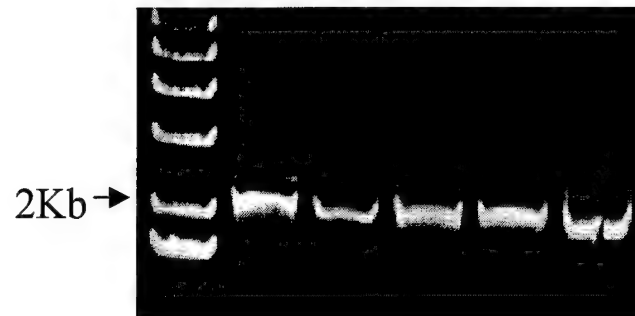
Figure 4.
Toxicity of the pLI50::*cna* construct in *E. coli*.

Figure 4a shows the results from *SacI/XbaI* digest of plasmids extracted from *E. coli* grown at 37° on TSA (top picture) and a *SacI/XbaI* digest of plasmids extracted from *E. coli* grown at 30° on 1/2 LB agar (bottom picture).

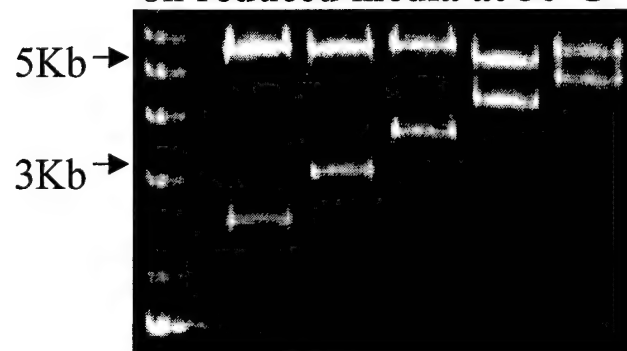
Figure 4b represents the frequency of isolating intact pLI50::*cna* constructs from transformants grown on different media at varying temperatures.

(a)

SacI/XbaI cut plasmids grown
on enriched media at 37°C



SacI/XbaI cut plasmids grown
on reduced media at 30°C



(b)

Growth
Conditions

Frequency of
Vector + Insert

TSA @ 37°

1/250+

TSA @ 30°

0/124

LB @ 30°

0/212

1/2 LB @ 30°

8/120

M9 @ 30°

5/45

Figure 5.
Northern slot blot and Western analysis of UAMS-128 comparing the
pLI50::0B_{Phillips} *cna* variant with its pLI50::2B_{Phillips} *cna* parent

Figure 5a depicts the Northern slot blot performed with mRNA extracted from the UAMS-128 parent (lane 1), UAMS-128 containing the pLI50::0B *cna* construct (lane 2), and UAMS-128 containing the pLI50::2B *cna* construct (lane 3). The amounts of total RNA (in μg) loaded in each slot and relative amounts of *cna* mRNA illuminated via a digoxigenin-labeled *cna* probe as shown. 5 μg of rRNA was used as a control and probed with digoxigenin-labeled rRNA DNA probe.

Figure 5b shows a Western blot (top picture) and SDS-PAGE control (bottom picture) performed using 25 μg of total cellular proteins in each extracted from the UAMS-128 parent (lane 2), UAMS-128 containing the pLI50::0B *cna* construct (lane 3), and UAMS-128 containing the pLI50::2B *cna* construct (lane 4). Cellular proteins used in the Western blot were blotted with anti-Cna antibody. The blot and gel shown were loaded with equal amounts of protein and ran simultaneously.

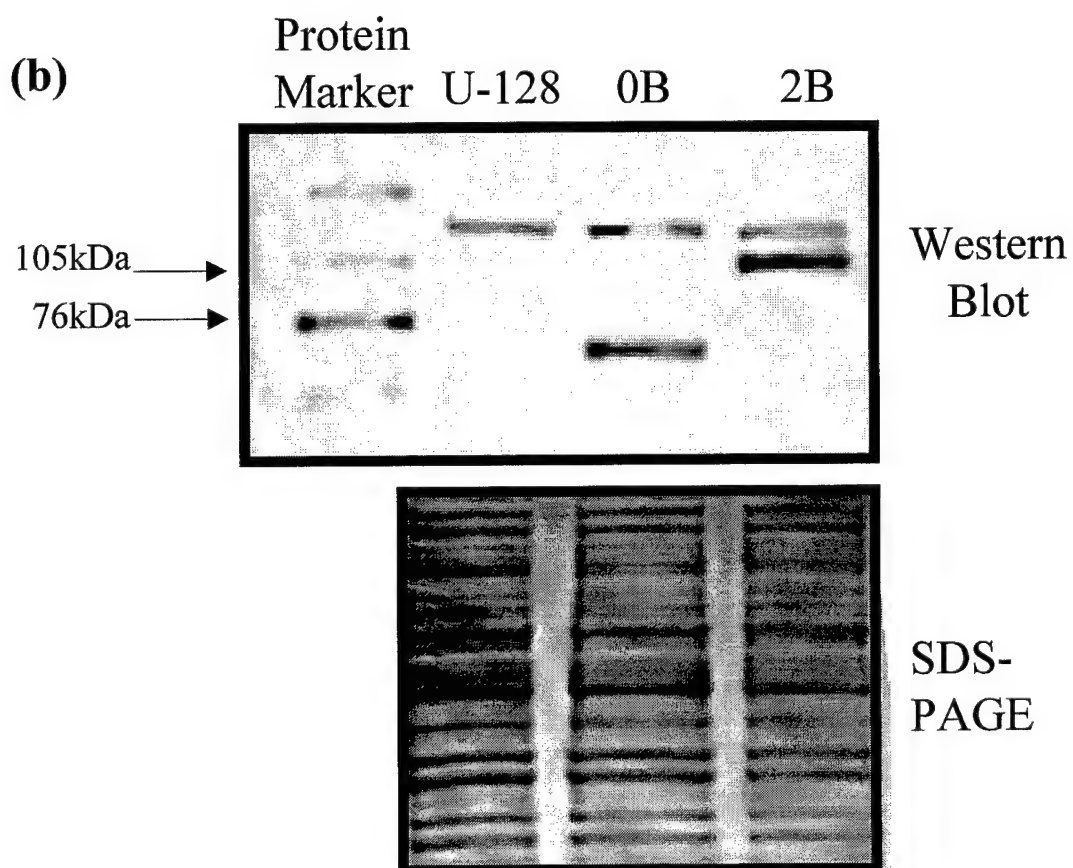
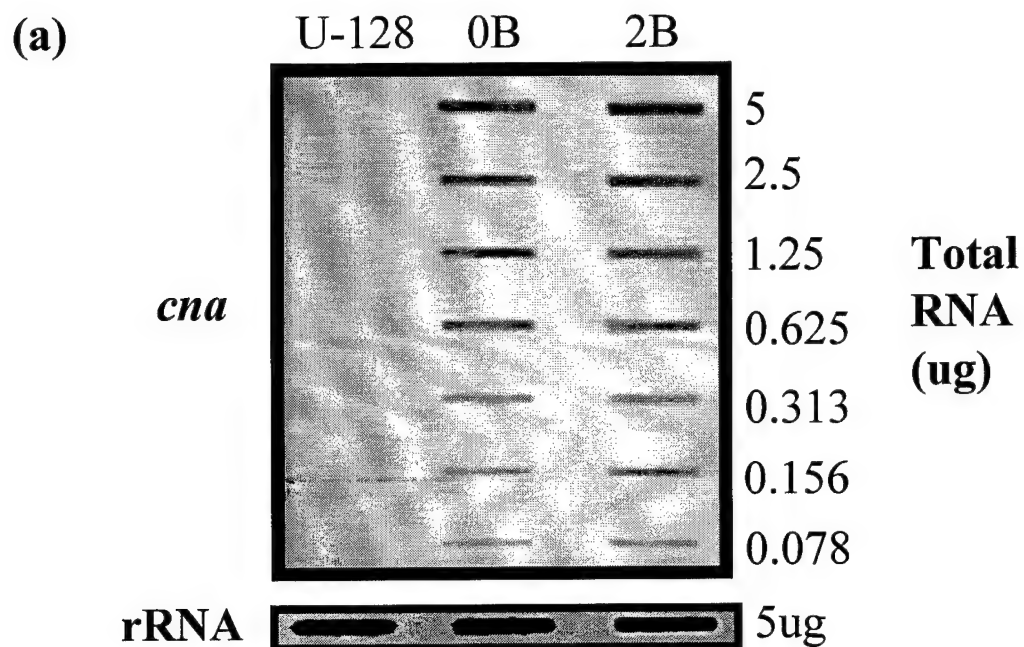


Figure 6.
Determination of surfaced expressed Cna by flow cytometry comparing the
pLI50::0B_{Phillips} *cna* variant with its pLI50::2B_{Phillips} *cna* parent

The mean fluorescent intensity (MFI) measured from three separate Cna-negative parent strains, each parent with the pLI50::0B *cna* variant, and each parent with the pLI50::2B *cna* variant as shown. Bacteria from an overnight TSB culture were standardized to an OD A₅₆₀ of 0.05 and subcultured to 20 ml TSB with chloramphenicol (10 µg/ml), where applicable. At approximately 4 hours, cells were harvested and standardized to approximately 10⁸ c.f.u. Once standardized, cells were resuspended in 100 mM NaPO₄ buffer containing 0.1% BSA and 0.1% Tween 20, pH 7.5. To minimize nonspecific binding of protein A, 27 µg of purified human Fc was added to cells and incubated with end-over-end rocking for 30 minutes. Cells were then pelleted at 9,300 × g at 4° C, the supernatant discarded, and then resuspended in 100 mM NaPO₄ buffer containing 0.1% BSA and 0.1% Tween 20, pH 7.5. Surface-bound Cna was detected using rabbit anti-Cna polyclonal antibody in conjunction with FITC-conjugated goat anti-rabbit IgG Fab₂ fragments. Data represents the average of two separate assays, each measuring 10,000 cells. The error bars designate the average standard deviation as calculated from the two separate assays.

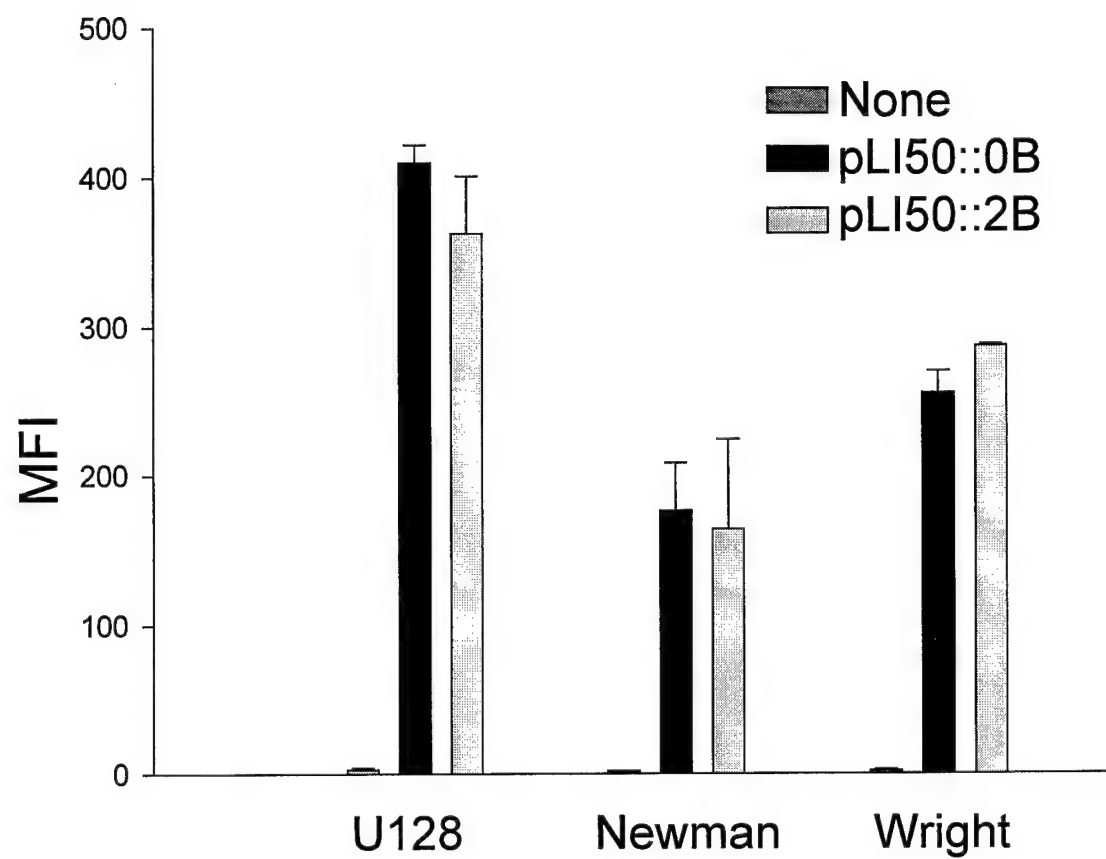
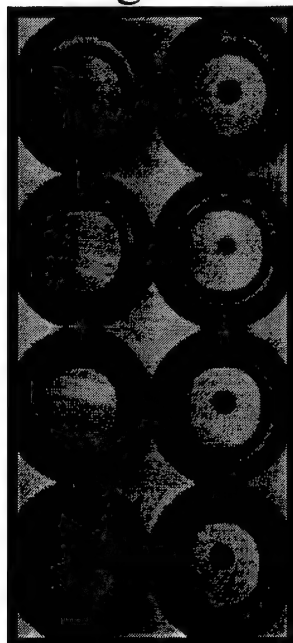


Figure 7.
Qualitative collagen binding assay of UAMS-128 comparing the
pLI50::0B_{Phillips} *cna* variant with its pLI50::2B_{Phillips} *cna* parent.

Picture represents a section of a 96-well microtiter plate in which column 1 was precoated with 20 µg of type I collagen and column 2 was precoated with 2% BSA in PBS. After overnight incubation, the wells were emptied and 200 µl of bacteria were added. After a 1 hour incubation with the *cna*-negative UAMS-128, *cna*-positive UAMS-1, and UAMS-128 containing the pLI50::0B and pLI50::2B constructs, the plate was centrifuged at 650 × g for 10 minutes. Bacteria that express functional Cna fail to form a pellet, binding to the collagen-coated wells.

Amount of collagen/well

20ug None



UAMS-128

UAMS-1

U128 (pLI50::0B_{Phillips} *cna*)

U128 (pLI50::2B_{Phillips} *cna*)

Figure 8.

¹²⁵I-labeled collagen binding assays comparing the pLI50::0B_{Phillips} *cna* variant with the pLI50::2B_{Phillips} *cna* variant in the UAMS-128 strain

UAMS-128, Newman, and Wright strains with the 0B and 2B variants were harvested from an overnight TSB culture, standardized to an OD A₅₆₀ of 0.05, and subcultured to 20 ml of TSB with chloramphenicol (10 µg/ml), where applicable. After approximately 4 hours, cells were harvested, standardized to an OD A₅₆₀ of 1.0, and pelleted. Once standardized, cells were resuspended in 100 mM NaPO₄ buffer containing 0.1% BSA and 0.1% Tween 20, pH 7.5. The 1.0 ml aliquot of standardized cell suspension was transferred to a microcentrifuge tube followed by the addition of 10⁵ dpm of ¹²⁵I-labeled type I collagen. Cells were incubated at RT with end-over-end mixing for 1 hour, pelleted at 15,000 × g for 10 minutes and the supernatant removed. Samples were recentrifuged and the remaining supernatant removed. The radioactivity retained in the pellet was measured in a BIOSCAN QC2000 gamma counter. All assays were done twice with duplicate samples each time and reported as an average with error bars representing the average standard deviation.

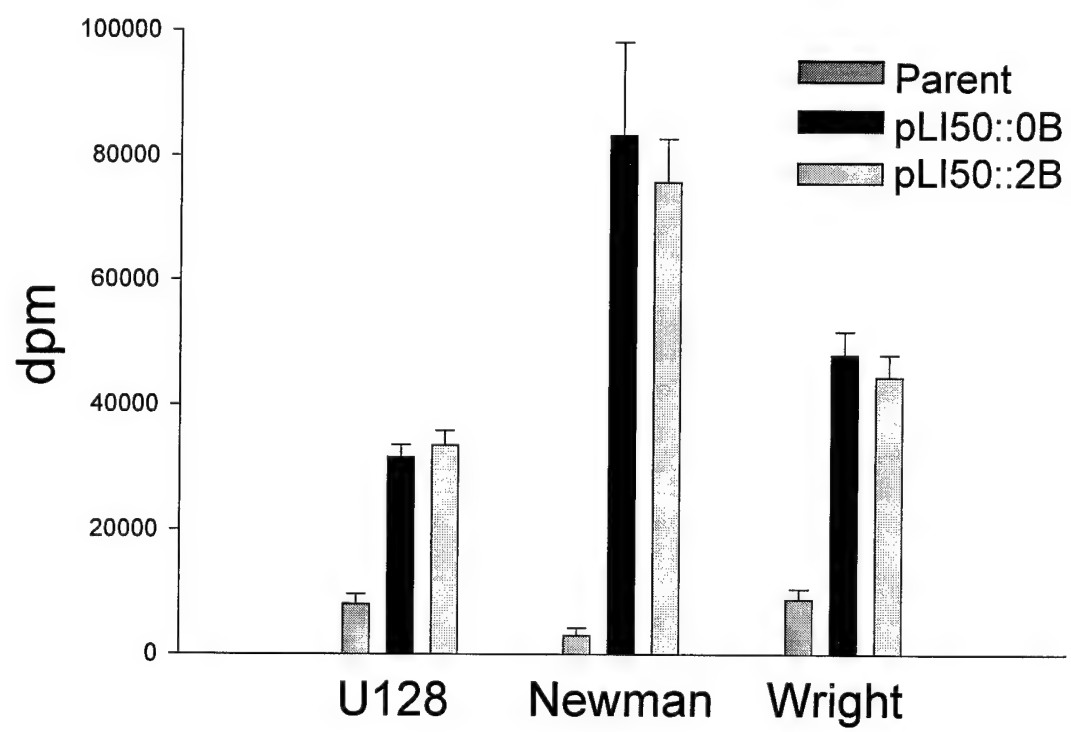


Figure 9.

Northern slot blot and Western analysis of UAMS-128 comparing the pLI50::*cna*_{UAMS-1} (1B), pLI50::*cna*_{Phillips} (2B), pLI50::*cna*_{FDA-574} (3B), and pLI50::*cna*_{UAMS-639} (4B) variants

Figure 9a shows a Northern slot blot performed with mRNA extracted from the UAMS-128 containing the pLI50::*cna*_{UAMS-1} construct (lane 1B), UAMS-128 containing the pLI50::*cna*_{Phillips} construct (lane 2B), UAMS-128 containing the pLI50::*cna*_{FDA-574} construct (lane 3B), UAMS-128 containing the pLI50::*cna*_{UAMS-639} construct (lane 4B), and the parent UAMS-128 strain. The amounts of total RNA (in µg) were loaded in each slot and relative amounts of *cna* mRNA illuminated via a digoxigenin-labeled *cna* probe. 5 µg of rRNA was used as a control and probed with digoxigenin-labeled rRNA DNA probe as shown.

Figure 9b shows a Western blot (top picture) and SDS-PAGE control (bottom picture) performed using 25µg of total cellular proteins extracted from the UAMS-128 parent (lane 2), UAMS-128 containing the pLI50::*cna*_{UAMS-1} construct (lane 3), UAMS-128 containing the pLI50::*cna*_{Phillips} construct (lane 4), UAMS-128 containing the pLI50::*cna*_{FDA-574} construct (lane 5), and UAMS-128 containing the pLI50::*cna*_{UAMS-639} construct (lane 6). Protein was loaded and run as described in figure 5b.

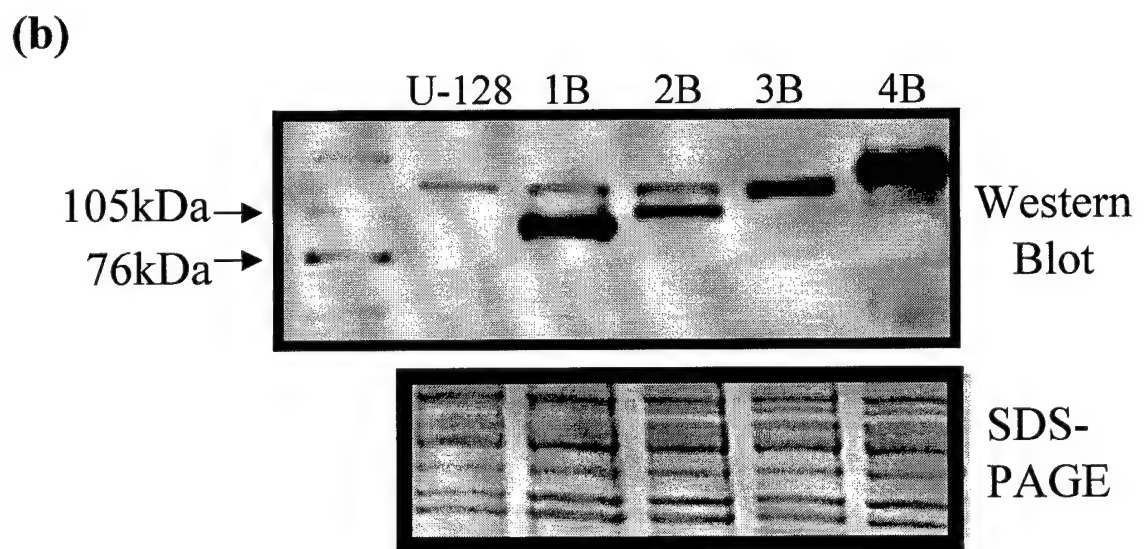
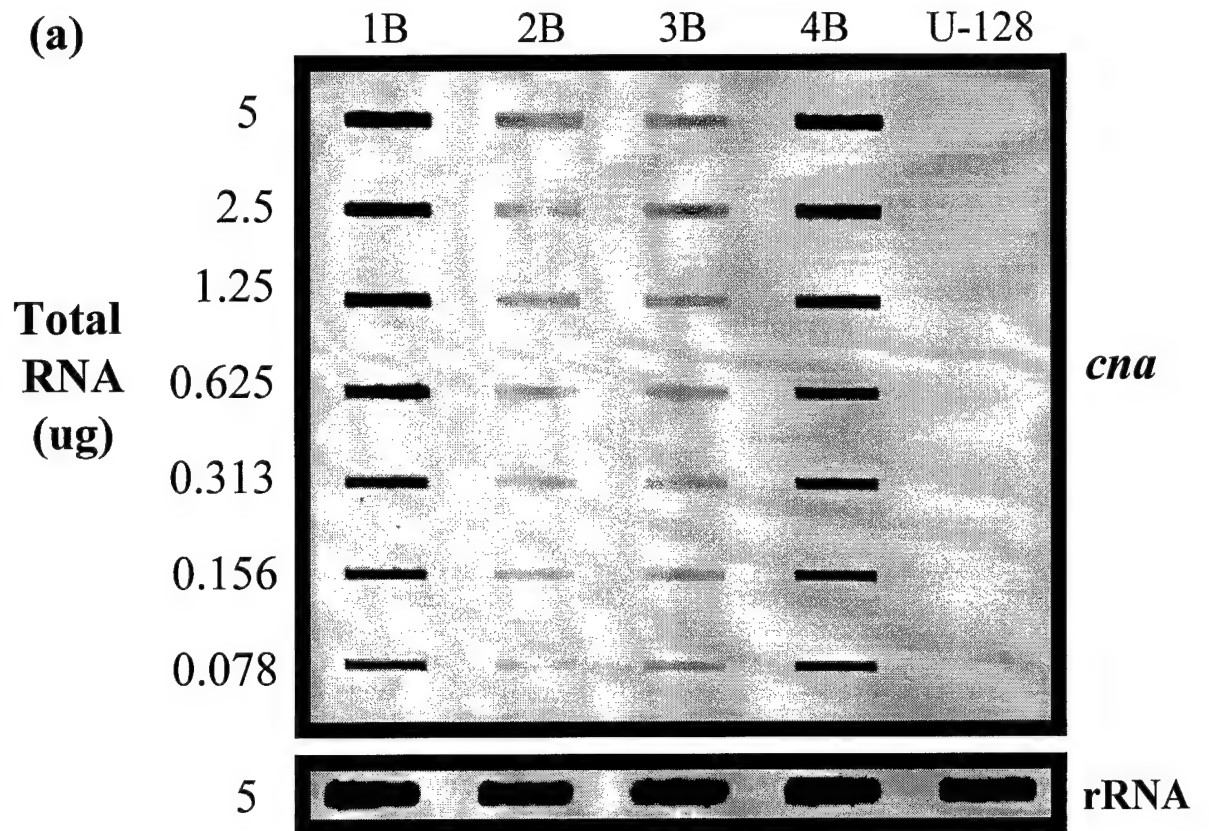


Figure 10.

Determination of surfaced expressed Cna of UAMS-128 by flow cytometry comparing the pLI50::*cna*_{UAMS-1} (1B), pLI50::*cna*_{Phillips} (2B), pLI50::*cna*_{FDA-574} (3B), and pLI50::*cna*_{UAMS-639} (4B) variants

Mean fluorescent intensity (MFI) measured from the Cna-negative UAMS-128 strain and UAMS-128 containing the natural *cna* constructs were performed as described in figure 6.

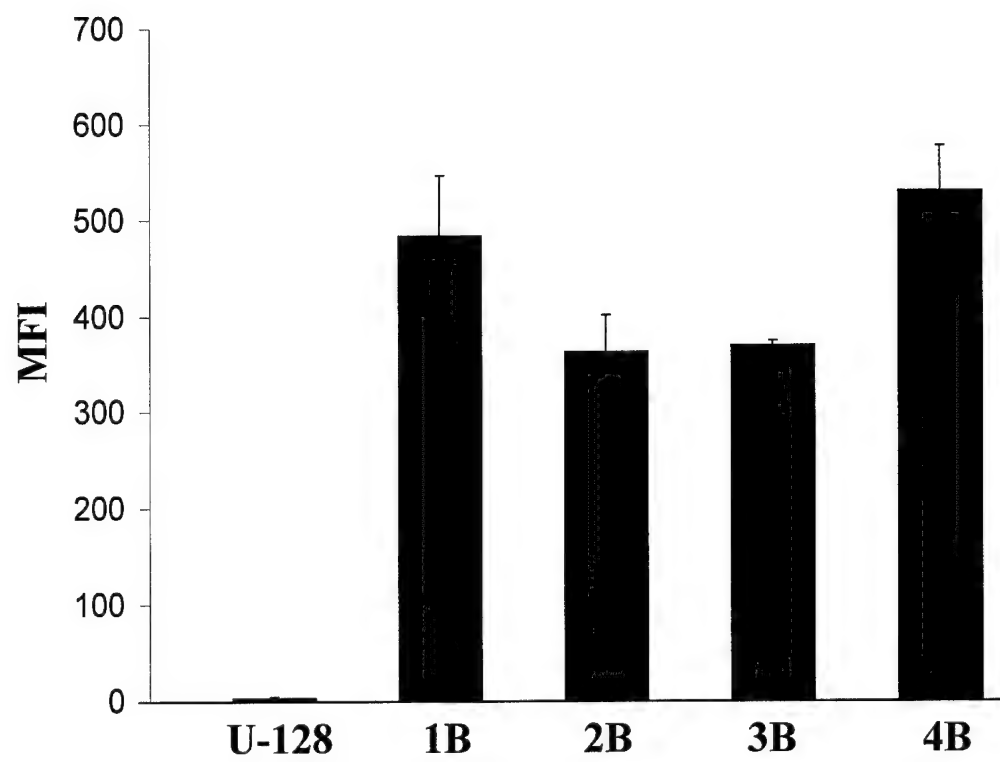
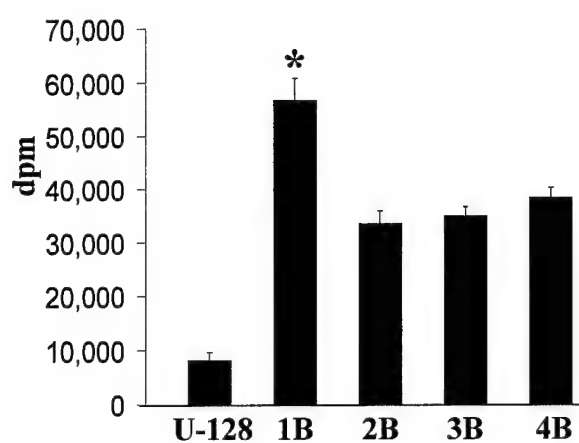


Figure 11.

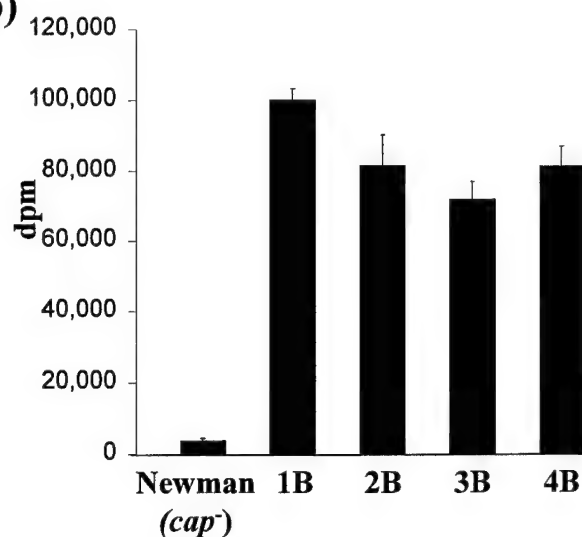
¹²⁵I-labeled collagen binding assays of 5 unencapsulated/microencapsulated strains comparing the pLI50::*cna*_{UAMS-1} (1B), pLI50::*cna*_{Phillips} (2B), pLI50::*cna*_{FDA-574} (3B), and pLI50::*cna*_{UAMS-639} (4B) variants

Collagen binding analysis was conducted using strains UAMS-128 (Fig 11a), Newman *cap* (Fig 11b), Newman (Fig 11c), Smith Compact (Fig 11d), and Wright (Fig 11e) strains. Each strain possessed the pLI50::*cna*_{UAMS-1} (1B), pLI50::*cna*_{Phillips} (2B), pLI50::*cna*_{FDA-574} (3B), and pLI50::*cna*_{UAMS-639} (4B) variants. This assay was performed as described in figure 8.

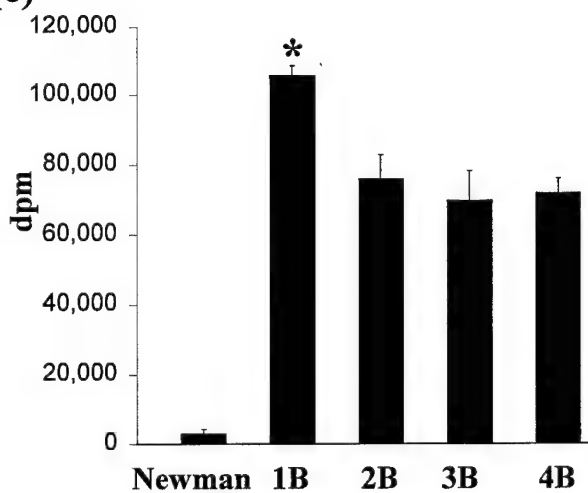
(a)



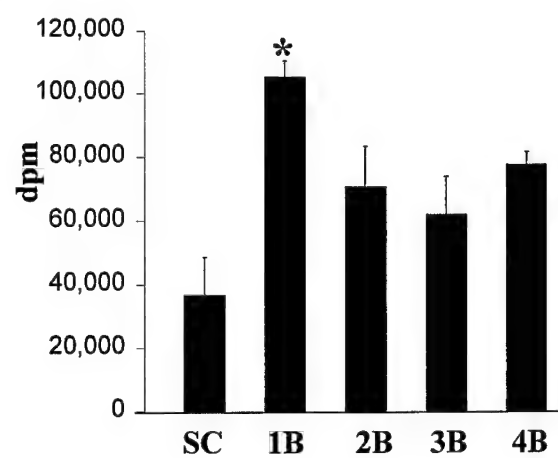
(b)



(c)



(d)



(e)

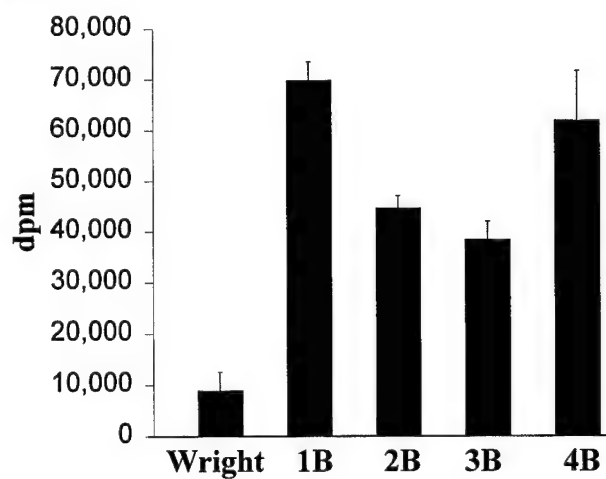
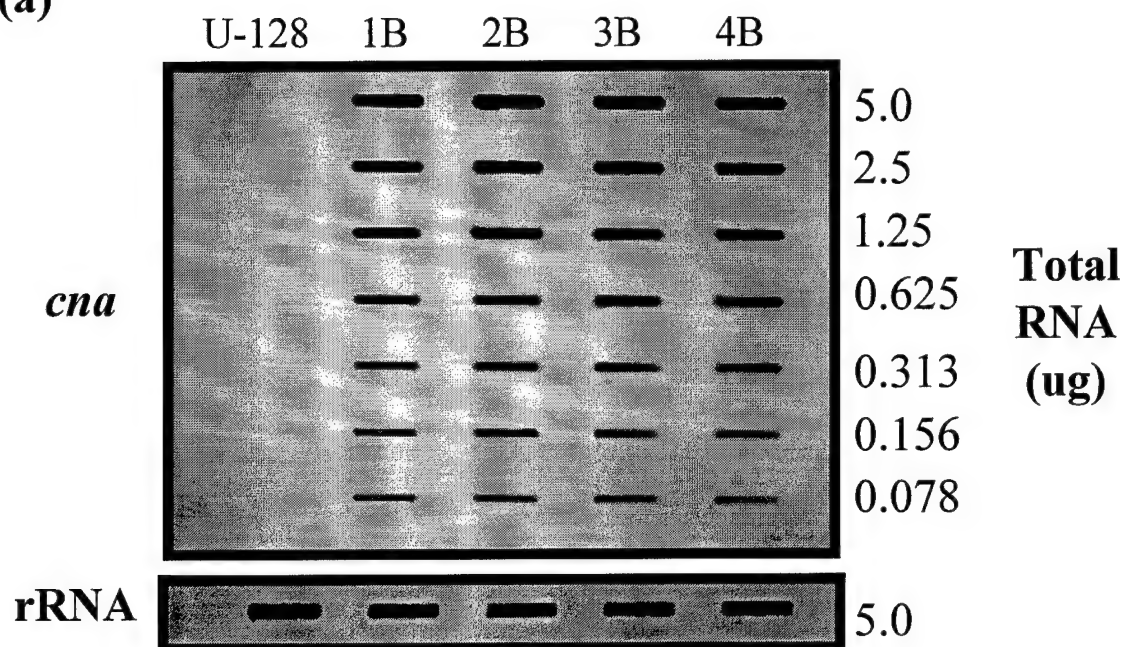


Figure 12.
Northern slot blot and Western analysis of UAMS-128 comparing the isogenic
pLI50::*cna*_{UAMS-639} (1B), pLI50::*cna*_{UAMS-639} (2B), pLI50::*cna*_{UAMS-639} (3B), and
pLI50::*cna*_{UAMS-639} (4B) variants

Figure 12a shows a Northern slot blot performed with mRNA extracted from the parent UAMS-128 strain (lane 1), the pLI50::*cna*_{UAMS-639} (1B) construct (lane 2), UAMS-128 containing the pLI50::*cna*_{UAMS-639} (2B) construct (lane 3), UAMS-128 containing the pLI50::*cna*_{UAMS-639} (3B) construct (lane 4), and UAMS-128 containing the pLI50::*cna*_{UAMS-639} (4B) construct (lane 5). The amounts of total RNA (in µg) were loaded in each slot and relative amounts of *cna* mRNA illuminated via a digoxigenin-labeled *cna* probe as shown. 5 µg of rRNA was used as a control and probed with digoxigenin-labeled rRNA DNA probe.

Figure 12b shows a Western blot (top picture) and SDS-PAGE control (bottom picture) performed using 25µg of total cellular proteins extracted from the UAMS-128 parent (lane 2), the pLI50::*cna*_{UAMS-639} (1B) construct (lane 3), UAMS-128 containing the pLI50::*cna*_{UAMS-639} (2B) construct (lane 4), UAMS-128 containing the pLI50::*cna*_{UAMS-639} (3B) construct (lane 5), and UAMS-128 containing the pLI50::*cna*_{UAMS-639} (4B) construct (lane 6). Protein was loaded and run as described in figure 5b.

(a)



(b)

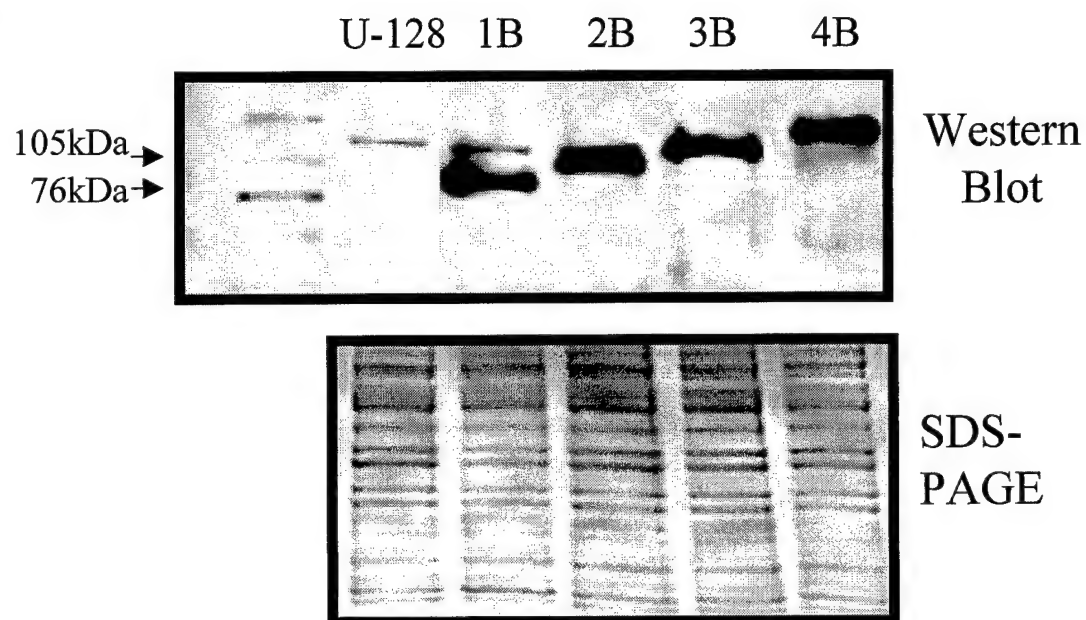


Figure 13.

Determination of surfaced expressed Cna of UAMS-128 by flow cytometry comparing the isogenic pLI50::*cna*_{UAMS-639} (1B), pLI50::*cna*_{UAMS-639} (2B), pLI50::*cna*_{UAMS-639} (3B), and pLI50::*cna*_{UAMS-639} (4B) variants

The mean fluorescent intensity (MFI) measured from the Cna-negative UAMS-128 strain and UAMS-128 containing the isogenic *cna* constructs are shown. This assay was performed as outlined in figure 6.

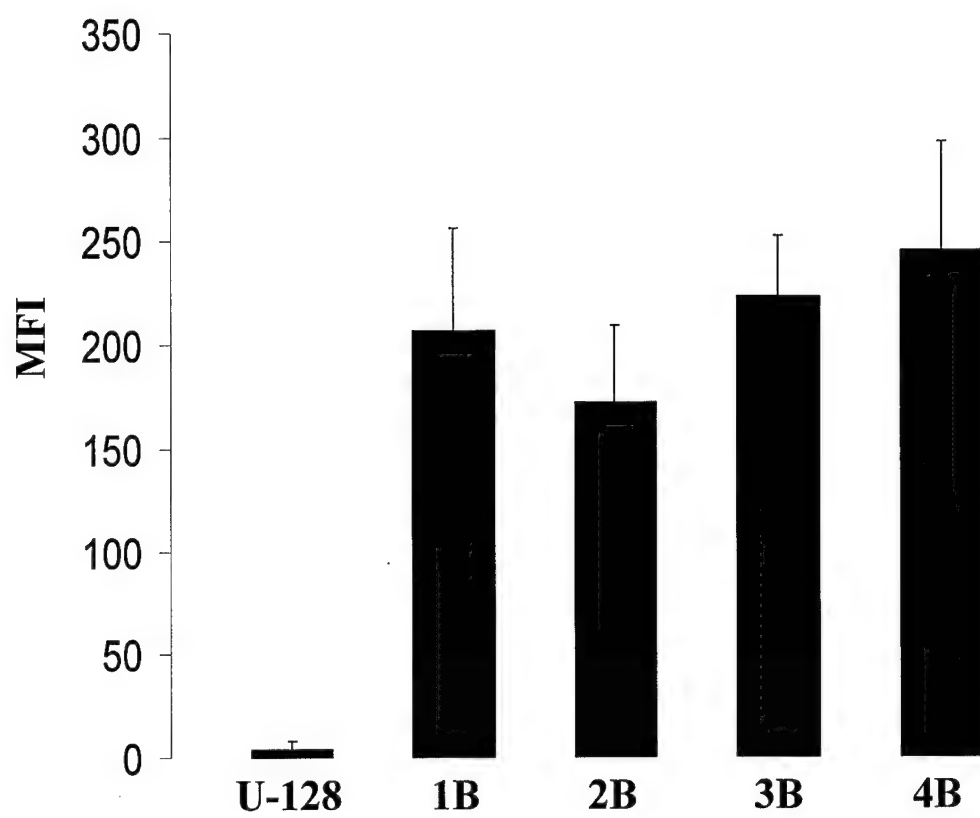


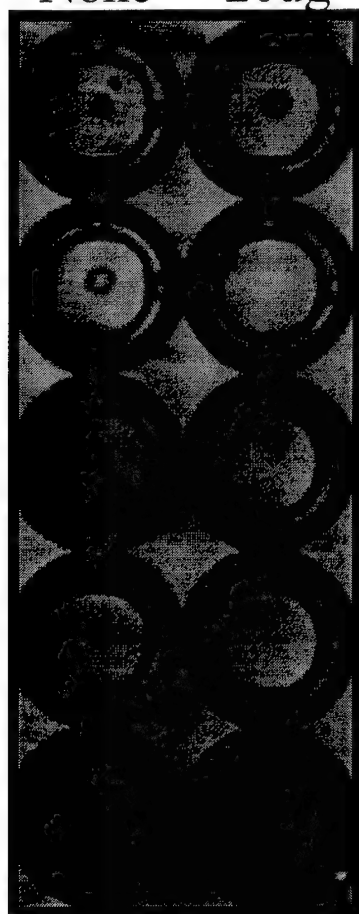
Figure 14.

Qualitative collagen binding assay of UAMS-128 comparing the isogenic pLI50::*cna*_{UAMS-639} (1B), pLI50::*cna*_{UAMS-639} (2B), pLI50::*cna*_{UAMS-639} (3B), and pLI50::*cna*_{UAMS-639} (4B)

Picture represents a section of a 96-well microtiter plate in which column 1 was precoated with 20µg of type I collagen and column 2 was precoated with 2% BSA in PBS. After overnight incubation, the wells were emptied and 200ul of bacteria were added. After a 1 hour incubation with the *cna*-negative UAMS-128 and UAMS-128 containing the isogenic *cna* constructs, the plate was centrifuged at $650 \times g$ for 10 minutes. Bacteria that express functional Cna fail to form a pellet, binding to the collagen-coated wells.

Amount of collagen/well

None 20ug



UAMS-128

U128 (pLI50::1B₆₃₉ *cna*)

U128 (pLI50::2B₆₃₉ *cna*)

U128 (pLI50::3B₆₃₉ *cna*)

U128 (pLI50::4B₆₃₉ *cna*)

Figure 15.

¹²⁵I-labeled collagen binding assays of UAMS-128 comparing the isogenic pLI50::*cna*_{UAMS-639} (1B), pLI50::*cna*_{UAMS-639} (2B), pLI50::*cna*_{UAMS-639} (3B), and pLI50::*cna*_{UAMS-639} (4B) variants

Collagen binding analysis was conducted of strain UAMS-128 possessing the isogenic *cna* variants as described in figure 8.

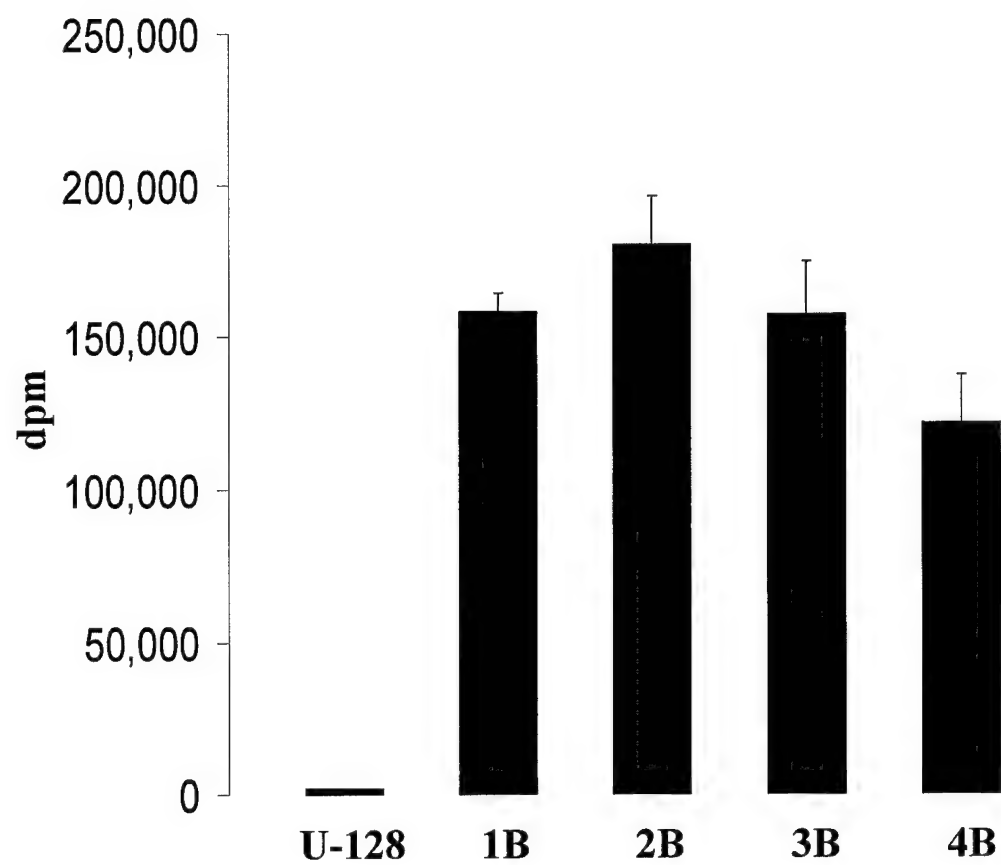


Figure 16.

Combined ^{125}I -labeled collagen binding capability of multiple strains comparing the isogenic pLI50::*cna*_{UAMS-639} (1B), pLI50::*cna*_{UAMS-639} (2B), pLI50::*cna*_{UAMS-639} (3B), and pLI50::*cna*_{UAMS-639} (4B) variants

The collagen binding data obtained from 7 strains (U-128, Newman, Wright, Smith Compact, Smith Diffuse, M variant, and M) were combined. All strains were assayed two times using duplicate samples and an additional assay of strain Wright grown on Columbia agar is included in the data summary to provide a total of 30 data points. Briefly, cells were harvested from an overnight TSB culture except Wright grown on Columbia agar (which was harvested from a plate). The bacteria were then standardized to an OD A_{560} of 0.05 and subcultured to 20 ml of TSB with chloramphenicol (10 $\mu\text{g/ml}$), where applicable. After approximately 4 hours, cells were harvested, standardized to an OD A_{560} of 1.0, and pelleted. Once standardized, cells were resuspended in 100 mM NaPO_4 buffer containing 0.1% BSA and 0.1% Tween 20, pH 7.5. The 1.0 ml aliquot of standardized cell suspension was transferred to a microcentrifuge tube followed by the addition of 10^5 dpm of ^{125}I -labeled type I collagen. Cells were incubated at RT with end-over-end mixing for 1 hour, pelleted at $15,000 \times g$ for 10 minutes and the supernatant removed. Samples were recentrifuged and the remaining supernatant removed. The radioactivity retained in the pellet was measured in a BIOSCAN QC2000 gamma counter. All assays were done in duplicate and reported as an average with error bars representing the average standard deviation.

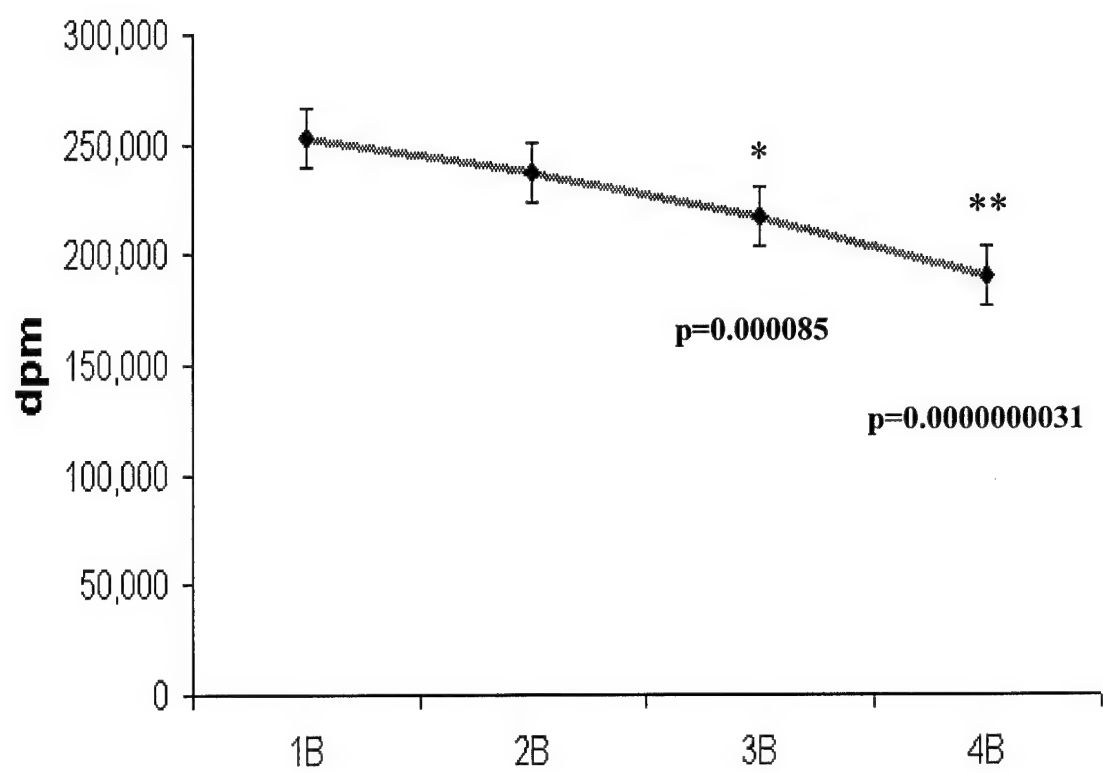


Figure 17.

125 I-labeled collagen binding capability of microencapsulated strain Newman and Newman *cap*⁻ comparing the pLI50::*cna*_{UAMS-1} (1B), pLI50::*cna*_{Phillips} (2B), pLI50::*cna*_{FDA-574} (3B), and pLI50::*cna*_{UAMS-639} (4B) variants

Figure 17a represents the collagen binding capability of the natural *cna* variants in strains Newman and Newman (*cap*⁻). Briefly, cells were harvested from an overnight TSB culture, standardized to an OD A_{560} of 0.05, and subcultured to 20 ml of TSB with chloramphenicol (10 μ g/ml), where applicable. After approximately 4 hours, cells were harvested, standardized to an OD A_{560} of 1.0, and pelleted. Once standardized, cells were resuspended in 100 mM NaPO₄ buffer containing 0.1% BSA and 0.1% Tween 20, pH 7.5. The 1.0 ml aliquot of standardized cell suspension was transferred to a microcentrifuge tube followed by the addition of 10⁵ dpm of 125 I-labeled type I collagen. Cells were incubated at RT with end-over-end mixing for 1 hour, pelleted at 15,000 \times g for 10 minutes and the supernatant removed. Samples were recentrifuged and the remaining supernatant removed. The radioactivity retained in the pellet was measured in a BIOSCAN QC2000 gamma counter. All assays were done in duplicate with two samples per assay and reported as an average. The error bars represent the average standard deviation.

Figure 17b expresses the obtained binding data as a simple ratio of the average Newman binding value divided by the average Newman (*cap*⁻) binding value. A value of 1.0 indicates when the binding of the encapsulated strain approaches its unencapsulated counterpart when the only difference between them is the presence of a capsule in the context of varying B domains.

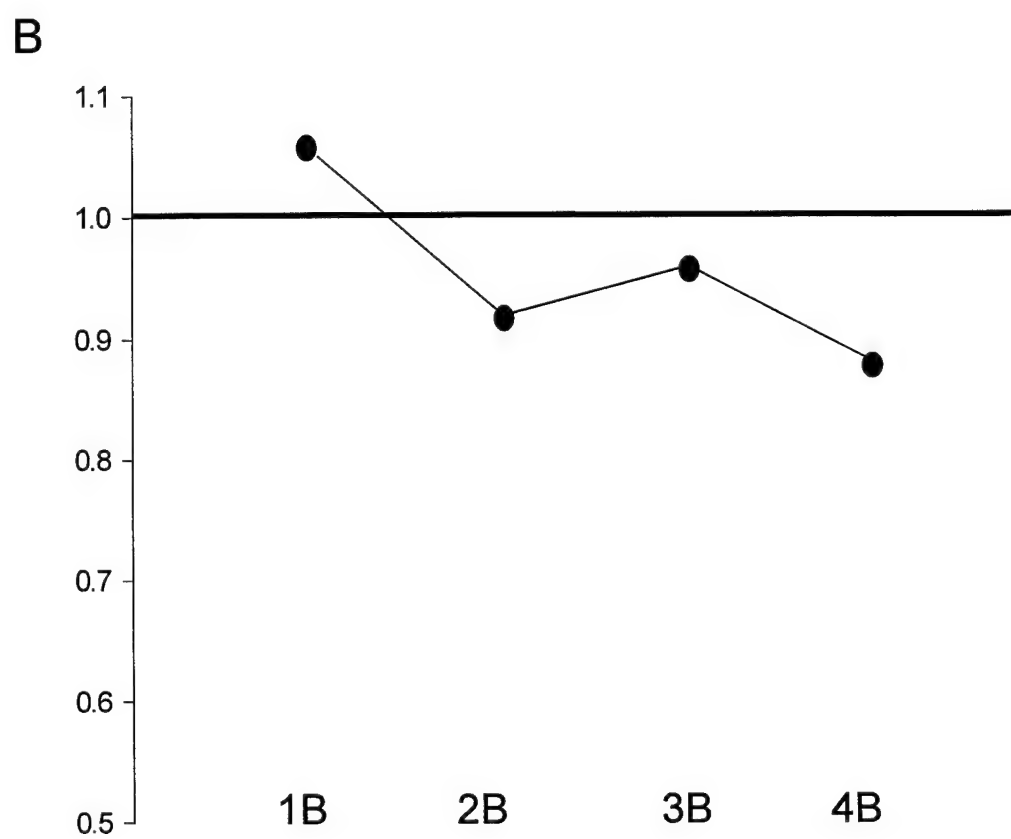
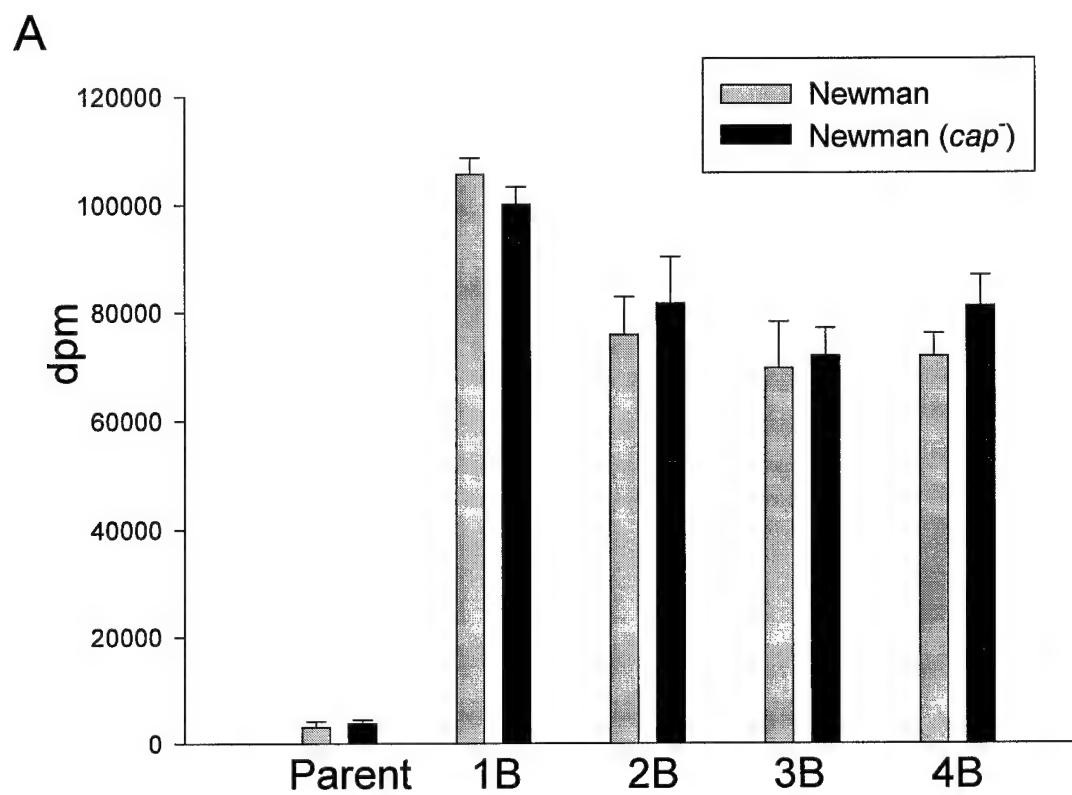


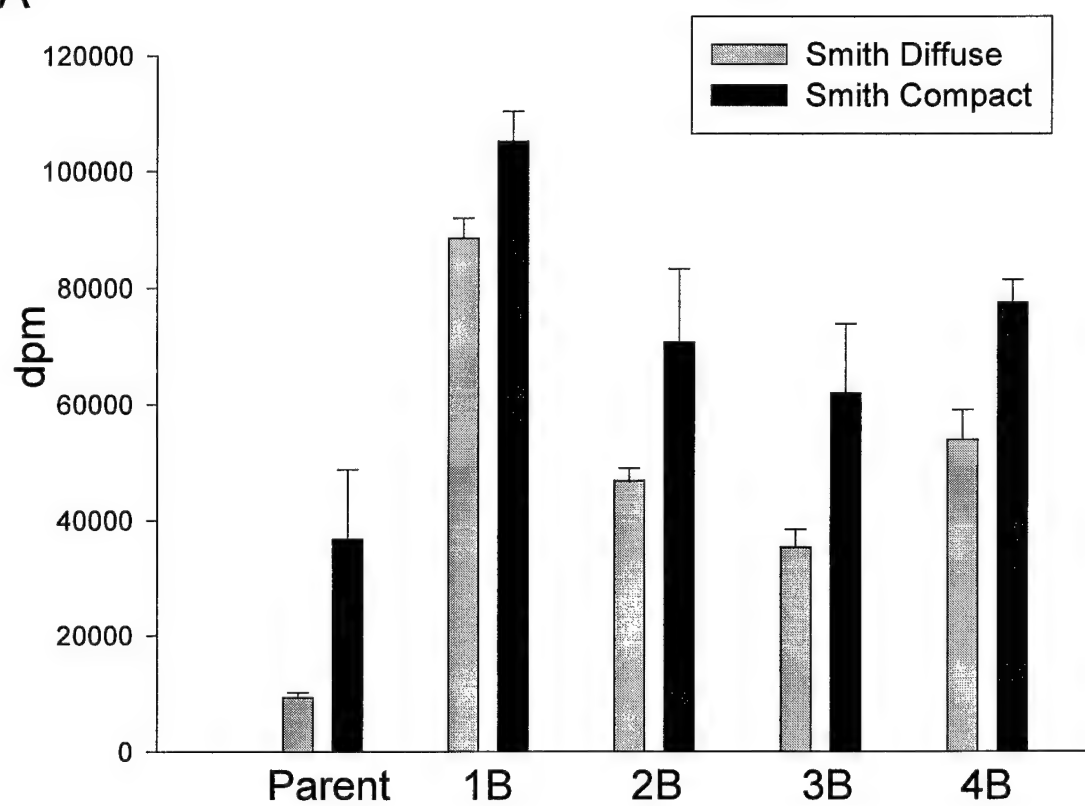
Figure 18.

¹²⁵I-labeled collagen binding capability of heavily-encapsulated strain Smith Diffuse and capsule knockout Smith Compact comparing the pLI50::*cna*_{UAMS-1} (1B), pLI50::*cna*_{Phillips} (2B), pLI50::*cna*_{FDA-574} (3B), and pLI50::*cna*_{UAMS-639} (4B) variants

Figure 18a represents the collagen binding capability of the natural *cna* variants in strains Smith Diffuse and Smith Compact. This assay was performed as outlined in figure 17a.

Figure 18b expresses the obtained binding data as a simple ratio of the average Smith Diffuse binding value divided by the average Smith Compact binding value. A value of 1.0 indicates when the binding of the encapsulated strain approaches its unencapsulated counterpart when the only difference between them is the presence of a capsule in the context of varying B domains.

A



B

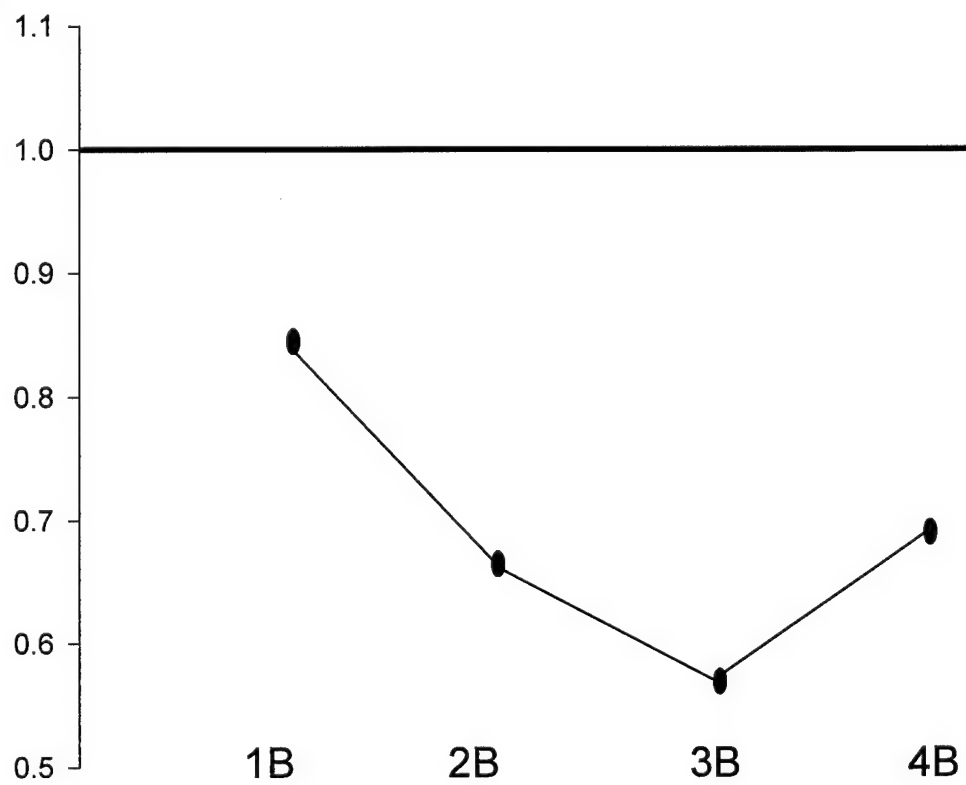


Figure 19.

¹²⁵I-labeled collagen binding capability of microencapsulated strains Newman and Wright comparing the isogenic pLI50::*cna*_{UAMS-639} (1B), pLI50::*cna*_{UAMS-639} (2B), pLI50::*cna*_{UAMS-639} (3B), and pLI50::*cna*_{UAMS-639} (4B) variants

Collagen binding analysis was conducted of strains Newman (Fig 19a) and Wright (Fig 19b) possessing the isogenic *cna* variants. This assay was performed as outlined in figure 8.

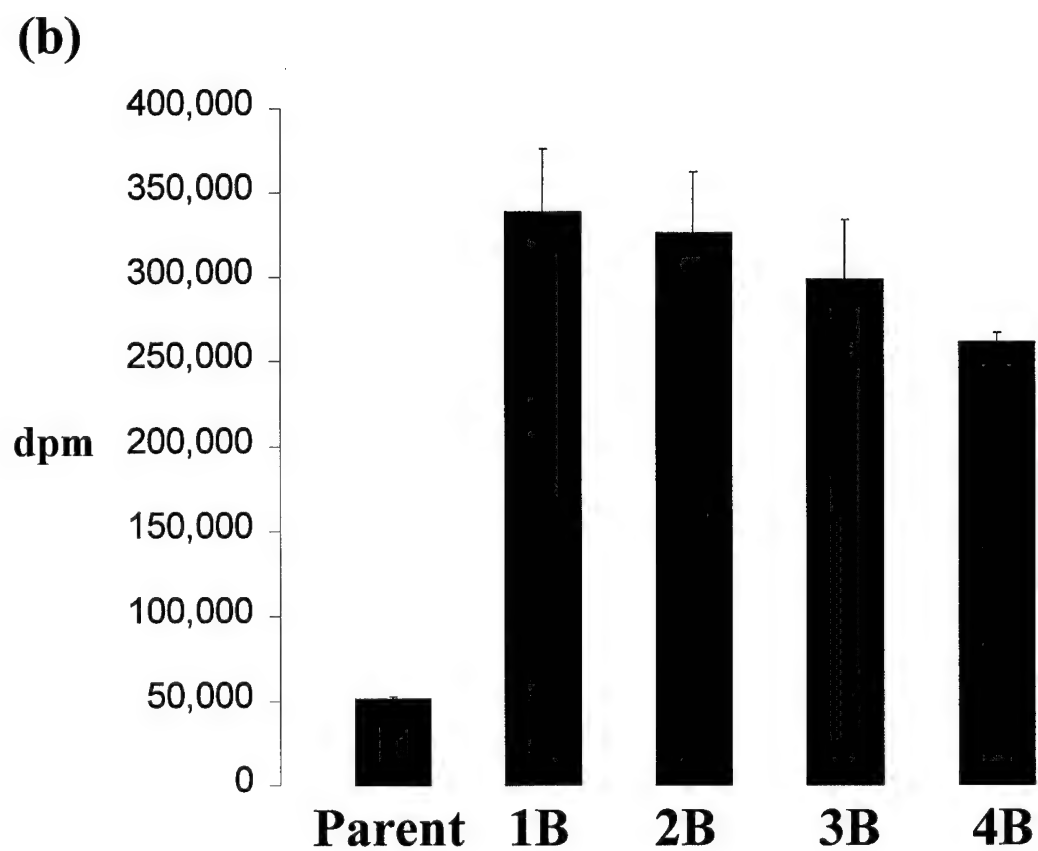
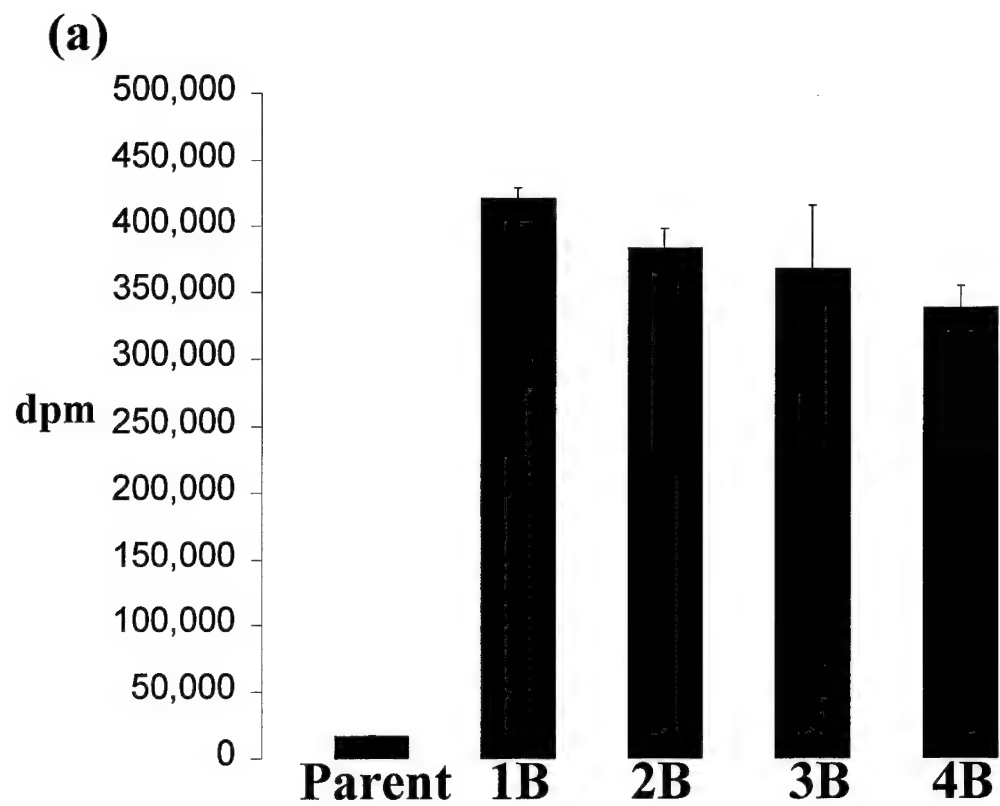
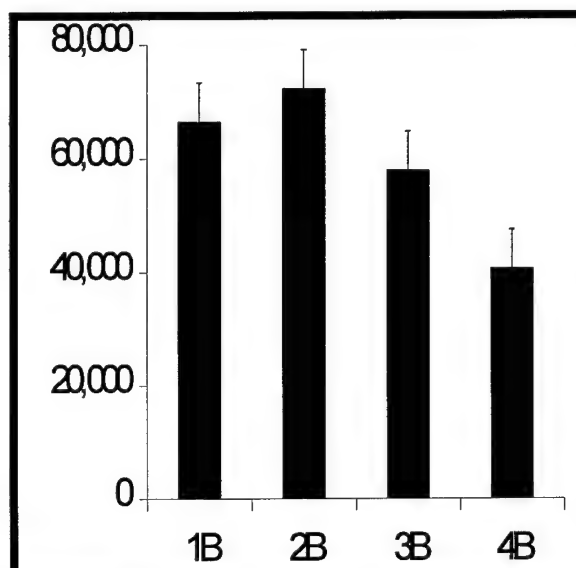


Figure 20.

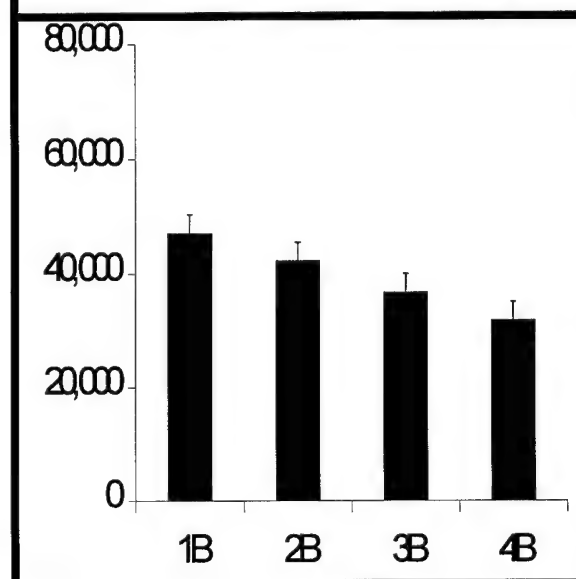
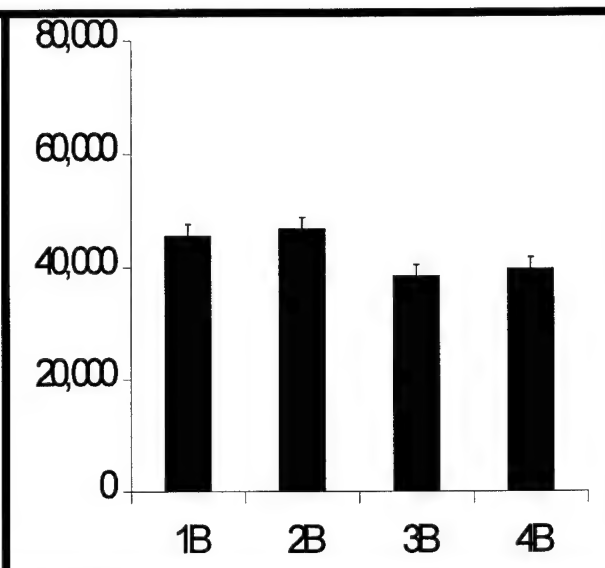
¹²⁵I-labeled collagen binding capability of strain Wright during a 12 hour timecourse study comparing the isogenic pLI50::*cna*_{UAMS-639} (1B), pLI50::*cna*_{UAMS-639} (2B), pLI50::*cna*_{UAMS-639} (3B), and pLI50::*cna*_{UAMS-639} (4B) variants

Collagen binding analysis was conducted of strain Wright possessing the isogenic *cna* variants. Briefly, cells were harvested from an overnight TSB culture, standardized to an OD A₅₆₀ of 0.05, and subcultured to 20 ml of TSB with chloramphenicol (10 µg/ml), where applicable. After approximately 4 hours, an aliquot of cells were harvested, standardized to an OD A₅₆₀ of 1.0, and pelleted. Once standardized, were resuspended in 100 mM NaPO₄ buffer containing 0.1% BSA and 0.1% Tween 20, pH 7.5. The 1.0 ml cell suspension was transferred to a microcentrifuge tube followed by the addition of 10⁵ dpm of ¹²⁵I-labeled type I collagen. Cells were incubated at RT with end-over-end mixing for 1 hour, pelleted at 15,000 × g for 10 minutes and the supernatant removed. Samples were recentrifuged and the remaining supernatant removed. The radioactivity retained in the pellet was measured in a BIOSCAN QC2000 gamma counter. The protocol was repeated every 2 hours throughout the time course. All assays were done in duplicate and reported as an average with designated error bars representing the average standard deviation.

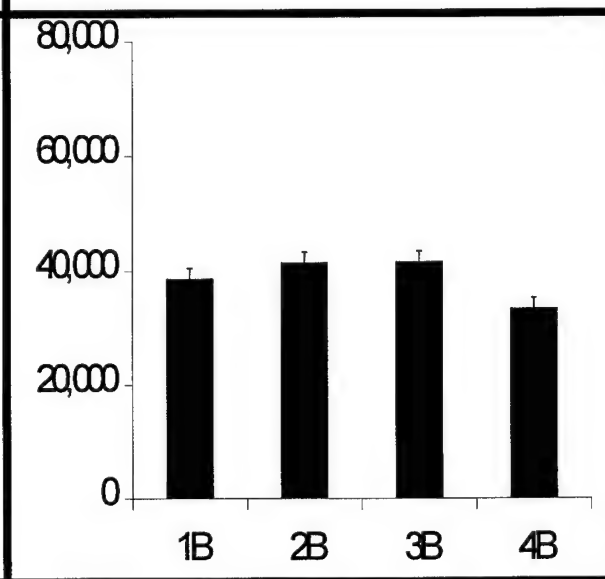
Wright in TSB @ 6 Hours



Wright in TSB @ 8 Hours



Wright in TSB @ 10 Hours



Wright in TSB @ 12 Hours

Figure 21.

^{125}I -labeled collagen binding capability of microencapsulated strain Wright, grown on Columbia agar, comparing the isogenic pLI50::*cna*_{UAMS-639} (1B), pLI50::*cna*_{UAMS-639} (2B), pLI50::*cna*_{UAMS-639} (3B), and pLI50::*cna*_{UAMS-639} (4B) variants

Collagen binding analysis was conducted of strain Wright possessing the isogenic *cna* variants. Briefly, cells were harvested from an overnight culture (≈ 24 hours) grown on Columbia agar, standardized to an OD A_{560} of 0.05, and resuspended in 100 mM NaPO_4 buffer containing 0.1% BSA and 0.1% Tween 20, pH 7.5. The 1.0 ml aliquot of standardized cell suspension was transferred to a microcentrifuge tube followed by the addition of 10^5 dpm of ^{125}I -labeled type I collagen. Cells were incubated at RT with end-over-end mixing for 1 hour, pelleted at $15,000 \times g$ for 10 minutes and the supernatant removed. Samples were recentrifuged and the remaining supernatant removed. The radioactivity retained in the pellet was measured in a BIOSCAN QC2000 gamma counter. All assays were done in duplicate and reported as an average with error bars representing the average standard deviation.

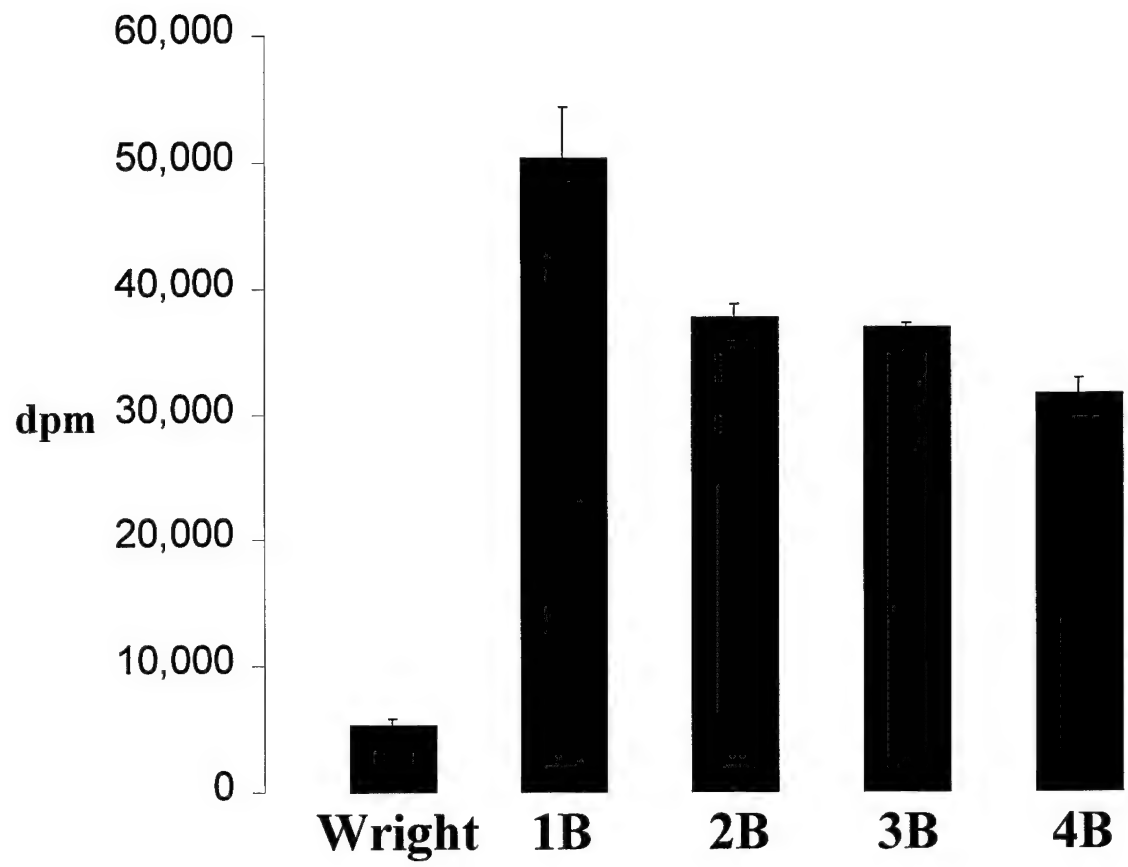


Figure 22.
¹²⁵I-labeled collagen binding capability of heavily-encapsulated strains Smith Diffuse and M comparing the isogenic pLI50::*cna*_{UAMS-639} (1B), pLI50::*cna*_{UAMS-639} (2B), pLI50::*cna*_{UAMS-639} (3B), and pLI50::*cna*_{UAMS-639} (4B) variants

Collagen binding analysis was conducted of strains Smith Diffuse (Fig 22a) and M (Fig 22b) possessing the isogenic *cna* variants. This assay was performed as outlined in figure 8.

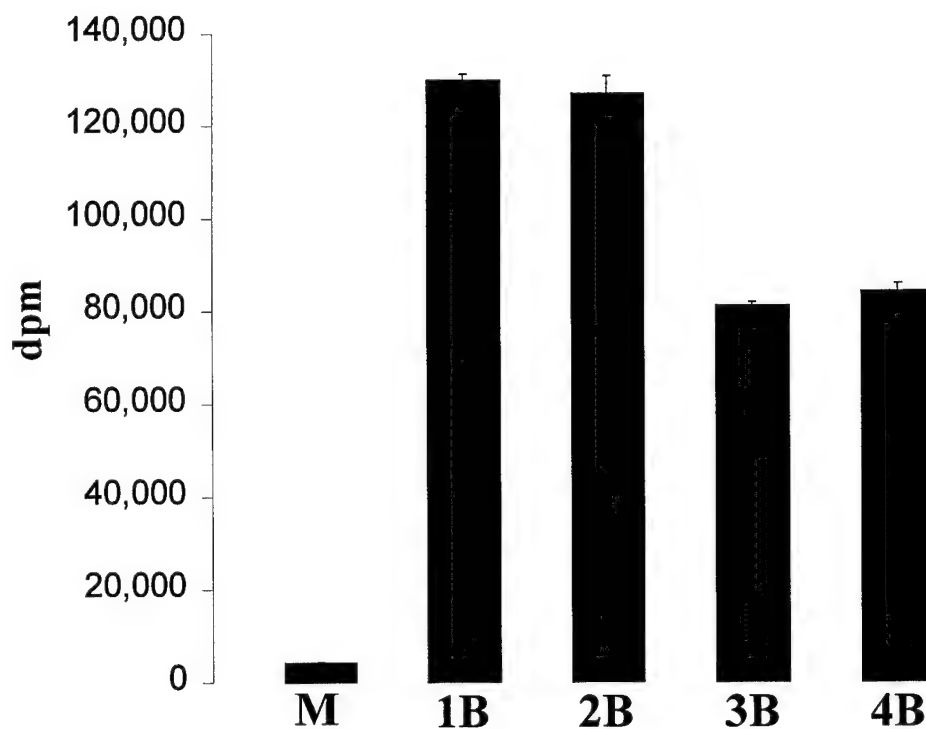
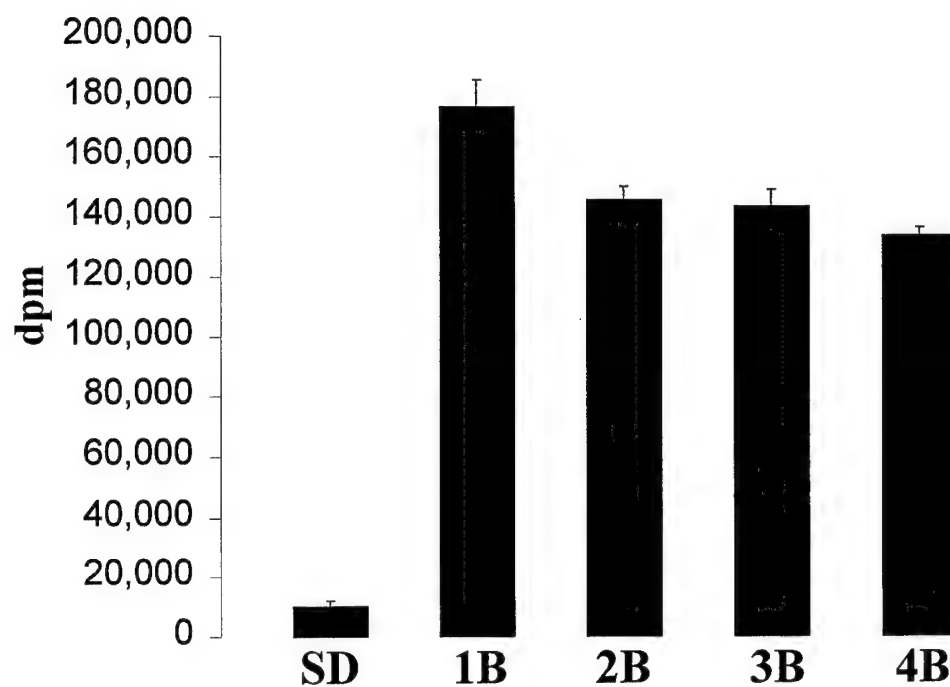
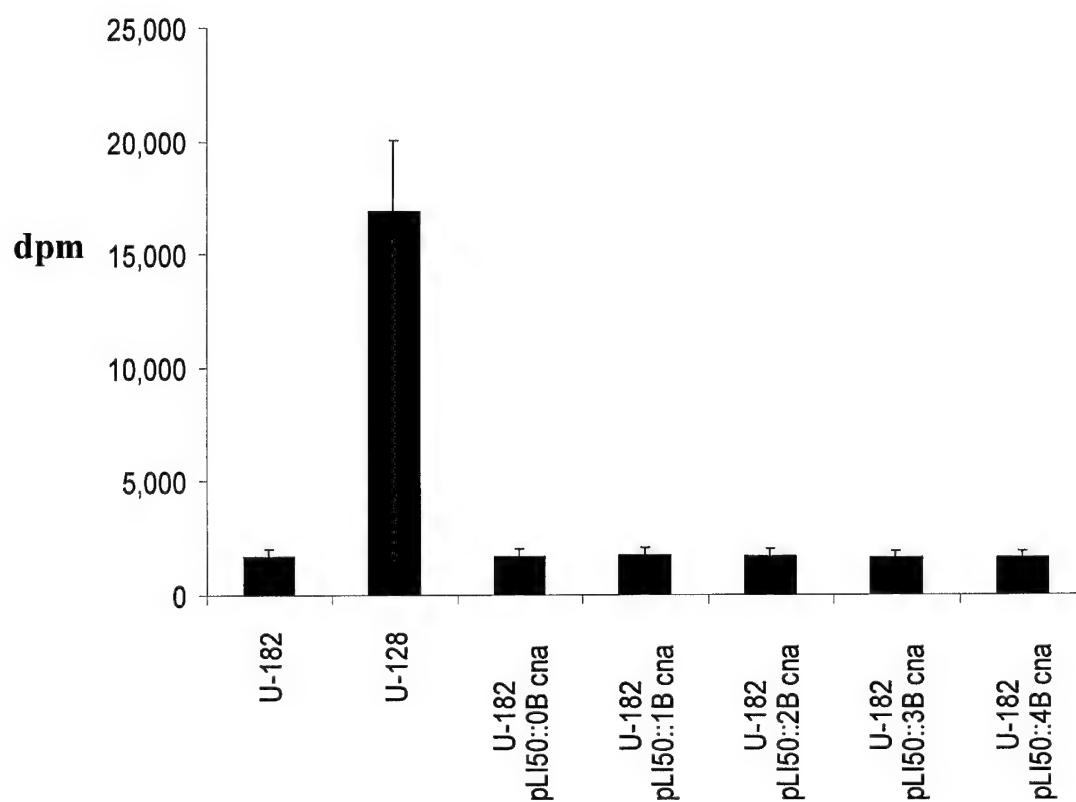


Figure 23.

¹²⁵I-labeled fibronectin binding assays assessing the B domain's ability to enhance fibronectin binding in strain UAMS-182 (*fnbA* and *fnbB* knockout)

Fibronectin binding analysis was conducted of strain UAMS-182 possessing the isogenic *cna* variants. Briefly, cells were harvested from an overnight TSB culture, standardized to an OD A₅₆₀ of 0.05, and subcultured to 20 ml of TSB with chloramphenicol (10 µg/ml), where applicable. After approximately 4 hours, cells were harvested, standardized to an OD A₅₆₀ of 1.0, and pelleted. Once standardized, cells were resuspended in 100 mM NaPO₄ buffer containing 0.1% BSA and 0.1% Tween 20, pH 7.5. The 1.0 ml aliquot of standardized cell suspension was transferred to a microcentrifuge tube followed by the addition of 10⁵ dpm of ¹²⁵I-labeled fibronectin. Cells were incubated at RT with end-over-end mixing for 1 hour, pelleted at 15,000 × g for 10 minutes and the supernatant removed. Samples were recentrifuged and the remaining supernatant removed. The radioactivity retained in the pellet was measured in a BIOSCAN QC2000 gamma counter. All assays were done in duplicate and reported as an average with error bars representing the average standard deviation.

Fibronectin binding capability of Cna variants



DISCUSSION

Staphylococcus aureus is an opportunistic pathogen capable of inducing many human diseases, primarily due to its vast array of virulence factors. Although frequently isolated from superficial skin infections, it is also responsible for many debilitating and life threatening diseases. For example, *S. aureus* is the most common etiological agent of both bacterial arthritis and acute osteomyelitis, responsible for nearly 80% of all reported cases (9, 69). Patients afflicted with these diseases endure a great deal of suffering and often require long term managed care. Interestingly, like many pathogens, the ability of *S. aureus* to cause disease largely depends on its capacity to adhere to host tissues. In many Gram-positive organisms, the bacterial proteins that facilitate attachment are termed adhesins.

The presence of Cna, the primary *S. aureus* collagen binding adhesin (19), may be important in certain diseases. Nearly all the *S. aureus* strains isolated from patients diagnosed with septic arthritis or osteomyelitis contained Cna (64). This is unlike wound infections, where only one-third of the isolated strains possessed this adhesin (64). Furthermore, Gillaspay et al. (18) demonstrated that Cna is present on the surface of *S. aureus* cells growing in bone tissue. These findings suggest Cna is a particularly important virulence factor in the causation of bone and joint diseases. Additionally, collagen binding is important in a variety of other diseases. For example, collagen binding in experimental infectious endocarditis is related to an increase in disease (24). Furthermore, inhibition of collagen binding reduces virulence in animal models of both endocarditis and septic arthritis (24, 51). These studies substantiate the role of collagen

binding in disease. However, more information is needed regarding the specific mechanisms that facilitate the binding process.

Based on function, Cna may be broken down into three distinct regions (Fig 1). Outside the cell, the outermost N-terminus of the protein is referred to as the A domain. This region is directly responsible for collagen binding (50). Within the cell, the C-terminus consists of a short cytoplasmic tail, followed by the membrane and wall spanning domains (58, 59). Common to most *S. aureus* surface bound proteins, this region anchors the adhesin to the cell. However, located between these regions is the B domain (58, 59). A single B domain is comprised of 187 amino acids and can be repeated in Cna (as many as four direct repeats per protein). Interestingly, the B domain has yet to be associated with any function. However, no *S. aureus* isolate has been reported to possess Cna in a form which lacks a B domain, which suggests a functional role for this domain. Therefore, we addressed two possible functions associated with the B domain. First, we determined whether Cna has a requirement for at least a single B domain to effectively bind collagen. Next, we proposed that multiple B domains may increase collagen binding, either by enhancing protein folding or overcoming capsule inhibition.

Initially, we created a 0B domain mutant from the Phillips' *cna* gene (a 2B variant). To ensure processing of the 0B domain mutant was comparable to that of the parent, we performed Northern slot blot analysis. As a result, both were shown to transcribe equal amounts of mRNA. However, Western analysis revealed slightly lower amounts of the translated 0B protein. To determine if this result was significant, we used flow cytometry to quantify the amount of cell-surface associated protein. Anti-Cna antibodies, specific for the A domain, bound both at similar levels. Therefore, we

concluded that both the 0B and 2B Cna variants were localized on the bacterial cell surface with equal efficiency. This suggested that elimination of the B domain did not significantly effect protein folding, or presentation, of the collagen binding A domain. This is unlike other *S. aureus* MSCRAMMs whose repeat regions are required for overall expression of the adhesin (20). Yet, equivalent expression did not ensure the 0B variant was completely functional.

To determine if the 0B domain variant was functional, we utilized a combination of immobilized and soluble collagen binding assays. Initially, the 0B mutant was shown to bind immobilized collagen as efficiently as the 2B parent. This provided early evidence that removing the B domain had negligible, if any, negative effects on collagen binding. However, as minor differences could go undetected in our immobilized plate assay, we used a soluble collagen binding assay to further assess function. Using ^{125}I -labeled type I collagen, the 0B domain mutant routinely bound collagen, in several cell lines, at levels resembling its 2B domain parent. As a result, we conclude that the B domain is neither required for proper presentation of the A domain nor necessary for efficient function. As a single B domain is not needed, and yet maintained in multiple forms within the population, further suggests it serves some function. Therefore, we investigated whether a specific number of B domains affected protein folding or enhanced collagen binding.

Using natural *cna* variants, we found that the resulting proteins bound collagen in a B domain independent manner. Specifically, increased collagen binding appeared to result from increased amounts of translated proteins. This observation is consistent with previous data that showed significant collagen binding to be in proportion to *cna* mRNA production (18). However, we observed that the 4B Cna variant transcribed and

subsequently translated as much Cna as the 1B variant, yet bound lower amounts of ^{125}I -labeled collagen. To determine if this result was directly attributed to increased B domains, we removed the apparent promoter-associated differences by creating and evaluating isogenic Cna variants.

Isogenic Cna variants, differing only in their number of B domains, were created from the UAMS-639 *cna* gene and subsequently evaluated on their ability to bind collagen. Unlike the natural *cna* variants, the isogenic variants showed equal amounts of transcribed mRNA and translated proteins. Flow cytometry confirmed the amounts of surface expressed protein were similar among all variants. From these data, we conclude that multiple B domains do not affect processing and expression of the protein.

With the confirmation of similar amounts of expressed protein, we next assessed the collagen binding capability of each variant. During functional evaluation, we found that multiple B domains failed to enhance collagen binding. In fact, an inverse trend was frequently observed in many strains. This suggested that multiple B domains reduced the overall binding capability. Utilizing a student's paired t-Test to compare binding data obtained from numerous strains, we found that the 3B and 4B variants bound significantly less collagen than the 1B version ($p < 0.001$).

Interestingly, a similar trend was observed utilizing these strains in a series of shear force studies performed by Dr. Julia Ross' lab at the University of Maryland Baltimore County (personal communication). At a medium shear rate of 500 s^{-1} , Dr. Ross' lab observed that the 1B version remained bound to a collagen matrix more efficiently than the 3B or 4B variants (personal communication). Results from their

studies suggest that multiple B domains may attenuate collagen binding. Exactly how this would benefit the organism is unclear. However, we speculate that an increased number of B domains may increase the disassociation constant between the adhesin and the collagen molecule. This would suggest that a possible function of multiple B domains is to prevent the organism from remaining constantly bound to the substrate. Therefore, immediately following initial binding, the organism could penetrate into deeper tissues. Experiments to further investigate this theory are currently ongoing. However, we also suspected that multiple B domains may facilitate collagen binding in the presence of a capsule. To address this question, we used a variety of *S. aureus* strains, each with different amounts of capsule production.

Capsular polysaccharides, comprising 11 different serotypes, are produced by more than 90% of *Staphylococcus aureus* isolates (48, 63). The prevalence of microencapsulated strains in the pathogenesis of human septicemia and septic arthritis is clear. Of all the serotypes, CP5 and CP8 comprise 80 to 85% of all clinical blood isolates (46). Such data, in correlation with the prevalence of Cna isolated from septic arthritis and osteomyelitis cases, would indicate the capsule and the adhesion can function as two independent and yet compatible macromolecular structures. Such a relationship has been established in other bacterial species (43). Utilizing our natural and isogenic variants, we searched for a condition in which multiple B domains enhanced collagen binding in microencapsulated strains.

Utilizing the microencapsulated CP5 and CP8 strains possessing our pLI50::*cna* constructs, we could not identify a condition where multiple B domains enhanced collagen binding. In fact, the binding trends both from the natural and isogenic variants

resembled those obtained from the previous unencapsulated U-128 experiments. The microcapsule may lack an ability to mask underlying surface proteins, including Cna. This would imply that the two structures are completely compatible. It is also possible that Cna and the microcapsule act in pathogenesis at different stages of the organism's development. Specifically, we observed that maximal Cna expression, *in vitro*, occurs during the mid-exponential growth phase (approximately 4-5 hours). This is in contrast to the capsule, which is maximally produced in stationary phase. Therefore, the microcapsule and Cna may not be required to be compatible, as they are utilized under different conditions.

Thakker et al. (65) recently reported that maximal CP5 expression, obtained from solid surface grown cultures, enhanced bacterial virulence for approximately 4 hours post infection in a murine model. However, both CP5 and CP8 microcapsules, when grown to exponential phase prior to inoculation, have been shown to provide little or no protection *in vivo* (1). Such data may provide an explanation for the coexistence of the capsule and the adhesin. Specifically, we propose a model where the compatibility between these structures stems from the organism's efficient regulation of both sets of genes in a cell-density dependent manner.

Upon introduction into the host from the environment, it is likely that the bacteria are in a stationary phase growth cycle, thus exhibiting maximal amounts of capsule. This facilitates the organisms' spread throughout the host with the antiphagocytic capsule acting as a protectant for a limited time. However, this dispersion leads to a state of low cell density, where *S. aureus* reacts by upregulating adhesins to facilitate binding to host matrices. Once binding occurs, the cell density increases followed by upregulation of the

protective capsular polysaccharide layer. Despite the feasibility of this model, it remains speculation. Therefore, the possibility exists where *in vivo*-like conditions simply were not identified in our experiments. Particularly, perhaps *S. aureus* produces significant amounts of capsule, *in vivo*, at times when Cna remains functional. This may facilitate the ability of multiple B domains to act as a stalk. Therefore, we tested our hypothesis in certain microencapsulated strains under conditions known to increase capsule production.

Lee et al. (34) demonstrated that *S. aureus* CP8 capsule expression is regulated by the microenvironment of the culture. Specifically, cultures grown on solid support yielded quantities of cell-associated capsule greater than 300-fold higher than those yielded by cells grown in liquid cultures. Following a similar protocol, we observed an increase in CP8 capsule production by strain Wright as evidenced by phenotypic appearance. Experiments measuring the adherence to soluble collagen showed a decrease in collagen binding under these conditions. This was probably due to an additive effect of decreased Cna expression with increased capsule production. However, our data indicated that the multiple B domain variants failed to provide the organism any significant advantage in collagen binding. This could be interpreted in two ways.

First, the amount of capsule produced by microencapsulated strains, under any condition, may be sufficiently low enough to mask any of the variants. However, during a 12 hour time course study of strain Wright grown in liquid medium, we observed a distinct decrease in collagen binding between the 6 and 8 hour time point. The level of collagen binding then remained consistent throughout the remainder of the study. We have also shown that *cna*-positive cells, grown overnight, retain the ability to bind substantial levels of collagen. Though it is possible that Cna's function dramatically fell

during the 6 and 8 hour time point, it is more likely that the observed decrease in collagen binding was due to the capsule. To further evaluate the possibility of insufficient capsule production, we utilized strains known to overproduce capsular polysaccharides sufficient to mask the function of Cna.

Gillaspy et al. (19) previously demonstrated a direct correlation of the presence of *cna* with the organism's ability to bind collagen, with one notable exception. Strains that produced an overabundance of capsular polysaccharide, namely Smith Diffuse (CP2) and M (CP1), bound collagen at significantly lower levels than their capsule knockout mutants. Importantly, Northern analysis revealed similar levels of *cna* mRNA in both the encapsulated and unencapsulated counterpart. Likewise, both of the heavily-encapsulated strains possessed *cna* with a single B domain. These findings suggested certain capsule types impaired the organism's ability to bind collagen. Yet this presents the organism with the paradox of utilizing one virulence factor (the capsule) at the expense of the other (Cna). However, if the organism possessed Cna with multiple B domains both structures may coexist and remain equally functional. Experiments focusing on the B domain secondary structure, and its interaction with multiple B domains, has recently been reported (56). These studies concluded that each B domain is comprised of approximately 40% beta sheet structure which folds independently of other Cna domains, appearing as a classic mosaic protein. More importantly, they propose that one possible function may be to act as a stalk, enhancing collagen binding in heavily-encapsulated strains (56). Therefore, to functionally address the question, we performed collagen binding assays with our natural and isogenic *cna* variants in M and Smith Diffuse.

Without exception, multiple B domains failed to significantly enhance collagen binding in heavily-encapsulated strains. The binding trend associated with the natural *cna* variants was similar to previous experiments. Specifically, the overall collagen binding capacity correlated with increased mRNA production. Further analysis of the isogenic variants in strains Smith Diffuse and M also revealed a slight increase collagen binding associated with fewer B domains. Surprisingly, we observed relatively high levels of collagen binding in our experimental strains, suggesting the capsule barrier may be inhibited by the overproduction of Cna.

Capsule disruption from the overproduction of Cna from a plasmid can not be disproved. However, several observations suggest that substantial capsule disruption did not occur. Specifically, we observed no detectable differences between the strains harboring our pLI50::*cna* constructs and the parent strain's capsule production, both exhibiting an extremely mucoid phenotype. More importantly, parental capsule-knockout strains bound, on an average, four times more collagen than that of their encapsulated counterpart. This was comparable to our experimental strains, in which unencapsulated bacteria bound three times more collagen than that of the encapsulated version. The slight reduction could be interpreted as a loss of inhibition due to decreased capsule production. However, it could also be a capsule-independent phenomenon.

Capsules, in strains such as M and Smith Diffuse, have been shown to be quite porous, allowing free passage of certain large molecules such as complement components and lysostaphin (30, 31, 71). These capsule types have also been shown to inhibit passage of bacteriophage particles possessing phage heads greater than 100 nm in diameter (70). Reduced binding is expected as many of the collagen molecules (having lengths greater

than 300 nm long) would lie across the pores being unable to penetrate. However, this pore size would easily allow the end-on penetration of soluble collagen. Likewise, as the *S. aureus* capsule is a hydrophilic, negatively charged moiety (29, 55) and the vast majority of amino acids that compose the tropocollagen molecule are nonpolar (35), it is unlikely that charge-associated repulsion would be a major factor. This premise is also supported by studies which demonstrate that size is the limiting factor for capsule penetration by a variety of substances, including host proteins (30, 31, 70, 71).

Therefore, it remains possible that the likelihood of binding could be determined by the proximity of the pore to a nearby Cna molecule. As a result, the increased binding we observed may be attributed to the increased likelihood of a Cna molecule, now in larger quantities on the cell surface, being in close proximity with a capsule pore. The end result would be increased collagen binding without altering overall capsule expression. Yet in both cases, capsule inhibition within the experimental strains still existed (as evidenced by a three-fold reduction in binding compared to the unencapsulated mutants). Therefore, the observation that the larger proteins failed to bind more collagen suggests their structures, regardless of the number of B domains, is unable to project the collagen binding domain passed the capsule barrier. In fact, even in heavily encapsulated strains, multiple B domains appeared to impair collagen binding.

The continual reemergence of this pattern, regardless of the presence of extensive capsule, was somewhat surprising. As discussed above, the B domain may function to increase steric hindrance, thus increasing the disassociation constant. Yet there are other possibilities which are equally plausible. Multiple B domains could simply be a genetic burden which the organism is in the process of eliminating. Though we do not have the

essential number of strains necessary to facilitate a large epidemiological study, we have noticed trends within our culture collection. Specifically, only one 4B variant has been identified in the literature. In fact, most of the Cna-positive organisms within our collection possess a 1B or 2B version. It is possible that the primordial staphylococci possessed Cna with numerous B domain repeat sequences. Over time, they have selected for their removal. Although we failed to identify a function, this does not mean there is not one. In an effort to identify a viable function, we compared the B domain sequence with other known bacterial proteins.

We compared the B domain with other reported protein sequences using Gene Bank. Cna showed an approximate 30%-40% homology at the protein level with various streptococcal fibronectin binding proteins. Interestingly, Hienz et al. (23) previously reported that the insertional inactivation of Cna had a pleiotropic effect, in which decreased fibronectin binding was observed. We performed fibronectin binding assays within an *fnAB*-knockout strain containing our pLI50::*cna* variants. However, no increase in fibronectin binding was observed between variants, providing evidence that the B domain serves no apparent role in fibronectin binding.

We conclude that the B domain within the *Staphylococcus aureus* collagen adhesion serves no function with respect to enhanced collagen binding. We have shown the B domain is not required for efficient adhesion to a collagen matrix and that multiple B domains do not enhance binding, *in vitro*. The significance, if any, of the reduced binding capability exhibited by the larger variants is unknown. The 3B and 4B variants may induce disease, *in vivo*, as efficiently as the 1B variant. Likewise, this data does not

preclude the ability of the B domain to function in some role unrelated to collagen binding.

Other direct repeat regions, with varying degrees of size, have been shown to benefit bacteria in numerous ways. For example, Han et al. (21) demonstrated that the *hagA* gene of *Porphyromonas gingivalis* contains as many as four direct repeats greater than 1,318 base pairs each (over twice the size of the B domain). Interestingly, their function was to increase hemagglutinin activity. As the B domain is conserved, it seems likely that it serves some function. One related possibility would be to determine if the B domains themselves could bind non-collagenous proteins to which a *S. aureus* adhesin has not yet been identified, such as laminin, bone sialoprotein, or osteopontin. Additionally, as complement-mediated opsonophagocytosis is the major mechanism by which *S. aureus* is cleared, the B domain may itself act to resist phagocytosis by binding complement inhibitors, such as Factor H or decay accelerating factor.

Still, the B domain may function, in some obscure way, to aid in collagen binding. For example, it remains possible that multiple B domains aid the bacterium in collagen binding in a non-encapsulated environment. As the bacterium enters the blood stream and is coated with host proteins, such as fibrinogen or fibronectin, multiple B domains may have the structure necessary to enhance collagen binding under those circumstances. Additionally, *Staphylococcus aureus* has been shown to inhibit the biosynthesis of bone matrix proteins by a yet undefined noncytotoxic mechanism (36). No evidence suggests or disputes that the B domain within Cna fulfills some role in that inhibition. This would afford the pathogen the ability to bind its host substrate while subduing the host's ability

to respond to disease. With all the possibilities, the identification of a B domain function may prove beneficial for reducing the overall virulence of the organism.

Future studies involving the B domain could be useful in addressing questions raised from this study. Particularly, what is the nature of collagen binding in the presence of other host proteins? Clearly the direct interactions between any host protein which coats *S. aureus in vivo* may have a direct impact on how other surface proteins (like Cna) interact with each other and the host. As a result, such a multifactorial interaction may favor the presence of multiple B domains associated with Cna. Similarly, we have shown that strains possessing certain capsule types (heavily encapsulated) tend to mask the function of Cna *in vitro* where others do not. This raises questions of capsule interactions with other bacterial surface-associated proteins. Specifically, is Cna unique in its interaction with the different capsules or is there a more global pattern of incompatibility? One could speculate that the heavily encapsulated strains, which are virulent in mice, are not found in human disease strictly due to their inability to colonize host tissue. Determining whether masking occurs utilizing various capsule types in conjunction with other host proteins could provide insight on the paradox that exists between the positively charged cell wall and the negatively charged capsule layer. Such experiments would almost certainly require nontraditional approaches in assessing the role B domains may have in *S. aureus* pathogenesis.

BIBLIOGRAPHY

1. Albus, A., Arbeit, R.D., and Lee, J.C. Virulence of *Staphylococcus aureus* mutants altered in type 5 capsule production. *Infect.Immun.* 59:1008-1014, 1991.
2. Albus, A., Fournier, J.M., Wolz, C., Boutonnier, A., Ranke, M., Hoiby, N., Hochkeppel, H., and Doring, G. *Staphylococcus aureus* capsular types and antibody response to lung infection in patients with cystic fibrosis. *J.Clin.Microbiol.* 26:2505-2509, 1988.
3. Arbeit, R.D., Karakawa, W.W., Vann, W.F., and Robbins, J.B. Predominance of two newly described capsular polysaccharide types among clinical isolates of *Staphylococcus aureus*. *Diagn.Microbiol.Infect.Dis.* 2:85-91, 1984.
4. Baddour, L.M., Lowrance, C., and Albus, A. *Staphylococcus aureus* microcapsule expression attenuates bacterial virulence in a rat model of experimental endocarditis. *J.Infect.Dis.* 165:749-753, 1992.
5. Bremell, T., Lange, S., Yacoub, A., Ryden, C., and Tarkowski, A. Experimental *Staphylococcus aureus* arthritis in mice. *Infect.Immun.* 59:2615-2623, 1991.
6. Campbell, K.M. and Johnson, C.M. Identificaiton of *Staphylococcus aureus* binding protein on isolated porcine cardiac valve cells. *J.Lab.Clin.Med.* 115:217-223, 1990.
7. Cheung, A.L., Eberhardt, K., and Heinrichs, J.H. Regulation of protein A synthesis by the *sar* and *agr* loci of *Staphylococcus aureus*. *Infect.Immun.* 65:2243-2249, 1997.
8. Christensen, G.D., Baddour, L.M., Madison, B.M., Parisi, J.T., Abraham, S.N., Hasty, D.L., Lowrance, J.H., Josephs, J.A., and Simpson, A. Colonial morphology of staphylococci on memphis agar: phase variation of slime production, resistance to β -lactam antibiotics, and virulence. *J.Infect.Dis.* 161:1153-1169, 1990.
9. Cierny, G., III. Classification and treatment of adult osteomyelitis. In: *Surgery of the Musculoskeletal System*, edited by Evarts, C.M. New York:Churchill Livingstone, 1990, p.4337-4379.
10. Crass, B.A. and Bergdoll, M.S. Toxin involvement in toxic shock syndrome. *J.Infect.Dis.* 153:918, 1986.
11. Fast, D.J., Schlievert, P.M., and Nelson, R.D. Toxic shock syndrome-associated staphylococcal and streptococcal pyrogenic toxins are potent inducers of tumor necrosis factor production. *Infect.Immun.* 57:291, 1989.

12. Fattom, A.I., Sarwar, J., Basham, L., Ennifar, S., and Naso, R. Antigenic determinants of *Staphylococcus aureus* type 5 and type 8 capsular polysaccharide vaccines. *Infect.Immun.* 66:4588-4592, 1998.
13. Fischetti, V.A., Jarymowycz, M., Jones, K.F., and Scott, J.R. Streptococcal M protein size mutants occur at high frequency within a single strain. *J.Exp.Med.* 164:971-980, 1986.
14. Foster, T.J. Potential for vaccination against infections caused by *Staphylococcus aureus*. *Vaccine* 9:221, 1991.
15. Fournier, J.M., Vann, W.F., and Karakawa, W.W. Purification and characterization of *Staphylococcus aureus* type 8 capsular polysaccharide. *Infect.Immun.* 45:87-93, 1984.
16. Gillaspy, A.F., Hickmon, S.G., Skinner, R.A., Thomas, J.R., Nelson, C.L., and Smeltzer, M.S. Role of the accessory gene regulator (*agr*) in the pathogenesis of staphylococcal osteomyelitis. *Infect.Immun.* 63:3373-3380, 1995.
17. Gillaspy, A.F., Patti, J.M., Pratt, F.L., Jr., Iandolo, J.J., and Smeltzer, M.S. The *Staphylococcus aureus* collagen adhesin-encoding gene (*cna*) is within a discrete genetic element. *Gene.* 196:239-248, 1997.
18. Gillaspy, A.F., Patti, J.M., and Smeltzer, M.S. Transcriptional regulation of the *Staphylococcus aureus* collagen adhesin gene, *cna*. *Infect.Immun.* 65:1536-1540, 1997.
19. Gillaspy, A.F., Sau, S., Lee, C.Y., Cheung, A.L., and Smeltzer, M.S. Factors affecting the collagen binding capacity of *Staphylococcus aureus*. *Infect.Immun.* 66:3170-3178, 1998.
20. Goldenberg, D.L. and Reed, J.I. Bacterial arthritis. *N.Engl.J.Med.* 312:764-771, 1985.
21. Han, N., Whitlock, J., and Progulske-Fox, A. The hemagglutinin gene A (*hagA*) of *Porphyromonas gingivalis* 381 contains four large, continuous, direct repeats. *Infect.Immun.* 64:4000-4007, 1996.
22. Hartford, O., Francois, P., Vaudaux, P., and Foster, T.J. The dipeptide repeat region of the fibrinogen-binding protein (clumping factor) is required for functional expression of the fibrinogen-binding domain on the *Staphylococcus aureus* cell surface. *Mol.Microbiol.* 25:1065-1076, 1997.
23. Hienz, S.A., Palma, M., and Flock, J.I. Insertional inactivation of the gene for the collagen-binding protein has a pleiotropic effect on the phenotype of *Staphylococcus aureus*. *J.Bacteriol.* 178:5327-5329, 1996.

24. Hienz, S.A., Schennings, T., Heimdahl, A., and Flock, J.I. Collagen binding of *Staphylococcus aureus* is a virulence factor in experimental endocarditis. *J.Infect.Dis.* 174:83-88, 1996.
25. Hochkeppel, H.K., Braun, D.G., Vischer, W., Imm, A., Sutter, S., Staeubli, U., Guggenheim, R., Kaplan, E.L., Boutonnier, A., and Fournier, J.M. Serotyping and electron microscopy studies of *Staphylococcus aureus* clinical isolates with monoclonal antibodies to capsular polysaccharide types 5 and 8. *J.Clin.Microbiol.* 25:526-530, 1987.
26. Holmberg, S.D. and Blake, P.A. Staphylococcal food poisoning in the United States. *JAMA* 251:487, 1984.
27. Joklik, W.K., Willett, H.P., Amos, D.B., and Wilfert, C.M. Staphylococcus. In: Zinsser Microbiology, 20th edition, edited by Joklik, W.K.: Appleton & Lange, 1992, p. 401-416.
28. Jonsson, K., McDevitt, D., McGavin, M.H., Patti, J.M., and Hook, M. *Staphylococcus aureus* expresses a major histocompatibility complex class II analog. *J.Biol.Chem.* 270:21457-21460, 1995.
29. Karakawa, W.W. and Vann, W.F. Capsular polysaccharides of *Staphylococcus aureus*. *Semin.Infect.Dis.* 4:285-293, 1982.
30. King, B.F., Biel, M.L., and Wilkinson, B.J. Facile penetration of the *Staphylococcus aureus* capsule by lysostaphin. *Infect.Immun.* 29:892-896, 1980.
31. King, B.F. and Wilkinson, B.J. Binding of human immunoglobulin G to Protein A in encapsulated *Staphylococcus aureus*. *Infect.Immun.* 33:666-672, 1981.
32. Lee, C.Y. Cloning of genes affecting capsule expression in *Staphylococcus aureus* strain M. *Mol.Microbiol.* 6:1515-1522, 1992.
33. Lee, J.C., Betley, M.J., Hopkins, C.A., Perez, N.E., and Pier, G.B. Virulence studies, in mice, of transposon-induced mutants of *Staphylococcus aureus* differing in capsule size. *J.Infect.Dis.* 156:741-750, 1987.
34. Lee, J.C., Takeda, S., Livolsi, P.J., and Paoletti, L.C. Effects of *in vitro* and *in vivo* growth conditions on expression of type 8 capsular polysaccharide by *Staphylococcus aureus*. *Infect.Immun.* 61:1853-1858, 1993.
35. Lehninger, A.L., Nelson, D.L., and Cox, M.M. The three-dimensional structure of proteins. In: *Principles of Biochemistry*, edited by Neal, V.:Worth Publishers, Inc. 1993, p.160-197.

36. Lerner, U.H., Sundqvist, G., Ohlin, A., and Rosenquist, J.B. Bacteria inhibit biosynthesis of bone matrix proteins in human osteoblasts. *Clin.Orthop.Rel.Res.* 346:244-254, 1998.
37. Lillibridge, C.B., Melish, M.E., and Glasgow, L.A. Site of action of exfoliative toxin in the staphylococcal scalded-skin syndrome. *Pediatrics* 50:728, 1972.
38. Lowy, F.D., Medical progress: *Staphylococcus aureus* infections. *N. Engl. J. Med.* 339:520-532, 1998.
39. Maki, D.G. Epidemic nosocomial bacteremias. In: *Handbook of hospital acquired infections*, edited by Wenzel, R.P. Boca Raton, FL: CRC Press. 1982, p.371-512.
40. Maki, D.G. Infections associated with intravascular lines. In: *Current clinical topics in infectious diseases, Vol 3*, edited by Remington, J.S. New York: McGraw-Hill, 1982, p.309-363.
41. McGavin, M.H., Krajewska-Pietrasik, D., Ryden, C., and Hook, M. Identification of a *Staphylococcus aureus* extracellular matrix-binding protein with broad specificity. *Infect.Immun.* 61:2479-2485, 1993.
42. Melish, M.E. and Glasgow, L.A. The staphylococcal scalded-skin syndrome: development of an experimental model. *N.Engl.J.Med* 282:1114, 1970.
43. Mesnage, S., Tosi-Couture, E., Gounon, P., Mock, M., and Fouet, A. The capsule and S-layer: two independent and yet compatible macromolecular structures in *Bacillus anthracis*. *J.Bacteriol.* 180:52-58, 1998.
44. Miller, K.D., Hetrick, D.L., and Bielefeldt, D.J. Production and properties of *Staphylococcus aureus* (strain Newman D2C) with uniform clumping factor activity. *Thrombosis Research.* 10:203-211, 1977.
45. Nemeth, J.A. Antibodies to capsular polysaccharides are not protective against experimental *Staphylococcus aureus* endocarditis. *Infect.Immun.* 63:375-380, 1995.
46. Nilsson, I.M., Lee, J.C., Bremell, T., Ryden, C., Tarkowski, A. The role of staphylococcal polysaccharide microcapsule expression in septicemia and septic arthritis. *Infect.Immun.* 65:4216-4221, 1997.
47. Novick, R.P., Ross, H.F., Projan, S.J., Kornblum, J., Kreiswirth, B., and Moghazeh, S. Synthesis of staphylococcal virulence factors is controlled by a regulatory RNA molecule. *The EMBO Journal.* 12:3967-3975, 1993.
48. Ouyang, S. and Lee, C.Y. Transcriptional analysis of type 1 capsule genes in *Staphylococcus aureus*. *Mol.Microbiol.* 23:473-482, 1997.

49. Patti, J.M., Allen, B.L., McGavin, M.J., and Hook, M. MSCRAMM-Mediated adherence of microorganisms to host tissue. *Annu.Rev.Microbiol.* 48:585-617, 1994.
50. Patti, J.M., Boles, J.O., and Hook, M. Identification and biochemical characterization of the ligand binding domain of the collagen adhesin from *Staphylococcus aureus*. *Biochemistry.* 32:11428-11435, 1993.
51. Patti, J.M., Bremell, T., Krajewska-Pietrasik, D., Abdelnour, A., Tarkowski, A., Ryden, C., and Hook, M. The *Staphylococcus aureus* collagen adhesin is a virulence determinant in experimental septic arthritis. *Infect.Immun.* 62:152-161, 1994.
52. Patti, J.M., Jonsson, H., Guss, B., Switalski, L.M., Wigberg, K., Lindberg, M., and Hook, M. Molecular characterization and expression of a gene encoding a *Staphylococcus aureus* collagen adhesin. *J.Biol.Chem.* 267:4766-4772, 1992.
53. Peterson, P.K., Quie, P.G., Youngki, K., Wilkinson, B.J., Verbrugh, H.A., and Verhoef, J. Recognition of *Staphylococcus aureus* by human phagocytes. *Scand. J. Infect. Dis.* 41:67-76, 1983.
54. Poutrel, B., Boutonnier, A., Sutra, L., and Fournier, J.M. Prevalence of capsular polysaccharide types 5 and 8 among *Staphylococcus aureus* isolates from cow, goat, and ewe milk. *J.Clin.Microbiol.* 26:38-40, 1988.
55. Reifsteck, F., Wee, S., and Wilkinson, B.J. Hydrophobicity-hydrophilicity of staphylococci. *J. Med. Micro.* 24:65-73, 1987.
56. Rich, R.L., Demeler, B., Ashby, K., Deivanayagam, C.C.S., Petrich, J.W., Patti, J.M., Narayana, S.V.L., and Hook, M. Domain structure of the *Staphylococcus aureus* collagen adhesin. *Biochem.* 37:15423-15433, 1998.
57. Salyers, A. and Whitt, D., Some Other Opportunists. In: *Bacterial pathogenesis: a molecular approach*, edited by various: ASM Press 1994, p.267.
58. Schneewind, O., Fowler, A., and Faull, K.F. Structure of the cell wall anchor of surface proteins in *Staphylococcus aureus*. *Science* 268, 1995.
59. Schneewind, O., Mihaylova-Petkov, D., and Model, P. Cell wall sorting signals in surface proteins of Gram-positive bacteria. *EMBO. J.* 12:4803-4811, 1993.
60. Signas, C., Raucci, G., Jonsson, K., Lindgren, P.E., Anantharamaiah, G.M., Hook, M., and Lindberg, M. Nucleotide sequence of the gene for a fibronectin-binding protein from *Staphylococcus aureus*: Use of this peptide sequence in the synthesis of biologically active peptides. *Proc.Natl.Acad.Sci.USA* 86:699-703, 1989.

61. Smeltzer, M.S., Gillaspy, A.F., Pratt, F.L., Jr., Thames, M.D., and Iandolo, J.J. Prevalence and chromosomal map location of *Staphylococcal aureus* adhesin genes. *Gene* 196:249-259, 1997.
62. Smith, I.M. and Vickers, A.B. Natural history of 338 treated and untreated patients with staphylococcal septicaemia (1936-1955). *Lancet*. 1:1318-1322, 1960.
63. Somploinsky, D., Samra, Z., Karakawa, W.W., Vann, W.F., Schneerson, R.S., and Malik, Z. Encapsulation and capsular types in isolates of *Staphylococcus aureus* from different sources and relationships to phage types. *J.Clin.Microbiol.* 22:828-834, 1985.
64. Switalski, L.M., Speziale, P., and Hook, M. Isolation and characterization of a putative collagen receptor from *Staphylococcus aureus* strain Cowan 1. *J.Bacteriol.* 264:21080-21086, 1989.
65. Thakker, M., Park, J.S., Carey, V., and Lee, J.C. *Staphylococcus aureus* serotype 5 capsular polysaccharide is antiphagocytic and enhances bacterial virulence in a murine bacteremia model. *Infect.Immun.* 66:5183-5189, 1998.
66. Ton-That, H., Faull, K.F., Schneewind, O., Anchor structure of staphylococcal surface proteins. *J.Biol.Chem.* 272:22285-22292, 1997.
67. Uhlen, M., Guss, B., Nilsson, B., Gatenbeck, S., Philipson, L., and Lindberg, M. Complete sequence of the staphylococcal gene encoding protein A. *J.Biol.Chem.* 259:1695-1702, 1984.
68. Vaudaux, P., Pittet, D., Haeberli, A., Lerch, P.G., Morgenthaler, J.J., Proctor, R.A., Waldvogel, F.A., and Lew, D.P. Fibronectin is more active than fibrin or fibrinogen in promoting *Staphylococcus aureus* adherence to inserted intravascular catheters. *J.Infect.Dis.* 167:633-641, 1993.
69. Waldvogel, F.A. and Vasey, H. Osteomyelitis: The past decade. *N.Engl.J.Med.* 303:360-370, 1980.
70. Wilkinson, B.J. and Holmes, K.M. *Staphylococcus aureus* cell surface: capsule as a barrier to bacteriophage adsorption. *Infect.Immun.* 23:549-552, 1979.
71. Wilkinson, B.J., Sisson, S.P., Kim, Y., and Peterson, P.K. Localization of the third component of complement on the cell wall of encapsulated *Staphylococcus aureus* M: implications for the mechanism of resistance to phagocytosis. *Infect.Immun.* 26:1159-1163, 1979.